USF Tampa Graduate Theses and Dissertations

3-27-2014

Neural Correlates of Spectral, Temporal and Spectro-temporal Modulation

Anusha Mohan
University of South Florida, mohan.anusha.1990@gmail.com

Neural Correlates of Spectral, Temporal and Spectro-Temporal Modulation

by

Anusha Mohan

A thesis submitted in partial fulfillment
of the requirements for the degree of
Master of Science in Biomedical Engineering
Department of Chemical and Biomedical Engineering
College of Engineering
University of South Florida

Major Professor: David A. Eddins, Ph.D.
Ann C. Eddins, Ph.D.
Joseph P. Walton, Ph.D

Date of Approval:
March 27, 2014

DEDICATION

I would like to dedicate this thesis to my Director and Program Coordinator Dr. Robert Frisina Jr. who has encouraged me and stood by my side in my tough times and to my parents, brother and soul-sister, who have been my four pillars of support through all the high and low tides in my life.

ACKNOWLEDGMENTS

TABLE OF CONTENTS

LIST OF TABLES

LIST OF FIGURES

ABSTRACT

Natural sounds are characterized by the distribution of acoustic power over different frequency regions and/or time. This is termed spectral, temporal or spectro-temporal modulation. The auditory system is equipped with banks of filters tuned to different spectral, temporal and spectro-temporal modulation frequencies (SM, TM, STM). The sensitivity of the peripheral system to these modulations can be measured by undertaking a linear systems approach. In addition to understanding the psychophysical sensitivity, studying the neural patterns of their processing is also critical. The current study is an attempt to understand the relationship between the behavioral and neural correlates of spectral, temporal and spectro-temporal processing in ten normal hearing subjects (age range 21-27 years; mean = 23.7 years). In the behavioral experiment, sensitivity to SM, TM and STM frequencies was estimated using a 3-interval, 3-alternative, forced-choice paradigm with a 3-down-1-up tracking algorithm. In the electrophysiological experiment, Electroencephalographs (EEGs) were recorded in a change-detection paradigm in response to the same set of modulation stimuli used in the behavioral experiment presented at 20 dB sensation level (SL). The EEG data were analyzed to determine the global field power and latencies of the N1and P2 components and the amplitude of the N1-P2 complex. Although an overall parietal dominance was observed for all of the components, the N1-P2 complex was strongly lateralized to the right hemisphere in the frontal region, but the hemispheric asymmetry decreased at central and parietal regions. A highly significant but weak to moderate negative correlation between individual behavioral thresholds and N1-P2 amplitudes

was observed, and this relationship also was observed when behavioral spectro-temporal transfer functions and N1-P2 amplitude transfer functions were examined together. Thus the current project reveals that a relationship exists between the behavioral measures and neural correlates and gives us hope to work towards establishing this relationship.

CHAPTER 1: INTRODUCTION

1.1 Problem Statement

To identify the neural correlates of spectral, temporal and spectro-temporal modulation by studying the perceptual and physiological responses to these modulation techniques in young, normal-hearing adults.

Spectral, temporal and spectro-temporal modulations are sinusoidal variations in the amplitude of the static spectrum, time waveform or a combination of the two. The rate of spectral modulation is varied in cycles/octave and that of temporal modulation is varied in cycles/second or Hz. Figure 1.1 shows the representation of spectral and temporal modulations in the time and frequency domains.

Spectral, temporal and spectro-temporal modulations are present in speech and music. The efficient processing of either of these complex stimuli involves the accurate resolution of its spectral and temporal components. This processing takes place in a two-step process involving perceptual and physiological correlates.

Following a linear systems approach, modulation transfer functions describe modulation depth detection thresholds as a function of modulation frequency. Each of these modulation techniques have been studied as the perceptual correlates to spectral, temporal and spectro-temporal processing (Viemeister, 1979; Eddins, 1993; Chi *et al*., 1999; Sabin *et al*., 2012; Bernstein *et al*., 2013) describing the spectral, temporal and spectro-temporal acuity of the

auditory system. Saoji and Eddins (2007) with their masking study suggested that the auditory system was organized into banks of filters each tuned to different spectral modulation frequencies and these filters were used in pure spectral modulation detection. Dau *et al*. (1997) also modelled the auditory system to be made of a bank of linear filters tuned to different temporal modulation frequencies.
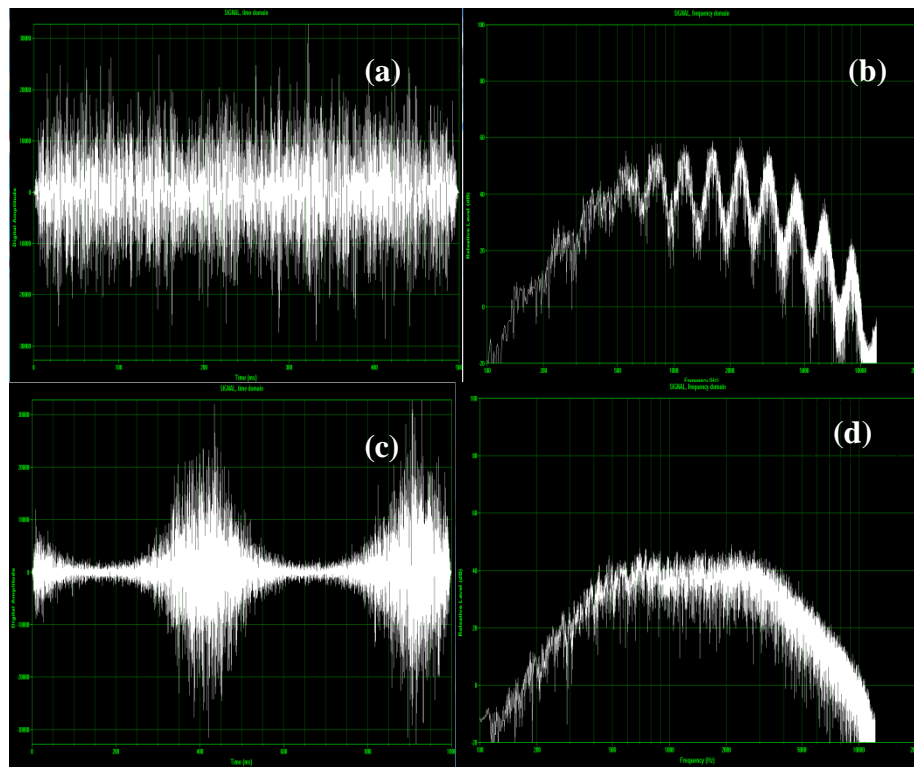
Figure 1.1 Spectral and temporal modulations in time (left panels) and frequency (right panels) domains. (a) 2 cyc/oct in time domain; (b) 2 cyc/oct in frequency domain; (c) 2 Hz in time domain; (d) 2 Hz in frequency domain.

Physiological recordings using different techniques such as functional magnetic resonance imaging (fMRI), magnetoencephalography (MEG) and electroencephalography (EEG) reveal differences in spectral and temporal coding by the auditory cortex as hemispheric differences and N1 latency shifts (Luo and Poppel, 2012; Draganova *et al*., 2009). The physiology describes the neural circuitry underlying the processing of these modulations which

gives a complete analysis of the processing of spectro-temporal stimuli along with the perceptual correlates.
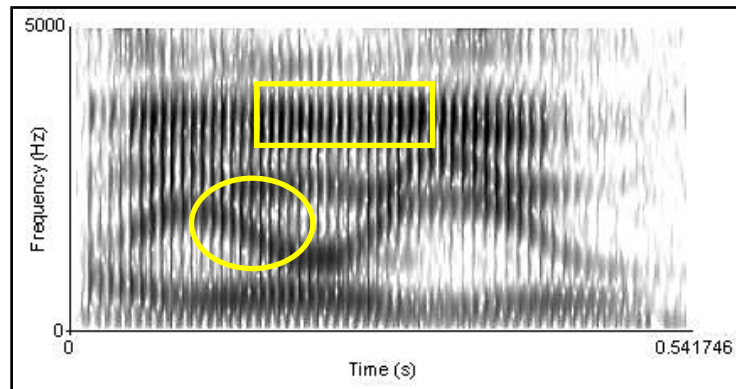
Figure 1.2 Spectrogram of "I owe you" showing spectro-temporal modulations[10]

The ability to perceive and process these modulations changes with hearing impairment (Bernstein *et al*., 2013). For example, persons with hearing loss have reduced frequency selectivity which degrades the perception of spectral modulations. Physiologically they also have reduced temporal fine structure coding, consistent with reduced coding of rapid temporal fluctuations (Korczak *et al*., 2012). This compromises the perception of speech in noise for these individuals. Spectro-temporal correlates of modulation sensitivity could be modelled to assess speech intelligibility and thereby provide a better discrimination between listeners with similar audiograms (Bernstein *et al*., 2013).

In order to study and understand the behavior and electrophysiological responses with different cohorts (age, hearing impairment etc.), it is essential to identify the perceptual and neural markers in a group of young, normal-hearing adults which would serve as a reference for other studies. This thesis aims at answering specific questions in the identification of the neural correlates of spectral, temporal and spectro-temporal modulation in a group of young normal-hearing adults.

CHAPTER 2: REVIEW OF LITERATURE

The auditory system is richly organized with neuronal banks of filters tuned to envelopes of spectral, temporal and spectro-temporal modulations at the different levels in the central auditory pathway (Langner and Shreiner, 1988; Langner, 1991; Shamma, 1993; Saoji and Eddins, 2007; Versnel *et al*., 2009). However, the perception of these features depends on the characteristics of the signal including stimulus duration, bandwidth of the carrier, depth of modulation, and modulation frequency (Viemeister, 1979; Eddins, 1993; Chi *et al*., 1999; Eddins and Bero, 2007). Modulation perception also may be affected by age, hearing loss, and other changes in the health of the auditory system (Summers and Leek, 1994; Bernstein *et al*., 2013). In addition to perceptual declines, declines in the neural encoding capacity under such conditions may result in poorer representation of these stimuli in the auditory system (Maurits *et al*., 2006; Berlingeri *et al*., 2012). Hence, it is equally important to understand the neural mechanisms encompassing the processing of different forms of modulation. In an attempt to explain the spectral, temporal and spectro-temporal processing by the auditory system, several models based on perceptual data and neural correlates have been proposed. This chapter outlines some of these important findings that serve as a motivation and basis for the hypotheses of the current study.

2.1 Linear Systems Approach

The characteristics of the any system can be assessed by feeding it with an input and studying the output. When the system is linear, a unit change in the input produces a homogenous output. The relationship between the input and output is characterized by a transfer

4

function which predicts the output of the system for any input. The predicted output is the input convolved with the transfer function in the time domain and input multiplied with the transfer function in frequency domain. Spectral, temporal and spectro-temporal modulations are created by modulating the amplitude of a carrier stimulus across the spectrum, across time, or a combination of the two. Variations in modulation frequency are essentially changes in the scale of modulation. Detecting spectral and temporal variations in amplitude is critical in phoneme identification and, in the bigger picture, the perception of speech and music as well as other complex environmental sounds.

In the time domain, the linear systems approach yields a temporal modulation transfer function (TMTF) and this is variously described as having a low-pass characteristic or a slightly band-pass characteristic with a minor reduction in the sensitivity to very low modulation frequencies. To measure the TMTF, sinusoidally amplitude modulated stimuli have served as input to the auditory system. The system output is indexed by either behavioral or physiological measures and these measures provide an index of the fidelity of coding the input modulation. By comparison of the output to the input, the TMTF of the system is described. In a behavioral paradigm, the depth of modulation is titrated to determine the minimum detectable depth of modulation. In this way, the sensitivity of the system is measured over a range of relevant modulation frequencies. Following a similar approach, a spectral modulation transfer function (SMTF) may be used to characterize the representation of spectral features by the auditory system. In this case, the carrier is shaped to have sinusoidal variations in amplitude (spectral modulation) over audio-frequency. Systematic manipulation of the spectral modulation frequency at the input to the system, and measurement of the sensitivity to that modulation at the output of the system, results in an SMTF. Such a linear system approach has been used to study

audition in various ways from pure tone audiometry and frequency tuning curves to speech intelligibility (Chi *et al*., 1999). The same methodology is used widely in the study of the visual and somatosensory systems. Remarkably, this linear systems approach appears to characterize these systems quite well despite the fact that they each have marked non-linear properties.

2.2 Spectral Modulation Detection (SM)
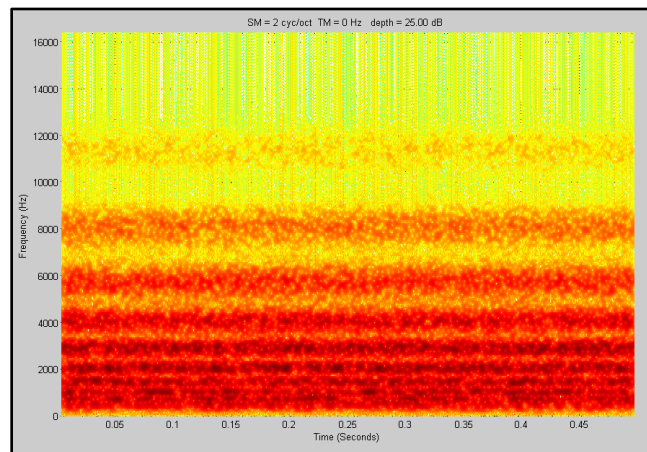
Figure 2.1 Spectrogram of 2 cyc/oct spectral modulation at 25 dB modulation depth

The ability of the auditory system to detect changes in amplitude across frequency, or the spectral shape of a stimulus, is fundamental to many aspects of audition including object identification, musical perception, and extracting meaning and nuance from speech. Applying a linear systems approach to studying spectral shape perception, one may measure the ability to detect sinusoidal spectral modulation as a function of the spectral modulation frequency. The resulting spectral modulation transfer function then is used to characterize spectral shape perception over a relevant range of parameters. Those parameters include carrier type (e.g., tonal vs. noise), carrier bandwidth (usually expressed in octaves), carrier range in audio frequency (Hz), modulation frequency, modulation phase, modulation amplitude, stimulus level, and stimulus duration. For perceptual tasks, it is typical for the listener to hear three intervals of

6

sound. Two of those intervals have no modulation and one interval has modulation (the signal interval). The listener must identify the interval with modulation. The minimum peak-to-valley depth required to detect the presence of modulation is termed the modulation detection threshold. This threshold is measured as a function of modulation frequency. A number of studies have investigated spectral envelope perception as a function of modulation frequency. Summers and Leek (1994) compared spectral modulation detection of listeners with hearing loss and listeners with normal hearing. They used logarithmically spaced tones as the carrier and varied the modulation frequency from 1 to 9 cyc/oct. They observed that the spectral modulation transfer function had a band-pass characteristic with best sensitivity from 2 to 4 cyc/oct and decreased sensitivity at frequencies above and below that range. Furthermore, they reported that performance was considerably worse for the listeners with hearing loss than the listeners with normal hearing. They attributed this difference, in part, to the frequency resolving power of the auditory periphery.

Eddins and Bero (2007) used a variety of band pass filtered noise carriers of different bandwidths (1, 2, 3, and 6 octave) in different frequency regions to systematically map out the effects of carrier parameters on spectral modulation detection. They concluded that the spectral modulation transfer function was not significantly dependent on carrier frequency or stimulus bandwidth.

Saoji and Eddins (2007) used a modulation masking paradigm to test the theory that the auditory system inherently has modulation specific tuning. To do so, they measured spectral modulation detection thresholds in the presence and absence of spectral modulation masking. In the case of masking, the stimulus had a fixed frequency, fixed depth masker modulation and the task was to detect the addition of signal modulation. Their results were consistent with the notion

7

that the auditory system has a bank of overlapping band-pass filters tuned to different spectral modulation frequencies. This is consistent with the physiological findings of Shamma *et al.* (1993) and others who have identified spectrally tuned receptive fields in the primary auditory cortex.

2.3 Temporal Modulation Detection (TM)
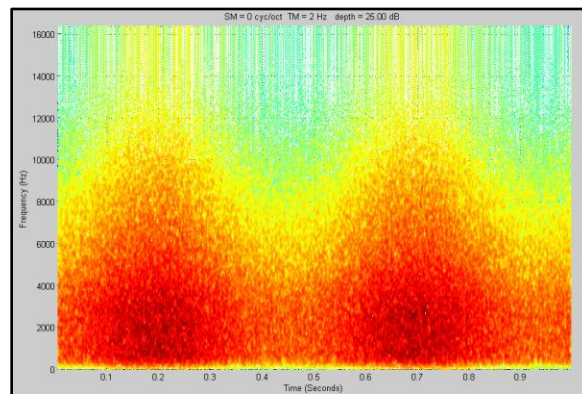
Figure 2.2 Spectrogram of a 2 Hz temporal modulation at 25 dB modulation depth

Most natural acoustic stimuli have an amplitude envelope that slowly changes over time. This temporal envelope carries meaning in speech, music, and provides identifying information for other acoustic events. The ability of the auditory system to follow these amplitude changes can be measured by studying the sensitivity of the auditory system to amplitude modulation. To fully map out the temporal sensitivity of the auditory system, modulation sensitivity may be mapped across a range of modulation frequencies. The resulting temporal modulation transfer function can then be used to define the temporal acuity of the auditory system. A number of investigators have used this approach to characterize temporal processing in humans and animals.

In his landmark study, Viemeister (1979) used broad band and narrow band noise carriers and sinusoidal amplitude modulation (SAM) to study the effects of stimulus intensity, center frequency (200, 1000, 10000 Hz), and carrier duration (250, 500, 1000, 1500 ms) on modulation perception. For broadband noise, he reported a temporal modulation transfer function that is characterized by a low-pass shape, with a cutoff frequency of about 60 Hz. This corresponds to a time constant of about 2 ms. To study the potential influence of audio-frequency region on the TMTF, he measured the TMTF for carrier center frequencies of 200 Hz, 1000 Hz and 10,000 Hz. The carrier bandwidth was approximately 50% of the center frequency. The resulting TMTFs were low-pass in shape with -3 dB cut-off frequencies that shifted from 27 Hz to 31 Hz to 45 Hz with increasing carrier center frequency. Thus, he reported that an increase in the carrier center frequency resulted in an increase in the -3 dB cut-off frequency despite the fact that the carrier bandwidth also increased proportionally. The change in TMTF could have been due to chances in carrier bandwidth (not mentioned by the authors). He also reported that a change in carrier duration had a substantial effect on the transfer function when the carrier duration was less than 250 ms and at low modulation frequencies. He investigated potential the intensity effects on the TMTF by changing the intensity of the carrier from 20 dB to 50 dB SPL and concluded that there was no substantial change in the transfer function; TMTFs had the same shape and were within a 1 dB across the three levels.

Eddins (1993) noted that in the Viemeister (1979) study, the carrier bandwidth changed as the center frequency was increased, thereby rendering it impossible to attribute changes in modulation detection to either bandwidth, center frequency, or some combination of the two. Therefore, he undertook a systematic investigation of the influence of stimulus bandwidth and center frequency on amplitude modulation detection using band-pass filtered noise carriers of

different bandwidths (200, 400, 800, 1600 Hz) in different frequency regions. To summarize the different temporal modulation transfer functions, he fitted a low-pass filter functions to the data and showed that the time constants were sensitive to stimulus bandwidth but not to center frequency. Specifically, the time constants decreased monotonically with increasing bandwidth (<=1600 Hz) but not across stimulus frequency region.

Physiological investigations have also mapped temporal modulation transfer functions at multiple levels in the central auditory pathway (e.g., cochlear nucleus - Frisina *et al*., 1985; inferior colliculus - Langner and Schreiner, 1988). Responses from single neurons demonstrate tuning to temporal modulation frequency and responses recorded across a population of neurons demonstrate tuning to a wide range of different best modulation frequencies. The resulting modulation transfer functions are similar to those from human perception. Based on the physiological and psychophysical evidence, Dau *et al*. (1997) proposed a filter-bank model for temporal processing with two domains of filters with different bandwidths. The first domain between 0 and10 Hz with a constant bandwidth of 5 Hz and a second domain between 10 and1000 Hz with logarithmic scaling of bandwidth with a *Q* value of 2. The model accounted for low-pass characteristic when the modulation frequency was less than half the bandwidth of the carrier frequency and high pass characteristic of the transfer function when the modulation frequency greater than half the bandwidth of the carrier frequency. They argued that the low-pass characteristic of the function was due to interaction amongst the filters.

2.4 Spectro-temporal Modulation Detection (STM)

Most natural acoustic stimuli have amplitudes that vary over time (temporal modulation), amplitude that varies across frequency (spectral modulation) and spectra that vary over time

10

(spectro-temporal modulation). In each case, the pattern of variation is complex. Adopting the same linear systems approach described above, in the laboratory we can use sinusoidal modulation and systematically vary the free parameters. Spectro-temporal modulation is related to the perception of prosody in speech and the melody of a song played on an instrument such as a guitar.
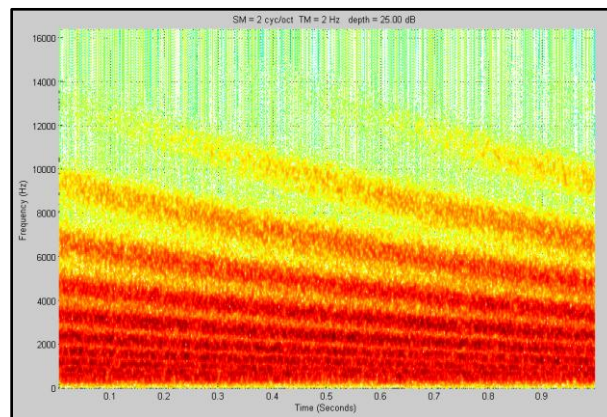
Figure 2.3 Spectrogram of a 2cyc/oct, 2 Hz spectro-temporal modulation at 25 dB modulation depth

Chi *et al*. (1999) mapped spectro-temporal modulation transfer functions in young, normal hearing adults using broad-band carriers with sinusoidal spectral and temporal profiles resulting in spectra that could drift downward or upward over time. They plotted modulation index, the percentage of modulation required to detect modulation, as a function of spectral (0.25 cyc/oct to 8 cyc/oct) and temporal modulation frequencies (1 Hz to 128 Hz) and concluded that the modulation transfer function had a low pass characteristic in both domains with high sensitivity at 2 to 8 Hz and 0.5 to 2 cyc/oct that was comparable to previous independent measurements of spectral and temporal modulation detection. Hence, they argued that it was a product of the two modulation transfer functions. Furthermore, they explained the relevance of using these transfer functions to speech intelligibility by stating that the most sensitive spectro-

11

temporal modulation frequencies (4 to 8 Hz and < 4 cyc/oct) correspond to the spectro-temporal properties greatest distinction among different speech sounds in speech perception.

Bernstein *et al*. (2013) expanded on the work of Chi *et al*. using a 4-octave bandwidth noise carrier with spectral modulation of 0.5, 1, 2 and 4 cyc/oct and temporal modulation of 4, 12 or 32 Hz. They compared the STM thresholds in subjects with normal hearing and impaired hearing in the age range of 24 to 60 years to other measures like frequency selectivity, audiometric thresholds, age and hearing impairment and concluded that STM sensitivity is directly affected by all the above mentioned parameters and that STM could be used as a good predictor for speech intelligibility.

An attempt to improve the perception of STM was proposed by Sabin *et al*. (2012). They tested their normal hearing listeners on spectral, temporal and spectro-temporal modulation detection before and after a training period (one hour per day for 7 days), compared the results and observed a significant improvement in the detection thresholds after training. The more interesting observation was that the subject groups that underwent training in spectral or temporal modulation detection did not perform as well in detecting spectro-temporal modulation and vise-versa suggesting that there was a separate bank of neural filters tuned to combinations of spectro-temporal modulations.

Physiological evidence of spectro-temporal modulation tuning has been found in the cochlear nucleus (Clopton and Backoff, 1990), inferior colliculus (Versnel *et al*., 2009) and the primary and secondary auditory cortices (Depireux *et al*., 1999). This has been reported as the presence of spectro-temporal receptive fields which are regions of increased single or multi-neuron activity in response to spectro-temporally modulated stimuli. All the studies report

12

sensitivity to spectro-temporal modulation at low modulation frequencies (< 4 cyc/oct), which is in close agreement with the behavioral data from humans (e.g., Chi *et al*., 1999). Depireux *et al*. (2001) studied both the upward and downward STM drift in the AI of a ferret and showed that the combined transfer function was not fully separable due to asymmetric units in the AI.

2.5 Human Electrophysiology

From previous studies, we have learned that perceptual measures of spectral, temporal and spectro-temporal processing are supported by physiological evidence from single neuronal recordings and receptive fields from the different nuclei in the central auditory pathway of animal models. Studying the functional organization of the human brain to speech and spectro-temporal modulations also has shown evidence for the existence of neural correlates of spectral, temporal, and spectro-temporal modulation processing.

Zatorre and Belin (2001) used positron emission tomography (PET) to image the activity of the brain while processing spectral and temporal changes in the stimuli. Their standard stimulus consisted of a two-tone complex alternating between 500 Hz and 1000 Hz. Each of the components had a standard duration of 667 ms with a random duty cycle. In the temporal condition, the alternate stimulus had a shorter duration than the standard stimulus that was randomly assigned to values from ½ to 1/32 of the standard duration (333, 162, 81, 40, and 21 ms). In their spectral condition, the duration of the stimulus was kept a constant and the frequency separation of the two tones was varied. Starting with a standard separation of one octave, 5 sets of stimuli were produced where the frequency separation in each set was half the previous set (ranging from ½ to 1/32 of an octave separation). The stimuli were presented continuously and bilaterally through headphones and their subjects were instructed to

concentrate on the stimuli. They observed that the spectral stimulus produced greater activity in the right hemisphere and the temporal change produced greater activity in the left hemisphere.

Jamison *et al*. (2006) replicated Zatorre and Belin's study with a few changes. They used fMRI to image their responses and their stimulus presentation paradigm was not continuous. The length of the stimulus was 6 s and the inter-stimulus interval was 23 s. The responses were imaged 15 s after stimulus onset and an 8 s period of silence followed every acquisition. They familiarized their subjects with the stimuli a priori and instructed them to not pay attention to the stimuli while they imaged the responses. They still observed an asymmetry in the lateralization of spectral and temporal stimuli where the temporal stimuli lateralized to the left and spectral to the right.

Zaehle *et al.* (2008) used mis-match negativity (MMNs) responses to study the cortical distributions of activity in response to spectrally (broadband noise of different center frequencies) and temporally (broadband noise bursts separated by a gap of varying duration) deviant stimuli in young, normal hearing adults. They recorded EEG activity using a 32-channel system. The standard stimuli consisted of two segments; a 7 ms leading wideband noise burst and a 300 ms trailing band-passed noise burst centered at 1000 Hz separated by a 5 ms gap. The spectral deviants were generated by changing the center frequency of the trailing element (1500, 1600, 1700 Hz with bandwidth of 250 Hz) and the temporal deviants were generated by changing the noise onset times (60, 80, 100ms). Thus, the presentation paradigm was essentially a temporal gap discrimination in which either the duration of the gap (temporal) or relative frequency of the noise after the gap (spectral) parameters were varied. The stimuli were presented using an oddball paradigm with the standards occurring 70% of the trials and a stimulus-onset-asynchrony of 750 ms. They also performed a source localization analysis to

14

estimate the location and position of the neural generators. They observed that the MMNs to spectral and temporal deviants were organized asymmetrically, with larger responses to spectral changes in the right hemisphere and larger responses to temporal changes to the left hemisphere. They also observed that the responses were most robust in the fronto-central region. The authors concluded that this asymmetry was supported by the 'asymmetric sampling in time' (AST) model proposed by Poeppel (2003) using fMRI studies, where that the right hemisphere has a longer temporal integration window of 150 to 250 ms and the left hemisphere has a temporal integration window of 20 to 40 ms. He concluded saying that the right hemisphere was more robust in processing slow spectral variations whereas the left hemisphere was more robust in processing rapid fluctuations in time.

Rao *et al*. (2010) used pure tones (1000 Hz and 3000 Hz) and filtered noise (low pass filtered at 2000 Hz and band-pass filtered between 2000 Hz and 4000 Hz) as targets and background maskers to create combinations of congruent and incongruent pitch perception conditions with constant or varying background stimuli. In the constant background conditions, the presentation consisted of a combination of tones and filtered noise with either one as the background. If a tone (1000 Hz or 3000 Hz) was used as the background, the pitch of the noise (high pass or band-pass used as target) was asked to be rated as 'hi' or 'low'. The opposite was done when the noise (high pass or band-pass) was used as background and a tone was used as target. In the varying background conditions, the presentation consisted of a tone (1000 Hz or 3000 Hz) or filtered noise (high-pass or band-pass) as the target. When the tone was used as the target the background consisted of a combination of both the filtered noises and for the noise target, both the tones were used as background. The pure tones were maintained at 15 dB above the noise. The stimuli were presented at 60 dB above their 1000 Hz threshold with an inter-

stimulus interval randomized between 1900 and 2100 ms. They played their stimuli binaurally using ER-3A insert earphones and simultaneously recorded the EEG during the behavioral task. They compared the amplitudes and latencies of the individual components (P1, N2 and P2) of the event related potential in response to the different tasks by applying averaging techniques and Global Field Power analyses. They also compared the amplitudes and latencies of the different components in different sites (frontal, central and parietal) and hemispheres (right and left). They reported that the N1 and P2 components were more robust in the frontal and central regions and the N1 components were right lateralized. They observed that the amplitude of the N1 response increased with increase in difficulty of the task and attributed this to recruitment of more neurons and increase in activity.

Okamoto *et al*. (2012) examined magnetoncephalographic (MEG) responses to spectral, temporal and a combined spectral-temporal change in a two-sound sequence of tonal and filtered pulse train. In one experiment, combinations of two-sound sequences were created from four stimuli; 500 Hz and 2000 Hz pure tones and 500 Hz and 2000 Hz amplitude modulated (40 Hz) stimuli. Spectral change sensitivity was measured in response to a 500 Hz pure tone followed by a 2000 Hz pure tone or vice versa or to a 500 Hz AM followed by a 2000 Hz AM tone or vice versa. Temporal change sensitivity was measured in response to a 500 Hz or 2000 Hz tone followed immediately by a 500 Hz AM or 2000 Hz AM tone, respectively, or to a 500 Hz AM or 2000 Hz AM tone followed by a 500 Hz or 2000 Hz tone. Finally, spectral-temporal change sensitivity was measured in response to a 500 Hz pure tone followed by a 2000 Hz AM tone, 500 Hz AM followed by 2000 Hz pure tone, etc. In the second experiment the pure tones were replaced by 32 Hz and 48 Hz pulse trains and the AM tones were replaced by these pulse trains filtered between 2800 Hz and 4000 Hz or between 4000 Hz and 5600 Hz. The stimuli were 1600

ms in duration and were presented binaurally with an inter-stimulus interval of 800 ms using insert earphones. The responses were collected when the subjects watched a silent movie. They studied the P1m, N1m and P2m response amplitudes and latencies in the three conditions and two experiments and examined the difference between spectral, temporal and spectral-temporal change. They reported that the strengths of the responses elicited by the spectral and spectral-temporal changes were comparable and were statistically different from the strength of the responses elicited by the temporal change. They also noted a delayed occurrence of the N1m with temporal change compared to the spectral and spectral-temporal change.

2.6 Goal and Hypotheses of the Current Study

Previous studies have shown that spectral, temporal and spectro-temporal modulations are coded with high specificity by different types of cells in different regions in the auditory pathway. Analyzing psychophysical responses provides an index of the perceptual sensitivity to these modulation techniques and how it varies with modulation frequencies. The neurophysiological responses provide information on the neuronal representation, coding mechanism and the potential neural circuitry involved, especially during passive listening. To date, however, it is still not clear which electrophysiological measures of spectral, temporal and spectro-temporal modulation processing are best correlated and/or predictive of comparable psychophysical measures in the same group of young, normal-hearing listeners. The aim of the current study was to identify neural correlate(s) of spectral, temporal and spectro-temporal processing using both psychophysical measures and cortical auditory evoked potentials (CAEPs) obtained with multi-channel EEG in young, normal-hearing participants. Based on previous studies, we hypothesize that the CAEPs, characterized by a positive peak (P1) at about 50 ms, a negative peak (N1) at about 100 ms, and a positive peak (P2) at about 200 ms, would lateralize

17

more robustly to the right for spectral and spectro-temporal modulations and to the left for temporal modulation. Alternatively, it was also hypothesized that we might observe no overt lateralization for spectro-temporal modulations if they were to be considered a product of spectral and temporal activity. A second hypothesis was that the responses to all stimuli would be most robust in the fronto-central regions and smallest in the parietal region. Lastly, we hypothesized that behavioral measures and neurophysiological measures for component amplitude and/or latency would show a strong correlation for different modulation frequencies if they reflect similar underlying processes.

CHAPTER 3: METHODS

This chapter describes in detail the stimuli and the conditions tested in the behavior and evoked potential sessions, the hardware and software used for data collection, the subject criteria and hearing evaluation, the protocols followed for data collection in both sessions and finally the steps followed in the analysis of the data collected.

3.1 Participants

A group of ten young, normal-hearing individuals participated in this study (range: 21-31 years, mean: 23.86 years). All participants were briefed about the aim of the project, the evaluation and testing methods, benefits and risks, compensation and rights, prior to obtaining their written informed consent. Once the participant was consented, his/her hearing was evaluated based on otoscopy, tympanometry, and pure-tone audiometry. All participants had normal otoscopic exams and tympanometric results indicating normal outer and middle ear function, and pure-tone thresholds $\leq$ 20 dB hearing level (HL) at octave frequencies from 250 Hz and 8000 Hz. Additional inclusion criteria for participation in the study was; (1) no middle ear pathology, (2) no history of neurological or psychiatric disorders, and (3) passing score of 26 out of 30 on the Montreal Cognitive Assessment (MOCA) test battery. Participants were paid an hourly rate for their participation at the conclusion of the study.

3.2 Stimuli and Stimulus Conditions

Two sets of stimuli used in this study, signals and standards, were generated using MATLAB^{TM}. The stimuli were broad-band noise carriers band-limited between 400 Hz and 3200 Hz with a slope of 48 dB/octave on both ends. These carriers were amplitude modulated with spectral, temporal or spectro-temporal modulation and sampled at 24414 Hz. The different spectral, temporal and spectro-temporal modulations were:

- Spectral: 0.5 cyc/oct, 2 cyc/oct and 8 cyc/oct

- Temporal: 2 Hz, 8 Hz, 32 Hz, and 64 Hz

- Spectro-temporal: (0.5 cyc/oct, 2 Hz); (0.5 cyc/oct, 8 Hz); (0.5 cyc/oct,32 Hz); (0.5 cyc/oct, 64 Hz); (2 cyc/oct, 2 Hz); (2 cyc/oct, 8 Hz); (2 cyc/oct, 32 Hz); (2 cyc/oct, 64 Hz); (8 cyc/oct, 2 Hz); (8 cyc/oct, 8 Hz); (8 cyc/oct, 32 Hz); (8 cyc/oct, 64 Hz)

The stimuli were generated by modulating the band-limited carrier using peak-to-valley depths from 50 dB to 0.155 dB in steps of 6 points/octave (50 steps). Each of the stimuli was generated with 20 random starting phases at each modulation depth, resulting in 20 different stimuli at the same modulation depth. Hence, for a particular condition there resulted 20*50 = 1,000 stimuli. For the 19 conditions, there was a library of 19*1000 = 19,000 stimuli. The standard stimuli were unmodulated band-limited noise carriers with random starting phases. The stimulus duration depended upon the temporal modulation frequency. All stimuli were 500 ms in duration except the conditions with 2 Hz temporal modulation, which were 1000 ms in duration. Table 3.1 lists the 19 test conditions, corresponding SM and TM frequencies, and the duration of the stimuli.

Table 3.1 Spectral, temporal and spectro-temporal modulation testing conditions

Condition Number	SM frequency (cyc/oct)	TM Frequency (Hz)	Duration (ms)
1	0	2	1000
2	0	8	500
3	0	32	500
4	0	64	500
5	0.5	0	500
6	0.5	2	1000
7	0.5	8	500
8	0.5	32	500
9	0.5	64	500
10	2	0	500
11	2	2	1000
12	2	8	500
13	2	32	500
14	2	64	500
15	8	0	500
16	8	2	1000
17	8	8	500
18	8	32	500
19	8	64	500

The signal and the standards were saved in .wav format and 16-bit integer format. The .dat files were used by the TDT SykofizX software application in the behavioral experiments and .wav files were used in the evoked potential experiments.

In anticipation of future studies with participants who have hearing loss, it was desirable to minimize the potential spread of excitation in the cochlea which likely would differ between listeners with different degrees and configurations of hearing sensitivity. The masker was played continuously during behavioral and electrophysiological testing and was composed of a broadband noise (0 Hz to 44100 Hz) notched between 400 Hz to 3200 Hz with a 48 dB/oct slope and attenuated 25 dB sound pressure level (SPL) re: the signal level.

3.3 Hardware Circuitry

Figure 3.1 illustrates the hardware circuit for both behavioral and electrophysiological testing. The modulated signals were routed from output channel A of the TDT RZ6 to the input channel A of the signal mixer SM3. The notched noise masker was routed from the PC soundcard to the programmable attenuator, PA4 and then to input channel B of the SM3. The signal plus masker output was routed to the left channel output of the head phone buffer HB6 and then to the left channel of the Etymotic Tubephone^{TM} ER-2 earphones.

The ANT-Neuro high-speed amplifier was connected to the RZ6 via an RS-232 cable with a custom adapter. This served to deliver software triggers to the amplifier via TDT's Real-time Processor Visual Design Studio (RPvdsEx), Advanced Source Analysis (ASA) and MATLAB^{TM}-based custom software (ANTsc).
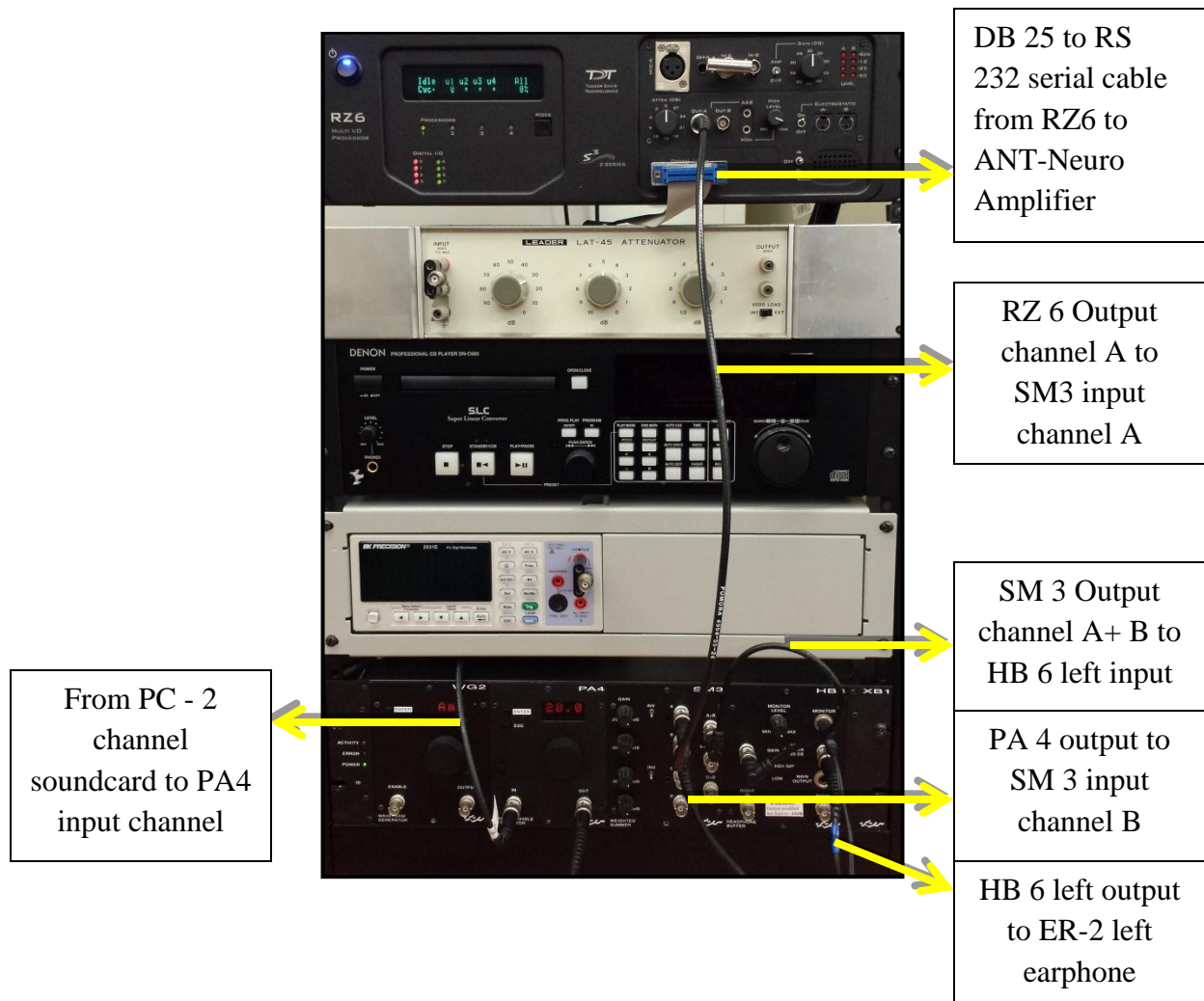
Figure 3.1 Connections in the hardware circuitry

3.4 Calibration

The Etymotic ER-2 insert earphones were calibrated to ensure that they delivered the stimulus at an accurate presentation level. The hardware was connected as follows: the output of channel A of the RZ6 was routed to input A of the SM3, one channel of the PC soundcard was routed to the PA4 then to input B of the SM3, the output of the SM3 to the HB6, and the output to the left channel of the ER-2 earphones. First, a 1000 Hz, 94 dB SPL calibration tone was generated with a B&K Type 4230 Calibrator (SN 449327) and recorded with a B&K 4134 ½" microphone (SN 532794) and B&K 2669 pre-amplifier (SN 2363780) routed to a BK Precision

voltmeter. Next, the Calibrator was replaced in the circuit by the ER-2 earphone, and the SykofizX calibration stimulus was played through the earphones and the output of the earphone was recorded in SykofizX. The calibration file for each earphone was saved and used later by SykofizX and ANTsc software applications during stimulus delivery for the behavioral and electrophysiological testing, respectively.

3.5 Behavioral Design and Data Acquisition

The behavioral part of the experiment was designed to determine the psychophysical threshold for each of the conditions outlined in Table 3.1. The pre-computed stimuli were controlled and played through SykofizX, routed through the RZ6, PA4, SM3, HB6 and delivered to the left earphone for each subject. The experimental protocol employed a 3-interval-3-alternative-forced-choice paradigm with an adaptive, 3-down, 1-up tracking rule (Levitt, 1971). Subjects were seated in the sound booth and attended to a subject interface displayed on a computer monitor. The interface included three images marked "Interval 1", "Interval 2" and "Interval 3" (see figure 3.11). Using a PC mouse, the subject was instructed to select the interval that contained the modulated noise by clicking on the appropriate image. Visual feedback regarding which interval contained the correct signal was provided after each presentation.

All subjects were provided with practice trials prior to data collection. During data collection, the first three reversals were discarded, and threshold was estimated based on the average of the final six reversals. Thresholds were estimated for a minimum of three runs for each of the 19 conditions. Mean thresholds and standard deviations were computed across the runs for each condition. Subjects were provided with regular breaks throughout testing. Figure 3.2 illustrates the graphic representation of one threshold run for a subject.
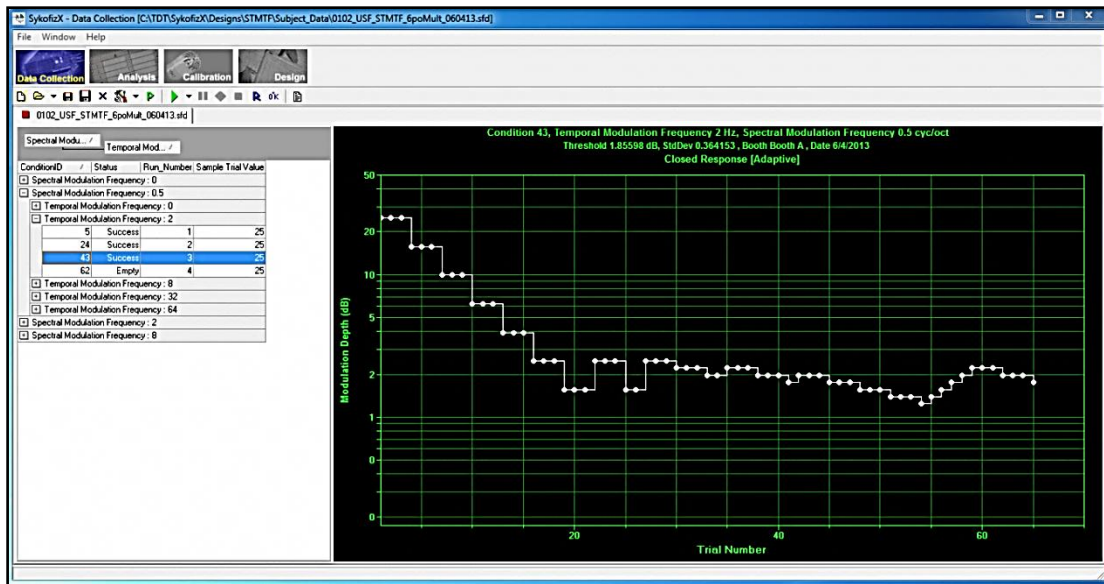
Figure 3.2 Representation of one threshold run for a subject

3.6 Electrophysiological Design and Data Acquisition

Electrophysiological testing was completed in a double-walled sound attenuating booth. Stimulus design and control were implemented using custom ANTsc software integrated with ASA-Lab and Experiment Manager (ExMan). To determine proper placement of the waveguard cap, the distance between nasion and inion and between the two tragus' were measured to estimate the center of the subject's head. The Cz electrode was placed at this position and the cap was then fitted snuggly but comfortably on the subject's head. Starting with the ground electrode, each electrode site was filled with electrode gel using a syringe and blunt-end needle. The gel reduces the impedance between the scalp and the electrodes in order to improve electrical conductivity and minimize unwanted physiological noise in the recording. Electrode impedances were kept below 10 kOhm. The cap was held tightly in place at the mastoids by placing an expanding mesh band around the head. The skin above and below the right eye and at the outer canthus of each eye was cleaned using alcohol wipes and Nuprep skin prep gel. Bipolar

Ag/AgCl cup electrodes filled with Ten20 conductive paste were placed at these eye locations to monitor horizontal and vertical electro-occulography (HEOG/VEOG) responses. After the cap and eye electrodes were position, ER-2 insert earphones were inserted in both ears. The subject was allowed to watch a closed-captioned movie of their choice or read silently while testing was in progress.

Using ASA-Lab, electrode impedance was checked prior to data collection, as shown in Figure 3.3. ANTsc software (a custom, MATLAB^{TM}-based stimulus generation and presentation control software package) was launched and the stimulus condition parameters were entered. Continuous EEG responses were obtained for all 19 stimulus conditions at a fixed supra-threshold level of 20 dB SL relative to each subjects' behavioral modulation detection threshold for that condition. The software delivered approximately 230-250 triggered events that were recorded in ASA-Lab and online averaged across a small subset of electrodes (Fz, Cz, Pz). A screen shot of the continuous EEG (left) and online averages (right) is shown in Figure 3.4. The continuous data were stored offline for later analysis. Subjects were provided regular breaks during testing to minimize fatigue. EEG data were obtained for all conditions over 2 test sessions lasting about 3 hours per session (including about 30 minutes for cap placement).

3.7 Data Analysis

The raw EEG collected by ASA was processed in the same way for all ten subjects. The data were batch processed in Experiment Manager, an Excel application that comes along with ASA, to save processing time. The data were first filtered using a band-pass filter with a lower cut off frequency of 0.3 Hz and an upper cut off frequency of 30 Hz. The data were corrected for any trends or slow drifts that might have occurred during recording using the de-trending feature.

The data were corrected for baseline shifts and ensured that there were no DC offsets to the averaged response.
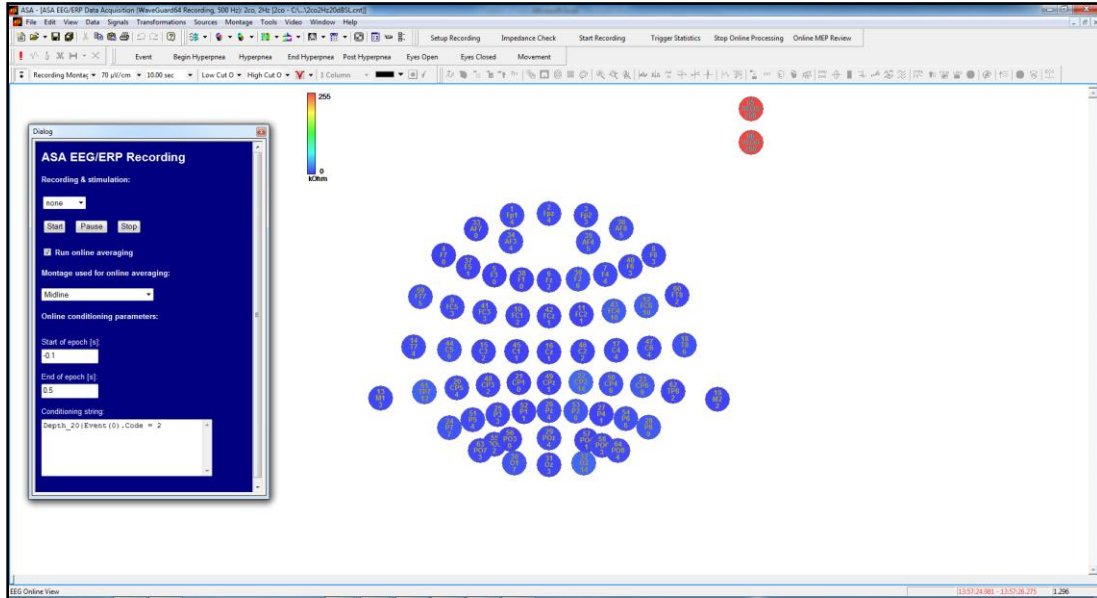
Figure 3.3 Impedance check and online averaging
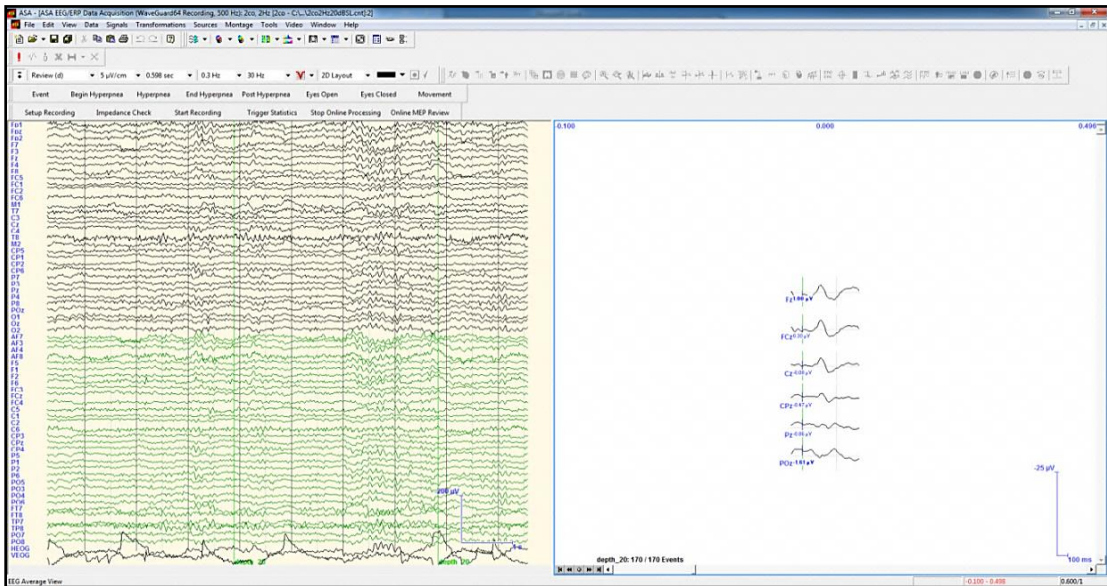
Figure 3.4 Online recording view. Left panel: Run-time continuous EEG recording, Right Panel: EEG online average

The responses that were greater than an absolute value of 150 µV were considered artefacts and marked using the artefact detection feature. The eye leads helped to record the artefacts due to eye blinks and saccades and could also be easily detected by the artefact detection feature. The averaging feature of the ASA Experiment Manager software was configured to epoch the data (-100 ms to 500 ms), reject the artefacts and average all the artefact-free epochs. Even though the data were batch processed, each condition generated a separate .avr file (average file). The averaged waveform resembled the auditory late evoked potential responses with a negative peak between 70 and 170 ms and a positive peak between 170 and 280 ms depending upon the condition tested and electrode location.

The main questions asked in this study were if the characteristics of these responses changed with hemisphere (right and left), location (Frontal, Central and Parietal), modulation type (spectral, temporal and spectro-temporal modulation) and modulation frequency and if there was a relationship between these characteristics and the behavioral data obtained so that we could define a neural marker that was predictive of the behavioral correlate. Using the data reduction methods of Rao *et al*. (2009), activity from the 64 channels were combined into seven subgroups – Frontal Left, Frontal Right, Central Left, Central Right, Parietal Left, Parietal Right and Midline. The electrodes that were used to form the subgroups are listed below

- Frontal Left (FL): F1, F3, F5, F7, FC1, FC3, FC5, FT7
- Frontal Right (FR): F2, F4, F6, F8, FC2, FC4, FC6, FT8
- Central Left (CL): C1, C3, C5, T7, CP1, CP3, CP5, TP7
- Central Right (CR): C2, C4, C6, T8, CP2, CP4, CP6, TP8
- Parietal Left (PL): P1, P3, P5, P7, PO3, PO5, PO7
- Parietal Right (PR): P2, P4, P6, P8, PO4, PO6, PO8

- Midline: Fz, FCz, Cz, CPz, Pz, POz

Figure 3.5 shows the positions of these electrodes on the 64 channel recording montage. The data from each of these montages was exported as an ASCII file from ASA from every condition and every subject for further processing.
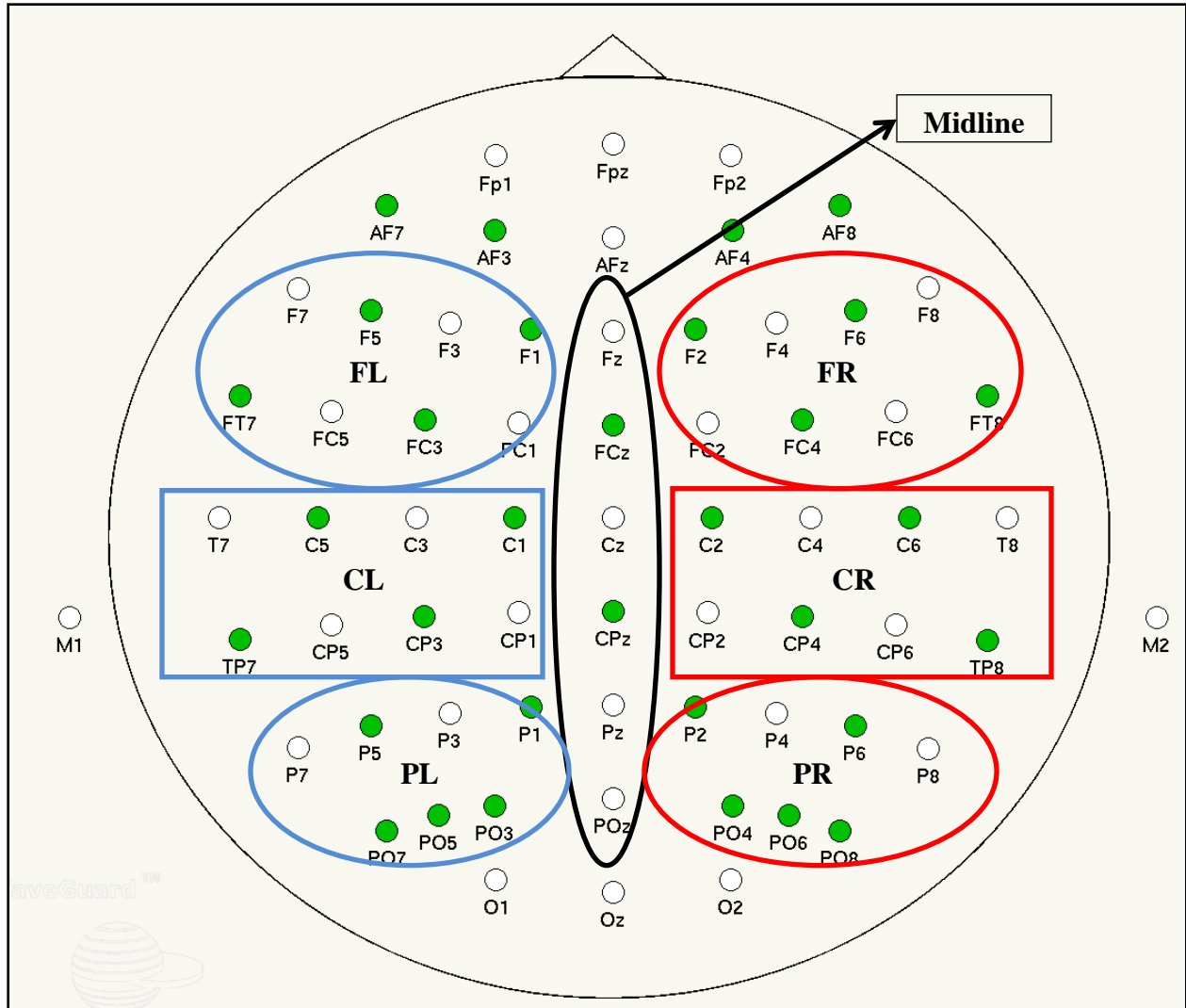
Figure 3.5 Electrode positions of the 7 sub-groups used for data analysis[11]

The general observation made during the recording was that lower spectral and temporal modulation frequencies elicited a more robust response in contrast to the higher modulation

frequencies. The next chapter explains in detail the data analyses performed on these responses from these sub-groups and compares statistical differences in the characteristics of the late potential components across hemisphere, location, modulation technique and modulation frequency.

CHAPTER 4: RESULTS AND DISCUSSION

The analyses for the behavioral and electrophysiological sections of the study will be reported separately. As detailed in Chapter 3, the aim of the behavioral part of the study was to determine the modulation depth detection thresholds for the different spectral, temporal and spectro-temporal conditions described in Table 3.1 Following collection of behavioral data, electrophysiological data were collected.

4.1 Behavioral Experiment Results

The behavioral data was analyzed separately for the different stimulus manipulations– pure spectral, pure temporal, and spectro-temporal modulation using three separate one way Analyses of Variance (ANOVA). Statistical analyses were executed using the IBM SPSS Statistics 21 software package.

4.1.1 Spectral Modulation Transfer Function (SMTF)

A spectral modulation transfer function describes the minimum perceivable modulation depth as a function of modulation frequency. When measured behaviorally, a SMTF provides a means of systematically defining the spectral acuity of the auditory system. Such acuity is important in differentiating sounds that differ in spectral energy (e.g., the spoken words "sing" versus "song" or in differentiating the sound of the same note played on a piano or a guitar). Recall that in this experiment, sinusoidal spectral modulation was superimposed on a noise carrier that was 3 octaves wide (400 Hz to 3200 Hz). The average (panel (a)) and individual

31

(panel (b)) results are shown in Figure 4.1. Spectral modulation frequency (0.5, 2.0, and 8.0 cyc/oct) is shown on the abscissa and spectral modulation depth at threshold (peak-to-valley difference in dB) is shown on the ordinate. In panel (a), error bars indicate the standard deviation about the mean.
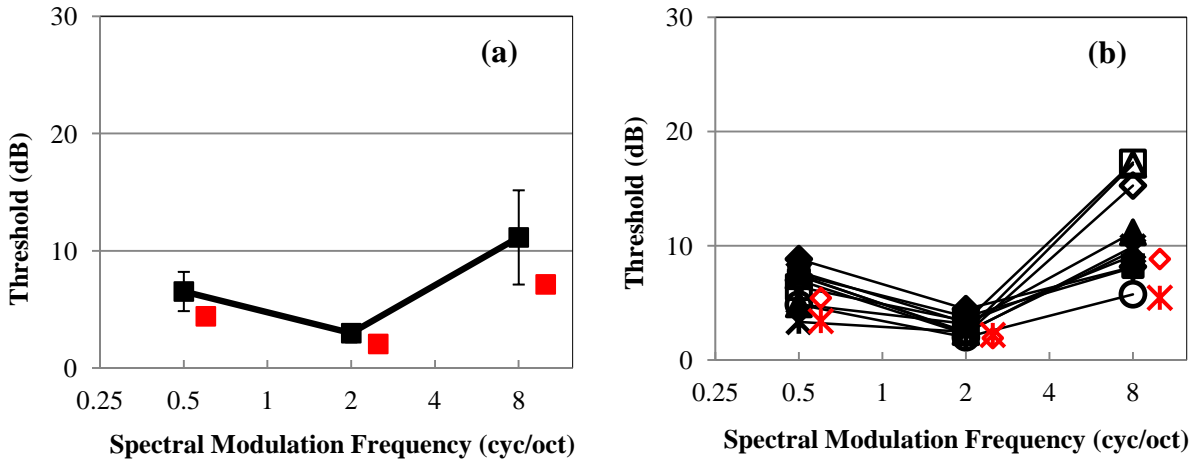
Figure 4.1 Spectral modulation depth detection thresholds plotted as a function of spectral modulation frequency. (a) Mean spectral modulation depth detection thresholds plotted as a function of spectral modulation frequency in the presence (10 subjects) and absence (2 subjects) of the continuous masker. (b) Individual spectral modulation depth detection thresholds plotted as a function of spectral modulation frequency in the presence (10 subjects) and absence (2 subjects) of the continuous masker. See text for details.

Focusing on the group mean data (black squares) in panel (a), it is clear that sensitivity is best at 2.0 cyc/oct (3.0 dB) and increases below (0.5 cyc/oct; 6.53 dB) and above (8.0 cyc/oct; 11.14 dB) this frequency. A one-way ANOVA with spectral modulation frequency as the between subject variable showed that the threshold at each of the modulation frequency was significantly different from each other ($F_{(2,27)} = 25.71$, $p < 0.001$), indicating a significant increase in modulation depth detection threshold at 0.5 cyc/oct and 8 cyc/oct in comparison to 2 cyc/oct. Post Hoc analysis also revealed that the mean thresholds at each of these frequencies

belonged to different sub-sets ($p_{0.5-2} = 0.012$, $p_{2-8} < 0.001$, $p_{0.5-8} = 0.001$). Thus spectral modulation depth detection worsened at lower and higher spectral modulation frequencies.

In panel (b) of Figure 4.1, the black symbols show thresholds at each modulation frequency for each of the ten subjects, indicated by different symbol types. Thresholds were most similar across subjects at 2 cyc/oct while the variability across subjects was greatest at 0.5 and 8.0 cyc/oct. For example, the thresholds of the individual subjects all fall within one standard deviation of the mean at 2 cyc/oct. This increases to 1.67 standard deviations at 0.5 cyc/oct and to 4.02 standard deviations at 8 cyc/oct. The thresholds of the individual subjects at 8 cyc/oct vary between 5.75 dB and 17.27 dB.

Greater variability at 8.0 cyc/oct may be related to the presence of the continuous notched-noise background sound intended to limit the upward spread of excitation. To test this possibility, two subjects participated in a post-hoc test that included threshold measurements for each of the 8 cyc/oct conditions but with no background noise present. The solid red squares in panel (a) represent the mean threshold of the two subjects at the different spectral modulation frequencies in the absence of the masker (the symbols have a horizontal offset for clarity). The red symbols in panel (b) show the individual thresholds of the two subjects in the absence of the masker. Comparing the values of the solid red squares with the solid black squares in panel (a) and also comparing the red symbols to the black symbols in panel (b), one can gauge the effect of the masker on modulation depth detection. The mean threshold at 8 cyc/oct in the presence of background noise is 11.14 dB. The mean threshold obtained from the two subjects in the absence of the masker is 7.13 dB. Thus the presence of the masker led to an increased (worse performance) threshold by about 4 dB. Comparing the thresholds of the two subjects with and without the masker, it is clear that the effect of the masker is much more evident at 8 cyc/oct than

0.5 cyc/oct and 2 cyc/oct. At this 8 cyc/oct, the subject represented by the open diamond is 6.43 dB worse and the subject represented by the asterisk is 4.11 dB worse than their individual thresholds in the absence of the masker.

4.1.1.1 Discussion

The current data is consistent with several previous studies of spectral modulation detection. Summers and Leek (1994) examined spectral modulation detection for a carrier ranging from 1000 Hz to 4000 Hz in normal and impaired listeners. They reported spectral modulation detection thresholds that were best at 2 cyc/oct and worse above and below this frequency. Thus, the pattern of thresholds was similar to the current data. The spectral modulation transfer function reported in the current study is more sensitive than Summers and Leek (1994) by almost 4 dB at 2 cyc/oct which is reduced to 2 dB at 8 cyc/oct. This may be due to several factors including their use of a narrower carrier band (2 octave rather than 3 octave), greater carrier component spacing, and the use of randomized presentation level from stimulus to stimulus.

Amagai *et al*. (1996) studied spectral modulation transfer functions with budgerigars, applying a sinusoidal modulation to log-spaced tones between 500 Hz and 10,000 Hz. Comparing the results of the current study with their study, we observe similar sensitivity to modulation at 2 cyc/oct. They reported substantially lower thresholds than those reported here at 0.5 cyc/oct (4 dB lower) and 8 cyc/oct (7 dB lower). Again, there are several factors that may have contributed to these differences, including the presence of a masker in the current study and species differences. In the absence of a masker, thresholds in the present study remain 2.4 dB

higher at 0.5 cyc/oct and 2.6 dB higher at 8 cyc/oct. Thus, differences in sensitive to spectral modulation across species may be the most likely explanation of the results.

Eddins and Bero (2007) compared spectral modulation transfer functions across different carrier frequency regions and bandwidths. Their study concluded that spectral modulation transfer functions were independent of carrier frequency region (with the exception of very low audio frequency region) and carrier bandwidths (from 1 to 6 octaves). The transfer function of the current study is less sensitive than that reported by Eddins and Bero (2007). The difference in sensitivity is more pronounced at the lower and higher modulation frequencies than at the best frequency. The current study is worse by 2 dB at 0.5 cyc/oct and 7 dB worse at 8 cyc/oct. Comparing the thresholds in the absence of the masker, the slightly better sensitivity in the current study may be attributed to minor differences in stimulus generation.

The presence of the continuous masker has a greater influence on thresholds at 8 cyc/oct that for lower modulation frequencies. The reason for this differential effect is not known with any certainty, however, one may speculate based on previous data. For example, Eddins and Bero (2007) used excitation pattern simulations (i.e., simulations of the output of the cochlea) to show that the peak-to-valley contrast at the cochlear output is dramatically reduced at higher modulation frequencies. At 8 cyc/oct, an input contrast of 5 dB resulted in an output contrast of about 1 dB. It may be that the addition of just a small amount of background noise has a severe influence on the residual peak-to-valley contrast, rendering thresholds much higher than without a masker.

4.1.2 Temporal Modulation Transfer Function (TMTF)

A temporal modulation transfer function quantitatively describes the temporal resolution of the auditory system. It is plotted with sensitivity to modulation on the ordinate as a function of temporal modulation frequency on the abscissa. Studying amplitude modulation depth detection thresholds is a conventional way of studying the temporal acuity of the system. In the present study, temporal modulation depth detection thresholds are measured by varying the peak-to-valley depth of the sinusoidal modulation in the amplitude of the stimuli over time starting at 25 dB. The sensitivity to modulation is expressed as 20 log (1/m) where m is the modulation depth. The average (panel (a)) and individual (panel (b)) results are shown in Figure 4.2. Temporal modulation frequency (2, 8, 32, and 64 Hz) is shown on the abscissa and temporal modulation depth at threshold is shown on the ordinate. Note that the independent variable in the experiment was the peak-to-valley depth in dB. This is a difference limen (DL) value where the relation between modulation depth, m, and the DL is as follows: **DL in dB = 20 * log[(1+m)/(1-m)] (Eq.4.1)** (Rodenburg, 1977). Here, thresholds are plotted as 20 log (1/m) by convention with respect to temporal modulation detection and for ease of comparison to other data. The solid black squares in panel (a) show the mean thresholds for the ten normal-hearing subjects across the different temporal modulation frequencies and the solid red squares show the mean thresholds of the two subjects in the absence of the continuous masker. The error bars indicate the standard deviation about the mean.
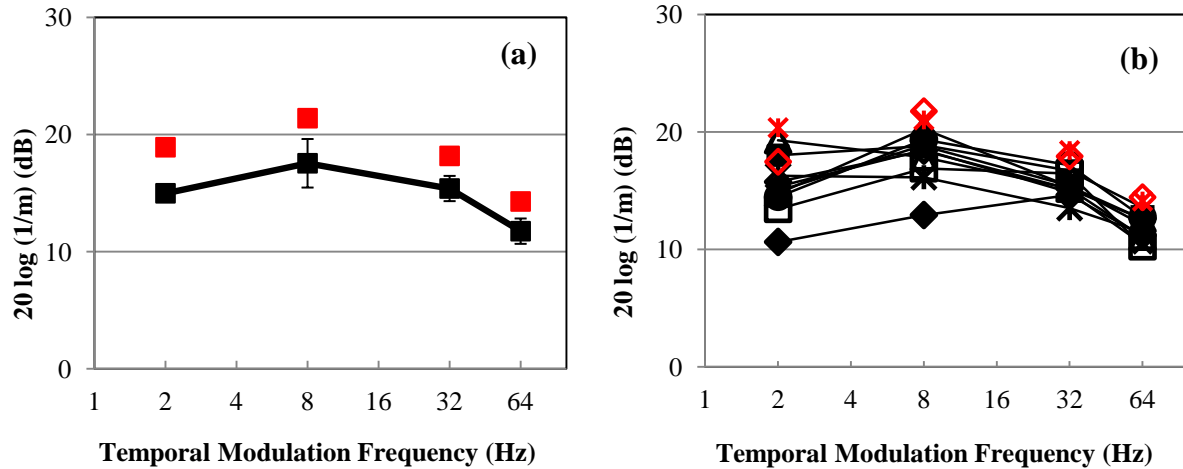
Figure 4.2 Sensitivity to temporal modulation depth detection plotted as a function of temporal modulation frequency. (a) Mean sensitivity plotted as a function of temporal modulation frequency in the presence (10 subjects) and absence (2 subjects) of the continuous masker. (b) Individual subject modulation sensitivities plotted as a function of temporal modulation frequency in the presence and absence of the masker.

Better sensitivity to modulation depth corresponds to larger values on the ordinate and decreases in sensitivity correspond to lower values. The mean modulation sensitivity is modulation-frequency dependent and ranges between 11.74 dB and 17.54 dB. The sensitivity is greatest at 8 Hz modulation frequency (17.54 dB) and decreases at lower and higher frequencies. A one-way ANOVA with temporal modulation frequency as the between subjects factor shows that there is a significant difference between the sensitivities at the different modulation frequencies ($F_{(3,36)}$ = 19.84, $p < 0.001$). Post hoc Tukey analysis reveals that sensitivities at 2 Hz and 32 Hz are not significantly different from one another ($p = 0.997$) but they are different from 8 Hz ($p_2 = 0.015$, $p_{32} = 0.024$) and 64 Hz ($p_2 < 0.001$, $p_{32} < 0.001$). The 8 Hz condition was also significantly different from the 64 Hz condition ($p < 0.001$). Increasing the modulation frequency initially improves modulation perception, but this worsens at modulation frequencies greater than 8 Hz.

Error bars in panel (a) and individual data in panel (b) indicate that thresholds vary more across individual subjects at the low than the higher modulation frequencies indicated by the closed and open symbols apart from the solid red squares, across the different modulation frequencies. At 2 Hz, the individual data fall within a 2.37 standard deviation range and at 8 Hz within a 2.07 standard deviation range. This variability decreases at 32 Hz and 64 Hz to a range of 1.08 standard deviations. One reason for this frequency dependent inter-subject variability may be due to the single subject identified by the diamonds in panel (b). For this subject, thresholds at 2 Hz and 8 Hz are much lower than the other subjects. The variability excluding this subject was 1.82 and 1.24 standard deviations at 2 Hz and 8 Hz respectively.

To evaluate the potential influence of the presence of background noise on thresholds, the same two subjects discussed above were tested in the temporal modulation conditions without a background noise. The mean modulation thresholds without background noise for those two subjects are shown by the solid red squares in panel (a) and their individual thresholds are shown by the red symbols in panel (b). Mean thresholds without the background noise higher (better) than with the background noise present by 3.94 dB at 2 Hz, 3.85 dB at 8 Hz, 2.79 dB at 32 Hz and 2.54 dB at 64 Hz. Despite the threshold differences, the same pattern of thresholds (greatest sensitivity at 8 Hz and poorer sensitive at 2 Hz, 32 Hz and 64 Hz) is observed.

4.1.2.1 Discussion

The present data are similar to data previously reported using similar band limited noise carriers and sinusoidal temporal modulation. For stimuli of similar duration as those used here, Viemeister (1979) reported a similar pattern of thresholds with modulation frequency though exact threshold values differed in several ways. Those differences likely depend on differences in

38

stimulus parameters and measurement methods. Using similar stimuli and methods, the results of Eddins (1993) were quite similar to the present data. When compared to the present data with background noise, current thresholds were slightly (1.10 to 2.30 dB) lower than those of Eddins (1993). When compared to the present data without background noise, current thresholds were 0.30 to 2.40 dB better than those of Eddins (2003). Thus, the present results are in line with data from previously published reports, thereby validating our methods.

4.1.3 Spectro-temporal Modulation Transfer Function (STMTF)

Spectro-temporal modulations are more complex signals that have both spectral and temporal modulation superimposed on the carrier frequency. In this case, the peak-to-valley depth of the sinusoidal modulation is constant over time but the location of the peaks and valleys changes with frequency over time. The rate of change is dependent on the temporal modulation frequency. To generate spectro-temporal modulation transfer functions a combination of the spectral modulation frequencies (0.5 cyc/oct, 2 cyc/oct and 8 cyc/oct) and the temporal modulation frequencies (2 Hz, 8 Hz, 32 Hz and 64 Hz) were used to give 9 different combinations of spectro-temporal modulation frequencies.

Figure 4.3 depicts a family of spectral modulation transfer functions (spectral modulation frequency on the abscissa and modulation depth on the ordinate) with temporal modulation frequency as the parameter of each individual function (colored lines). The data represent the average thresholds across ten subjects. The error bars depict the standard deviation about the mean for the different conditions. The transfer function labelled "Average – 0 Hz" is the same modulation transfer function shown in panel (a) of Figure 4.1.

Figure 4.3 Spectro-temporal modulation depth detection thresholds plotted as a function of spectral modulation frequency. Shown are different temporal modulation frequencies represented by the differently colored lines.

Visual inspection of the functions in Figure 4.3 show that the addition of temporal modulation to spectral modulation may lead to threshold changes as well as changes in the shape of the overall functions. To assess these changes, a univariate analysis on the spectro-temporal modulation detection threshold, taking into consideration all 19 conditions, was performed considering each spectro-temporal modulation condition separately across all 10 subjects. The analysis show significant main effects of spectro-temporal modulation frequency ($F_{(3,108)} = 24.74$, $p < 0.001$). Post Hoc analysis (Tukey method) revealed a more detailed relationship between modulation detection threshold and modulation frequency. First, consider changes in detection threshold as a function of spectral modulation frequency (x axis values) by comparing across different temporal modulation frequencies. For pure spectral modulation, represented by the solid black line in Figure 4.3, the thresholds at all three spectral modulation frequencies are

significantly different from each other and the best threshold is at 2 cyc/oct (as described in Section 4.1.1). The introduction of 2 Hz temporal modulation (orange squares) results in a threshold improvement of 4.49 dB at 0.5 cyc/oct, 1.36 dB at 2 cyc/oct and 1.63 at 8 cyc/oct. This improvement in threshold is significant at 0.5 cyc/oct ($p = 0.001$) but not at 2 cyc/oct ($p = 0.205$) and 8 cyc/oct ($p = 0.129$). However, with increasing temporal modulation frequency, the sensitivity of the transfer functions (blue, red, and green functions) worsens as the compared to the function at 2 Hz (orange function). This effect is significant at 2 cyc/oct and 8 cyc/oct but not 0.5 cyc/oct. Further, at 2 cyc/oct the decrease in sensitivity with increase in temporal modulation frequency is not significant at 8 Hz (1.20 dB, $p = 0.264$), but significant at 32 Hz (3.11 dB, $p = 0.004$) and at 64 Hz (5.04 dB, $p < 0.001$). At 8 cyc/oct, the decrease in sensitivity with increase in temporal modulation frequency is significant at 8 Hz (5.61 dB, $p < 0.001$), 32 Hz (8.07 dB, $p < 0.001$) and 64 Hz (9.83 dB, $p < 0.001$).

From these results, we observe that an interaction between temporal and spectral modulation. With static spectral modulation as the reference (black squares in Figure 4.3), introduction of temporal modulation at 2 Hz results in a slight improvement in sensitivity. At 2 and 8 cyc/oct, however, sensitivity decreases systematically with increasing temporal modulation frequency.

We also observe that the variability of spectro-temporal modulation is less than one standard deviation for spectral modulation frequencies of 0.5 and 2 cyc/oct and all temporal modulation frequencies except 64 Hz. At 8 cyc/oct, the individual variability was greater than 3 standard deviations for all temporal modulation frequencies and was similar to the condition with spectral modulation frequency alone. Due to the high variability at 8 cyc/oct, the starting level of

a threshold run was increased to 31.10 dB if the participant could not identify the observation interval with spectro-temporal modulation on the first trial.
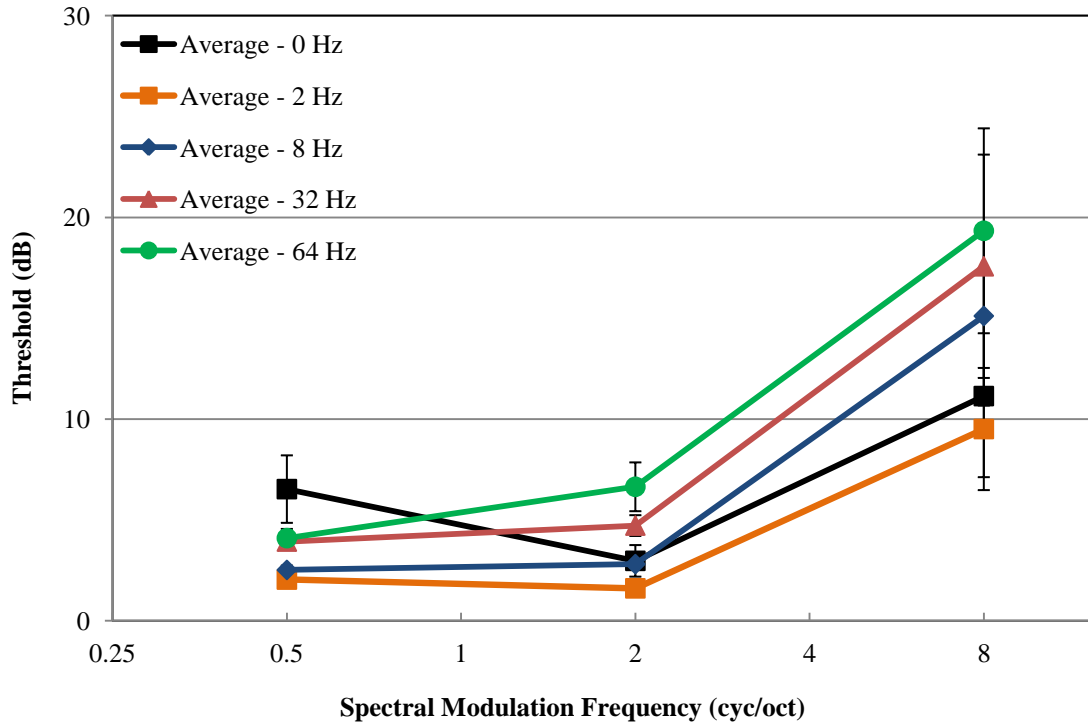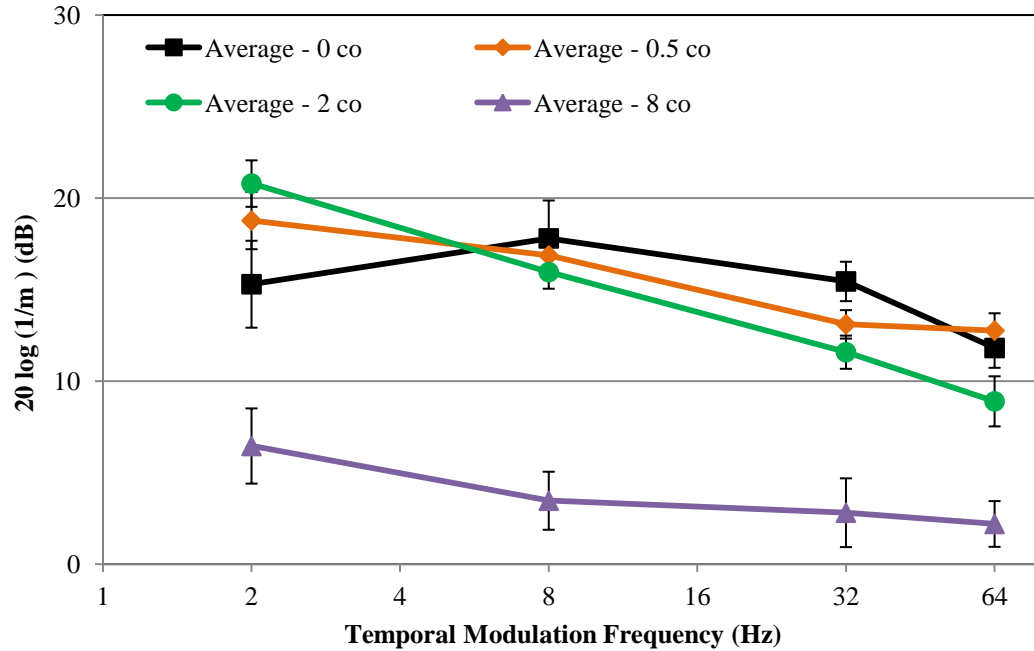

Figure 4.4 Spectro-temporal modulation depth detection thresholds plotted as a function of temporal modulation frequency. Shown are different spectral modulation frequencies represented by the differently colored lines.

Figure 4.4 shows an alternate way of representing the data, with thresholds plotted as a function of temporal modulation frequency rather than spectral modulation frequency on the abscissa. The results are a family of temporal modulation transfer functions with different spectral modulation frequencies indicated by color and symbol. The function represented by the black squares is the same temporal modulation transfer function detailed in section 4.1.2. The orange diamonds, green circles, and purple triangles represent TMTFs for spectral modulation frequencies of 0.5 and 2 and 8 cyc/oct, respectively. The error bars represent the standard deviation about the mean. From section 4.1.2, we know that temporal modulation detection thresholds in the absence of spectral modulation frequencies are best at 8 Hz and are

significantly worse at 2 Hz, 32 Hz and 64 Hz (black line in Figure 4.4). With the introduction of 0.5 and 2 cyc/oct (orange and green lines), the shape of the TMTF is altered slightly, becoming more linear with a steeper slope as a function of temporal modulation frequency.

Figure 4.5 shows thresholds for individual subjects with each panel showing data for a different temporal modulation frequency. This highlights the uniformity of thresholds across subjects at the low and mid spectral modulation frequency and greater inter-subject variability at the high spectral modulation frequency. As with static spectral modulation detection, it is possible that elevated and variable thresholds at 8 cyc/oct are influenced by the presence of background noise. The red symbols depict detection threshold of the two subjects at 8 cyc/oct in the absence of the continuous masker. Comparison of open and closed diamonds show the difference in thresholds with and without the background noise for one listener (a difference of 6.42, 8.97, 9.81 and 3.62 dB at 2, 8, 32 and 64 Hz, respectively). Similarly, comparison of the red and black asterisks shows the difference in thresholds with and without the background noise for a second listener (3.41, 3.13. 0.46 and 3.90 dB at 2, 8, 32 and 64 Hz, respectively).

4.1.3.1 Discussion

The present results are generally consistent with previous estimates of spectro-temporal modulation sensitivity in normal-hearing listeners. For example, Bernstein *et al*. (2013) reported thresholds for a similar range of spectral (0.5, 1, 2, 4 cyc/oct) and temporal (4, 12, 32 Hz) modulation frequencies. Figure 4.6 compares the modulation transfer function of the Bernstein study to the current study.
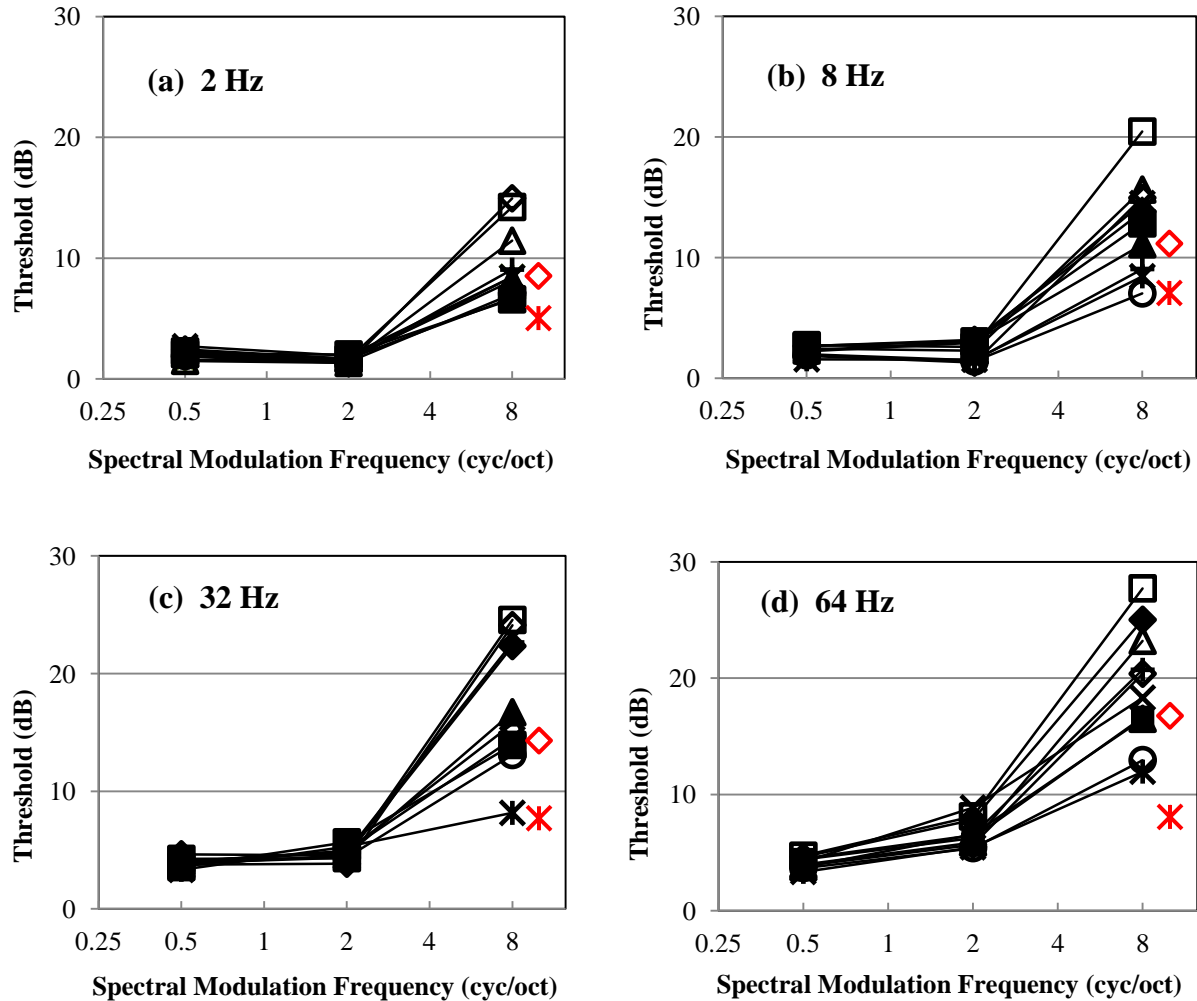
Figure 4.5 Individual subject thresholds for spectro-temporal modulation depth detection plotted as a function of spectral modulation frequency and temporal modulation frequencies. (a) 2 Hz, (b) 8 Hz, (c) 32 Hz and (d) 64 Hz

The black lines in Figure 4.6 represent data from the present study and duplicate the functions in Figure 4.4. The red dashed lines represent the data from Bernstein *et al*. (2013) after converting their threshold values into comparable units to those reported here using Equation 4.1. Only a few of the modulation frequencies match up exactly between studies; however, the parameters sampled are fairly similar. Importantly, the slopes of the functions are fairly similar across studies and thresholds differ by less than 3 dB at all common modulation frequencies. Comparing the 2 and 4 cyc/oct conditions from the Bernstein *et al*. (2013) to the 2 and 8 cyc/oct

conditions of the current study, we observe that the two functions are parallel to each other and that the functions of the current study are more sensitive. However, at 0.5 cyc/oct, data from Bernstein *et al*. (2013) are more sensitive than the current data by 3.06 dB at 32 Hz. The present results are also consistent with the results reported by Chi *et al*. (1999).
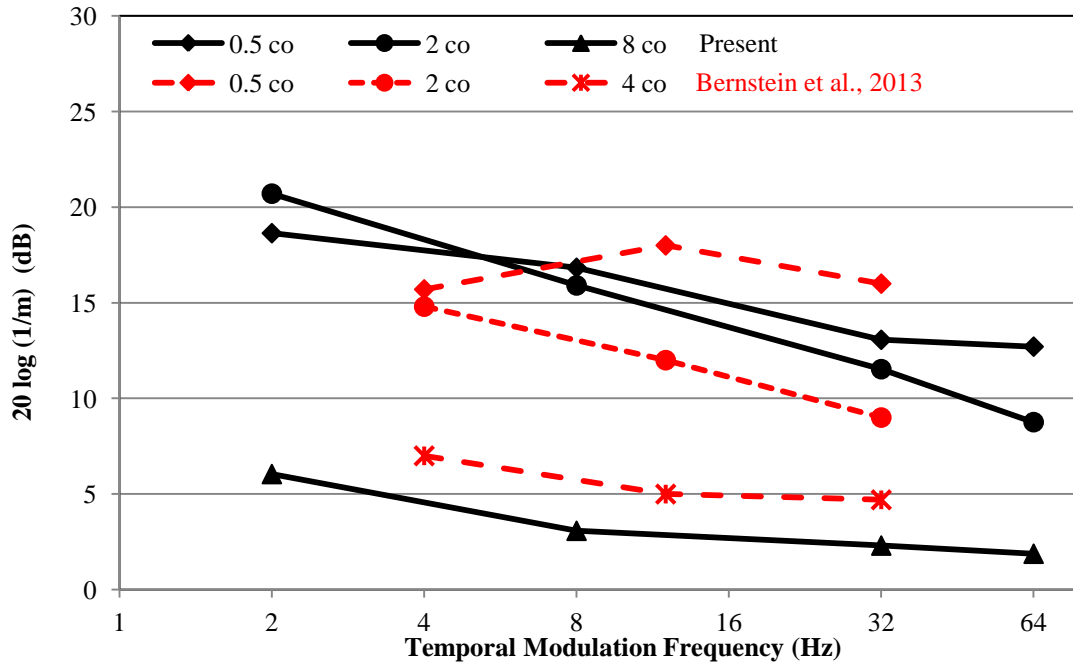
Figure 4.6 Comparison of spectro-temporal modulation detection thresholds of the current study (black) and Bernstein *et al*. (2013; red).

4.2 Electrophysiology Results

We hypothesized that CAEPs would have a tendency to lateralize to either hemisphere depending on the type of stimulus modulation that was being processed based on fMRI studies that show more robust processing in the right hemisphere for spectral modulation and in the left hemisphere for temporal modulation (Zatorre and Belin, 2001; Jamison *et al*., 2006). Other studies have observed the robustness of the signal in the frontal region versus the central and parietal by considering select electrode locations (Rao *et al*., 2010). To evaluate hemispheric

changes and cortical distribution of activity, we analyzed the data using two primary measures; global field power (GFP) and electrode cluster averaging. The grand averaged responses across subjects and the averaged responses for individual subjects for 14 out of the 19 conditions were grouped into seven clusters (refer to Chapter 3) and exported as ASCII files from ASA-Lab. The ASCII files contained the processed and epoched data (-100 to 500 ms). The five 8 cyc/oct spectral modulation conditions were excluded as their responses were not reliable for peak-identification. The waveforms from electrodes in each of the clusters were averaged to obtain an "average cluster waveform" for that region for the grand average response.

4.2.1 Analysis Techniques

The two types of analyses - global field power and the "average cluster waveform" were calculated as explained below. The Global Field Power was calculated for the grand average data and the "average cluster waveform" was calculated for both the grand average and the individual data.

4.2.1.1 Global Field Power

The GFP was calculated for each of the seven clusters and 14 stimulus conditions by computing the root mean square (RMS) amplitude at each time point in the grand average response for each electrode in the cluster and averaging across them. The GFP was calculated only for the grand average data. The N1 component power was identified as the maximum value of the response between 70 ms and 170 ms and the P2 component power was identified as the maximum value of the response between 170 ms and 280 ms. Figure 4.7 shows the GFP results for the midline electrode cluster and STM conditions with 0.5 cyc/oct spectral modulation. As

illustrated, the GFP waveforms consist of all positive values and characterize the strength of N1 or P2 components during the approximate 100 to 300 ms time interval following stimulus onset.
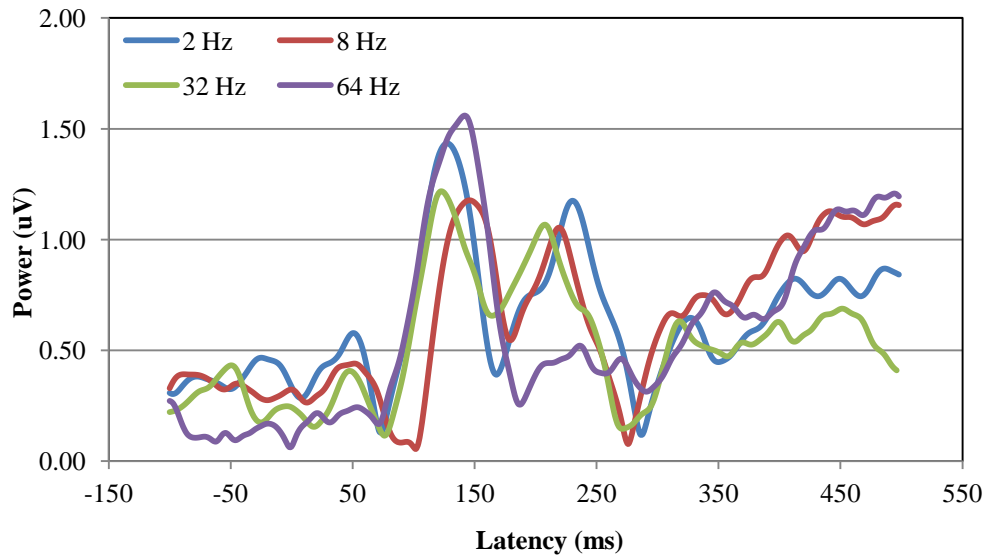
Figure 4.7 Example of global field power - calculated for the midline cluster for the different temporal modulation frequencies at 0.5 cyc/oct spectral modulation frequencies.

4.2.1.2 Average Cluster Waveform

The grand average response at each electrode in a cluster were averaged together to obtain one single waveform called the "average cluster waveform". Unlike the GFP, this waveform takes into account the negative and positive polarity of the N1 and P2 components and was used to quantify the N1 and P2 component latencies and N1-P2 peak-to-peak amplitude. These measures were quantified for both grand average responses across subjects as well as for individual subject data. Figure 4.8 shows the average cluster waveforms for the midline electrode cluster computed from the grand average data for STM conditions with 0.5 cyc/oct spectral modulation.
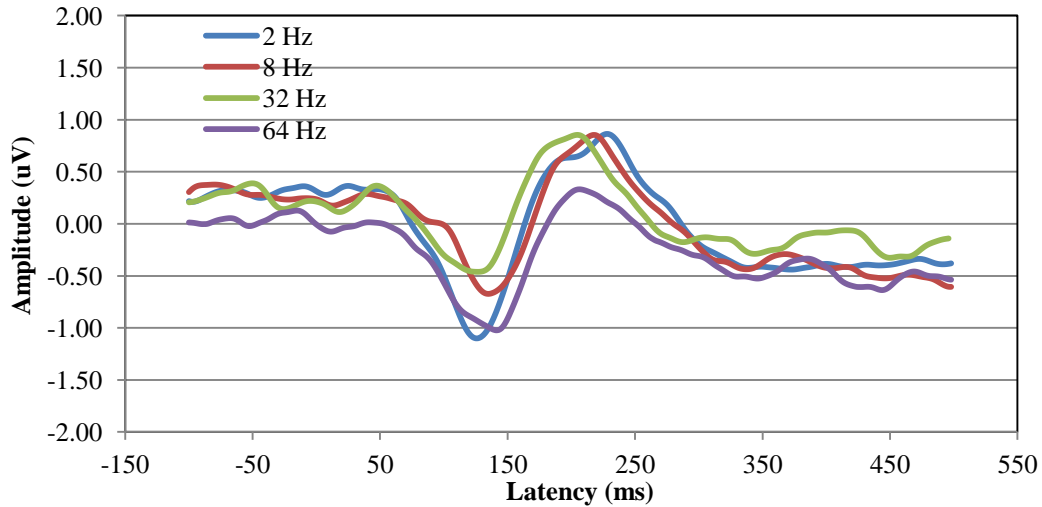
Figure 4.8 Example of the average cluster waveform – calculated for the midline cluster for all temporal modulation frequencies at 0.5 cyc/oct spectral modulation frequency.

In order to evaluate the influence of SM and TM processing on electrophysiological indices, N1 power, P2 power, N1 latency and P2 latency from the GFP responses and the N1-P2 amplitude and N1 latency from the average cluster waveforms were analyzed using a three-factor repeated measures ANOVA with cluster location (frontal, central, parietal) and hemisphere (right, left) as within subject factors and STM stimulus conditions (segmented by SM or TM) as a between subject factor. Table 4.1 and Table 4.2 summarize the F-values and the p-values of each of these factors across SM and TM respectively. To evaluate detailed comparisons of the seven electrode clusters, a two-factor ANOVA with location as a within subject variable and SM or TM frequency as a between subject variable was performed with N1 and P2 power, latency and peak-to-peak amplitude values for each of the clusters across stimulus conditions.

4.2.2 Grand Average Results

The results explained below reflect the analyses performed on the grand average responses, clustered and studied with respect to SM and TM processing.

48

Table 4.1. Results of three factor, repeated measures ANOVA for SM processing

Parameters	SM		Loc		Loc*SM		Hem		Hem*SM		Loc*Hem		Loc*Hem*SM	
N1 Power	$F_{(2,11)} =$ 3.18	$p =$ 0.081	$F_{(1,11)} =$ 52.58	$p <$ **0.001***	$F_{(2,11)} =$ 1.93	$p =$ 0.191	$F_{(1,11)} =$ 24.91	$p <$ **0.001***	$F_{(2,11)} =$ 0.441	$p =$ 0.654	$F_{(1,11)} =$ 0.016	$p =$ 0.903	$F_{(2,11)} =$ 0.504	$p =$ 0.617
N1 Latency	$F_{(2,11)} =$ 4.61	$p =$ **0.035***	$F_{(1,11)} =$ 0.72	$p =$ 0.414	$F_{(2,11)} =$ 0.07	$p =$ 0.934	$F_{(1,11)} =$ 75.21	$p <$ **0.001***	$F_{(2,11)} =$ 5.17	$p =$ **0.026***	$F_{(1,11)} =$ 28.58	$p <$ **0.001***	$F_{(2,11)} =$ 8.21	$p =$ **0.007***
P2 Power	$F_{(2,11)} =$ 2.60	$p =$ 0.119	$F_{(1,11)} =$ 27.98	$p <$ **0.001***	$F_{(2,11)} =$ 2.81	$p =$ 0.103	$F_{(1,11)} =$ 3.29	$p =$ 0.097	$F_{(2,11)} =$ 0.433	$p =$ 0.659	$F_{(1,11)} =$ 3.96	$p =$ 0.072	$F_{(2,11)} =$ 2.053	$p =$ 0.175
P2 Latency	$F_{(2,11)} =$ 3.71	$p =$ 0.059	$F_{(1,11)} =$ 0.81	$p =$ 0.386	$F_{(2,11)} =$ 0.92	$p =$ 0.429	$F_{(1,11)} =$ 0.03	$p =$ 0.860	$F_{(2,11)} =$ 3.93	$p =$ 0.051	$F_{(1,11)} =$ 0.01	$p =$ 0.947	$F_{(2,11)} =$ 1.81	$p =$ 0.210
N1-P2 Amp	$F_{(2,11)} =$ 2.85	$p =$ 0.101	$F_{(1,11)} =$ 51.37	$p <$ **0.001***	$F_{(2,11)} =$ 1.72	$p =$ 0.224	$F_{(1,11)} =$ 112.26	$p <$ **0.001***	$F_{(2,11)} =$ 0.07	$p =$ 0.181	$F_{(1,11)} =$ 2.87	$p <$ **0.001***	$F_{(2,11)} =$ 6.153	$p =$ **0.016***

Table 4.2 Comparison of F-value and p-values of different parameters with TM processing

Parameters	TM		Loc		Loc*TM		Hem		Hem*TM		Loc*Hem		Loc*Hem*TM	
N1 Power	$F_{(4,9)} =$ 2.73	$p =$ 0.097	$F_{(1,9)} =$ 68.02	$p <$ **0.001***	$F_{(4,9)} =$ 3.251	$p =$ 0.066	$F_{(1,9)} =$ 45.93	$p <$ **0.001***	$F_{(4,9)} =$ 2.792	$p =$ 0.092	$F_{(1,9)} =$ 0.09	$p =$ 0.769	$F_{(4,9)} =$ 9.18	$p =$ **0.003***
N1 Latency	$F_{(4,9)} =$ 1.02	$p =$ 0.312	$F_{(1,9)} =$ 0.61	$p =$ 0.454	$F_{(4,9)} =$ 0.06	$p =$ 0.992	$F_{(1,9)} =$ 42.16	$p <$ **0.001***	$F_{(4,9)} =$ 1.01	$p =$ 0.452	$F_{(1,9)} =$ 9.97	$p =$ **0.012***	$F_{(4,9)} =$ 0.49	$p =$ 0.746
P2 Power	$F_{(4,9)} =$ 1.05	$p =$ 0.433	$F_{(1,9)} =$ 20.73	$p =$ **0.001***	$F_{(4,9)} =$ 0.71	$p =$ 0.607	$F_{(1,9)} =$ 6.72	$p =$ **0.029***	$F_{(4,9)} =$ 4.37	$p =$ **0.031***	$F_{(1,9)} =$ 2.94	$p =$ 0.121	$F_{(4,9)} =$ 0.28	$p =$ 0.886
P2 Latency	$F_{(4,9)} =$ 1.04	$p =$ 0.440	$F_{(1,9)} =$ 1.86	$p =$ 0.206	$F_{(4,9)} =$ 1.01	$p =$ 0.409	$F_{(1,9)} =$ 0.16	$p =$ 0.700	$F_{(4,9)} =$ 0.28	$p =$ 0.884	$F_{(1,9)} =$ 0.03	$p =$ 0.864	$F_{(4,9)} =$ 0.26	$p =$ 0.899
N1-P2 Amp	$F_{(4,9)} =$ 1.91	$p =$ 0.194	$F_{(1,9)} =$ 59.63	$p <$ **0.001***	$F_{(4,9)} =$ 1.62	$p =$ 0.251	$F_{(1,9)} =$ 101.56	$p <$ **0.001***	$F_{(4,9)} =$ 0.92	$p =$ 0.495	$F_{(1,9)} =$ 39.77	$p <$ **0.001***	$F_{(4,9)} =$ 1.03	$p =$ 0.443

4.2.2.1 N1 Power with Spectral Modulation Frequency

The results of the three-factor ANOVA for N1 power and SM (location X hemisphere X SM) revealed a significant main effect of cluster location ($F_{(1,11)} = 52.58$, $p < 0.001$) and hemisphere ($F_{(1,11)} = 24.91$, $p < 0.001$) on N1 power. Pairwise comparisons show that the N1 was more robust in the parietal region than in the frontal and central ($p_{f-p} < 0.001$, $p_{c-p} < 0.001$) regions and more robust in the right hemisphere than in the left ($F_{(1,11)} = 24.91$, $p < 0.001$). This effect is shown in panels (a) and (b) of Figure 4.9. When location and hemisphere are considered together, panel (c) shows that there was a significant increase in N1 power from frontal to parietal regions consistent on both left ($p_{fl-pl} = 0.005$, $p_{cl-pl} < 0.001$) and right ($p_{fr-pr} = 0.040$, $p_{cr-pr} = 0.005$) hemispheres and hence there was no significant interaction of location and hemisphere. Pairwise comparisons of N1 power for each electrode cluster across location and hemisphere, show that N1 power was significantly greater in the right than in the left hemisphere in the central and parietal regions ($p_{cl-cr} < 0.001$, $p_{pl-pr} = 0.002$) but not in the frontal region. There also was a significant difference between N1 power at midline versus central left and right ($p_{cl-m} < 0.001$, $p_{cr-m} = 0.037$) and between midline and parietal left and right ($p_{pl-m} = 0.001$, $p_{pr-m} < 0.001$).

Figure 4.9 panel (d) shows the effect of SM frequency on N1 power. Although there was a trend for an increase in N1 power with the addition of low spectral modulation frequencies (e.g., 0.5 cyc/oct) and a decrease in N1 power with higher modulation frequencies (e.g., 2 cyc/oct), this effect was not statistically significant. Panels (e) and (f) show the change in N1 power with hemisphere and SM and with location and SM. As shown in Table 4.1, there was no significant interaction of hemisphere or location on N1 power with SM. The observed variation in N1 power with SM frequency is similar in both hemispheres and all three regions.

Figure 4.9 Main effects of location, hemisphere and SM and their interactions on N1 power. (a) Main Effect of Location; (b) Main Effect of Hemisphere; (c) Effect of Location x Hemisphere; (d) Main Effect of SM; (e) Effect of SM x Hemisphere; (f) Effect of Location x SM; *$p < 0.05$.

4.2.2.2 N1 Power with Temporal Modulation Frequency

The results of the three-factor ANOVA for N1 power and TM (location X hemisphere X TM) revealed a significant main effect of cluster location ($F_{(1,9)} = 68.02$, $p < 0.001$) and hemisphere ($F_{(1,9)} = 45.93$, $p < 0.001$) on N1 power for TM conditions. Similar to changes observed for SM, pairwise comparisons show that the N1 was more robust in the parietal region than in the frontal and central ($p_{f-p} < 0.001$, $p_{c-p} < 0.001$) regions and more robust in the right hemisphere than in the left ($F_{(1,9)} = 45.93$, $p < 0.001$). This effect is shown in panels (a) and (b) of Figure 4.10. When location and hemisphere are considered together, panel (c) shows that there was a significant increase in N1 power from frontal to parietal regions consistent on both left ($p_{fl-pl} = 0.002$, $p_{cl-pl} < 0.001$) and right ($p_{fr-pr} = 0.001$, $p_{cr-pr} = 0.004$) hemispheres and hence there was no significant interaction of location and hemisphere. Pairwise comparisons of N1 power for each electrode cluster across location and hemisphere, show that N1 power was significantly larger in the right than in the left hemisphere in the central and parietal regions ($p_{fl-fr} = 0.005$, $p_{cl-cr} < 0.001$, $p_{pl-pr} = 0.006$) but not in the frontal region. There also was a significant difference between N1 power at midline versus frontal left and right regions ($p_{fl-m} = 0.026$, $p_{fr-m} = 0.024$), midline versus central left and right ($p_{cl-m} < 0.001$, $p_{cr-m} = 0.017$) and between midline and parietal left and right ($p_{pl-m} = 0.003$, $p_{pr-m} < 0.001$). Figure 4.10 panel (d) shows the effect of TM frequency on N1 power that was not statistically significant. Panels (e) and (f) show the change in N1 power with hemisphere and TM and with location and TM. As shown in Table 4.2, there was no significant interaction of hemisphere or location on N1 power with TM. There was, however, a significant three-way interaction (Loc x Hem x TM) for N1 power and TM processing ($F_{(4,9)} = 9.18$, $p = 0.003$), due to the fact that N1 was equivalent or larger in frontal versus central for some but not all TM conditions.
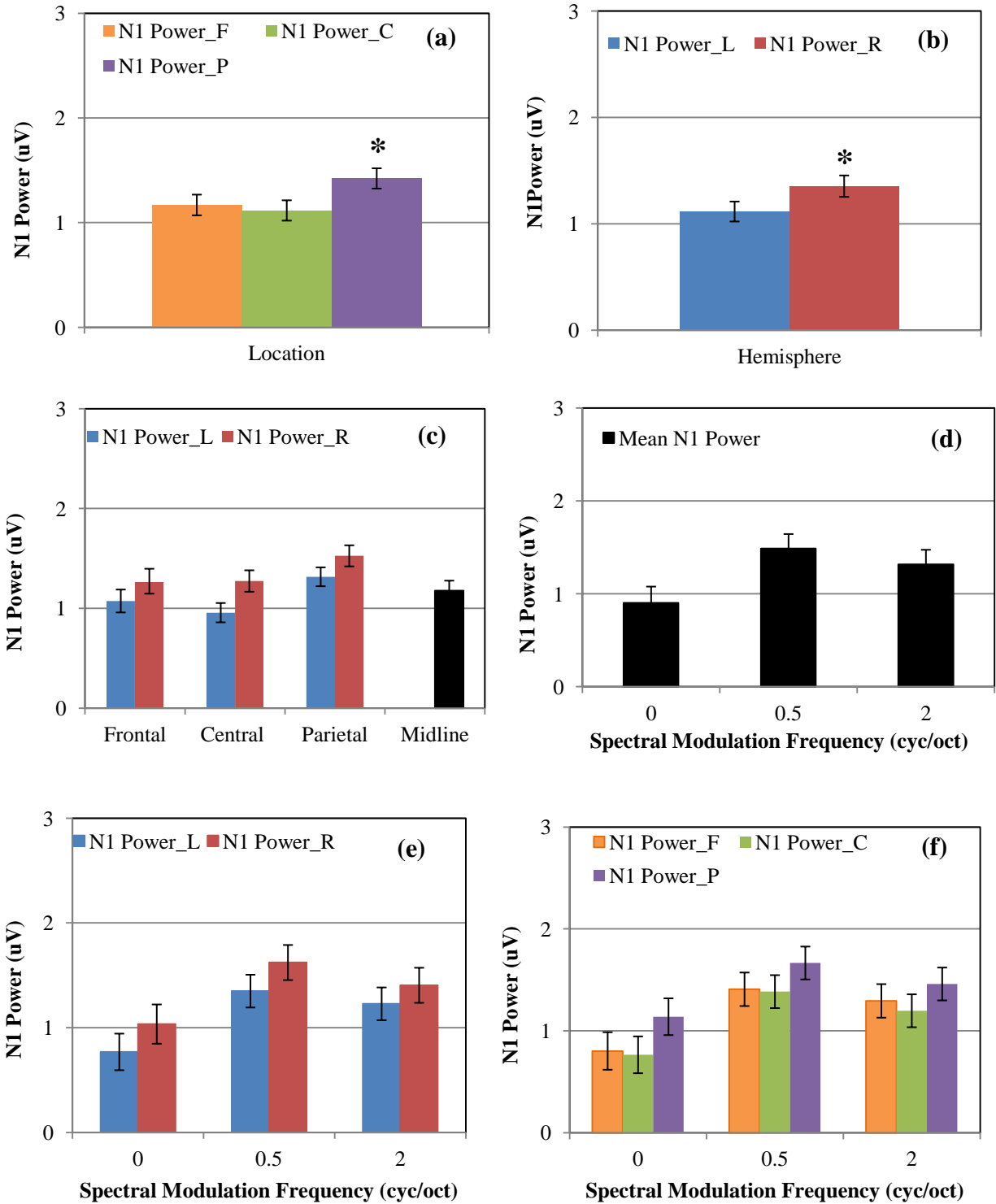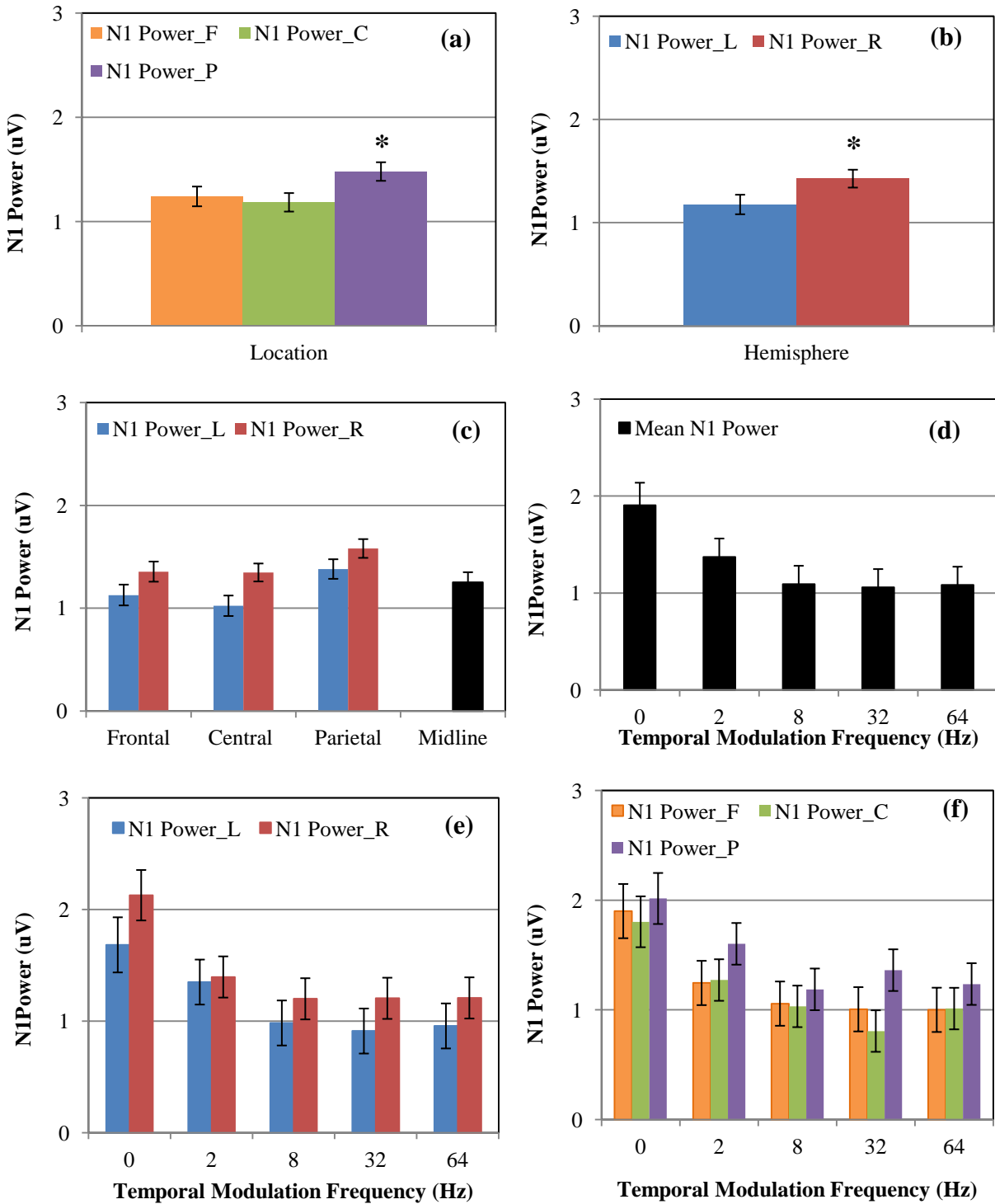
Figure 4.10 Main effects of location, hemisphere and TM and their interactions on N1 power. (a) Main Effect of Location; (b) Main Effect of Hemisphere; (c) Effect of Location x Hemisphere; (d) Main Effect of TM; (e) Effect of TM x Hemisphere; (f) Effect of Location x TM; *$p < 0.05$

4.2.2.3 N1 Latency with Spectral Modulation Frequency

The results of the three-factor ANOVA for N1 latency and SM (location X hemisphere X SM) revealed no significant main effect of cluster location but a significant main effect of hemisphere on N1 latency. Pairwise comparisons show that the N1 latency was shorter in the right hemisphere than in the left ($F_{(1,11)} = 75.21$, $p < 0.001$). This effect is shown in panels (a) and (b) of Figure 4.11. When location and hemisphere are considered together, panel (c) shows that there was a significant decrease in N1 latency from frontal to parietal regions in the right hemisphere ($p_{fr-cr} = 0.019$, $p_{fr-pr} = 0.005$) but a significant increase in N1 latency in the left hemisphere ($p_{fl-pl} = 0.002$) and hence there is a significant interaction of location and hemisphere ($F_{(2,11)} = 5.17$, $p = 0.026$). Pairwise comparisons of N1 latency for each electrode cluster across location and hemisphere, show that N1 latency was significantly shorter in the right than in the left hemisphere in the central and parietal regions ($p_{cl-cr} < 0.001$, $p_{pl-pr} < 0.001$) but not in the frontal region. There also was a significant difference between N1 latency at the midline versus frontal left ($p_{fl-m} = 0.018$), central left ($p_{cl-m} = 0.003$), parietal left and right ($p_{pl-m} = 0.002$, $p_{pr-m} = 0.007$) regions but not between the midline versus frontal right and central right regions. Figure 4.11 panel (d) shows the significant main effect of SM frequency on N1 latency ($F_{(2,11)} = 4.61$, $p < 0.035$). Pairwise comparisons reveal that N1 latency at 0.5 cyc/oct and 2 cyc/oct was significantly different from 0 cyc/oct (considering pure temporal modulation) ($p_{0-0.5} = 0.047$, $p_{0-2} = 0.015$) but was not significantly different from one another. Panels (e) and (f) show the change in N1 latency with hemisphere and SM and with location and SM. As shown in Table 4.1, there was no significant interaction of hemisphere or location on N1 latency with SM. There was, however, a significant three-way interaction (Loc x Hem x SM) for N1 latency and SM processing ($F_{(2,11)} = 8.21$, $p = 0.007$).

Figure 4.11 Main effects of location, hemisphere and SM and their interactions on N1 latency. (a) Main Effect of Location; (b) Main Effect of Hemisphere; (c) Effect of Location x Hemisphere; (d) Main Effect of SM; (e) Effect of SM x Hemisphere; (f) Effect of Location x SM; *$p < 0.05$

4.2.2.4 N1 Latency with Temporal Modulation Frequency

The results of the three-factor ANOVA for N1 latency and TM (location X hemisphere X TM) revealed no significant main effect of cluster location but a significant main effect of hemisphere on N1 latency. Pairwise comparisons show that the N1 latency was shorter in the right hemisphere than in the left ($F_{(1,9)} = 42.16$, $p < 0.001$). This effect is shown in panels (a) and (b) of Figure 4.12. When location and hemisphere are considered together, panel (c) shows that there was a significant decrease in N1 latency from frontal to parietal regions in the right ($p_{fr-cr} = 0.025$, $p_{fr-pr} = 0.025$) and a significant increase in N1 latency from frontal to parietal regions in the left hemisphere ($p_{fl-pl} = 0.040$) hence there is a significant interaction of location and hemisphere ($F_{(1,9)} = 2.94$, $p = 0.012$). Pairwise comparisons of N1 latency for each electrode cluster across location and hemisphere, show that N1 latency was significantly shorter in the right than in the left hemisphere in the central and parietal regions ($p_{cl-cr} < 0.001$, $p_{pl-pr} = 0.003$) but not in the frontal region. There also was a significant difference between N1 latency at the midline versus frontal left ($p_{fl-m} = 0.025$), central left ($p_{cl-m} = 0.010$), and parietal left and right ($p_{pl-m} = 0.016$; $p_{pr-m} = 0.022$) regions.

Figure 4.12 panel (d) shows the change in N1 latency with TM. Although there was a trend for an increase in N1 latency with increasing temporal modulation frequency, except at 32 Hz where there is a decrease, this effect was not statistically significant. Panels (e) and (f) show the change in N1 latency with hemisphere and TM and with location and TM. As shown in Table 4.2, there is no significant interaction of hemisphere or location on N1 latency with TM. The observed variation in N1 latency with TM frequency is similar in both hemispheres and all three regions.
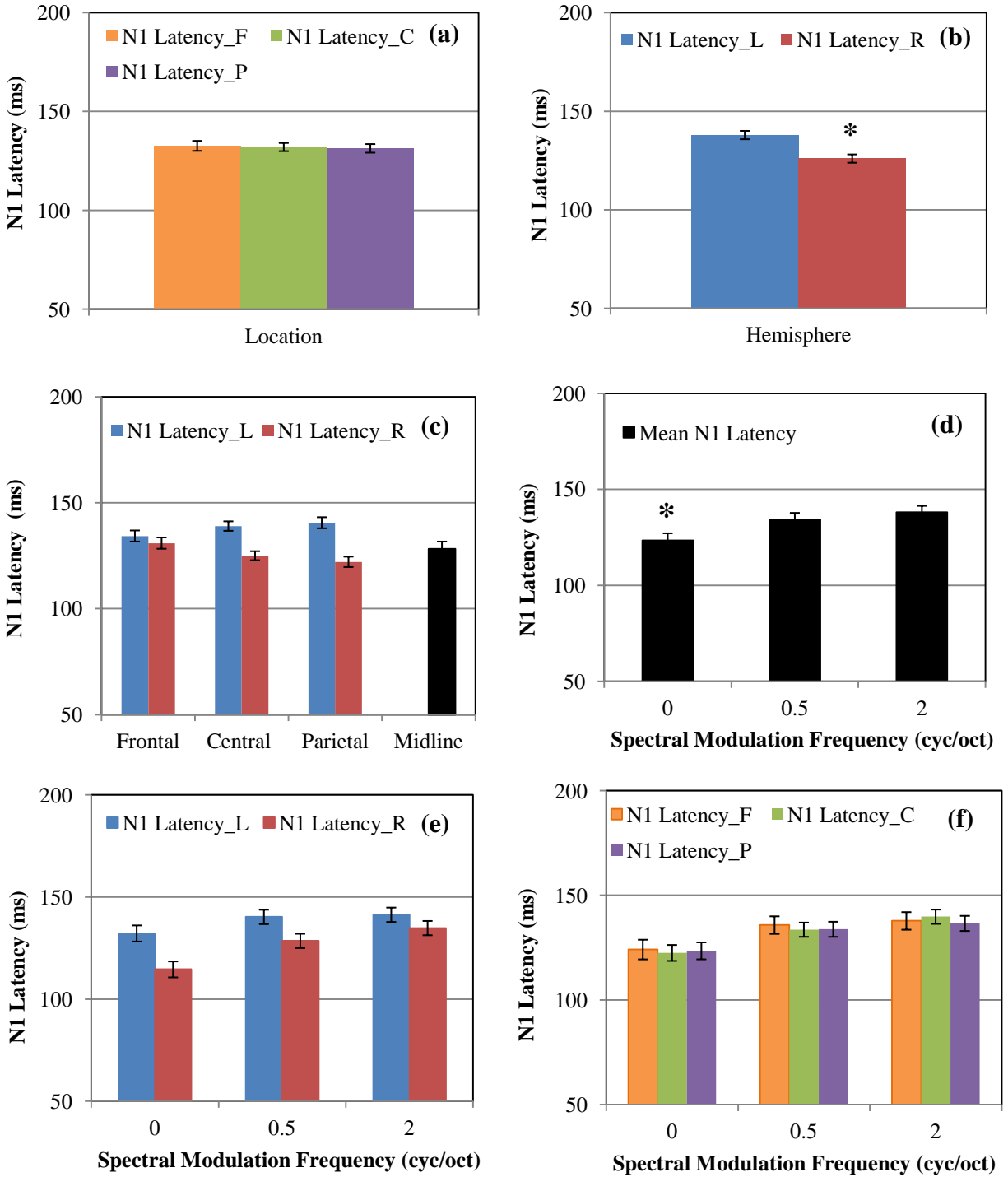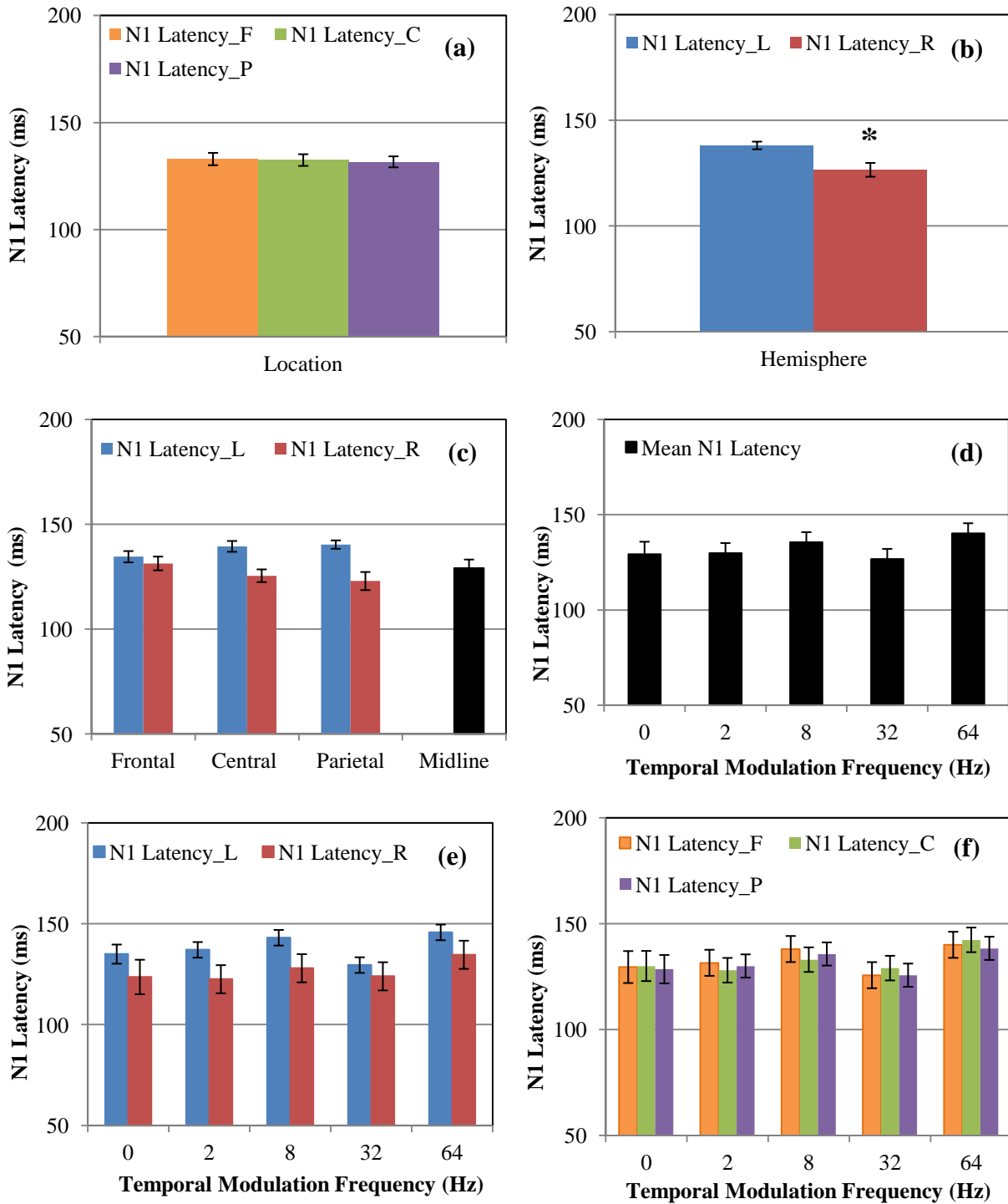
Figure 4.12 Main effects of location, hemisphere and TM and their interactions on N1 latency. (a) Main Effect of Location; (b) Main Effect of Hemisphere; (c) Effect of Location x Hemisphere; (d) Main Effect of TM; (e) Effect of TM x Hemisphere; (f) Effect of Location x TM; *$p < 0.05$

4.2.2.5 P2 Power with Spectral Modulation Frequency

The results of the three-factor ANOVA for P2 power and SM (location X hemisphere X SM) revealed a significant main effect of cluster location ($F_{(1,11)}$ = 27.98, $p < 0.001$) but no significant main effect of hemisphere on P2 power. Pairwise comparisons showed that P2 was more robust in the frontal region than in the central and parietal ($p_{\text{f-p}} < 0.001$, $p_{\text{c-p}} = 0.023$) regions. These effects are shown in panels (a) and (b) of Figure 4.13. When location and hemisphere are considered together, panel (c) shows that there was a significant decrease in P2 power from frontal to parietal regions consistent on both left ($p_{\text{fl-pl}} = 0.033$) and right ($p_{\text{fr-pr}} = 0.001$, $p_{\text{cr-pr}} = 0.001$) hemispheres and hence there was no significant interaction of location and hemisphere. Pairwise comparisons of P2 power for each electrode cluster across location and hemisphere showed that P2 power was not significantly different between left and right hemispheres in the frontal, central and parietal regions. There was a significant difference in P2 power between midline and central left and right ($p_{\text{cl-m}} < 0.000$, $p_{\text{cr-m}} = 0.013$), between midline and parietal left and right ($p_{\text{pl-m}} < 0.001$; $p_{\text{pr-m}} = 0.001$) and midline and frontal left ($p_{\text{fl-m}} < 0.001$) but not frontal right. Figure 4.13 panel (d) shows the effect of SM frequency on P2 power. Although there was a trend for an increase in P2 power for low spectral modulation frequencies (e.g., 0.5 cyc/oct) and decrease in P2 power for higher modulation frequencies (e.g., 2.0 cyc/oct), this effect was not statistically significant. Panels (e) and (f) show the change in P2 power with hemisphere and SM and with location and SM. As shown in Table 4.1, there was no significant interaction of hemisphere or location on P2 power with SM. The observed variation in P2 power with SM frequency was similar in both hemispheres and all three regions.

Figure 4.13 Main effects of location, hemisphere and SM and their interactions on P2 power. (a) Main Effect of Location; (b) Main Effect of Hemisphere; (c) Effect of Location x Hemisphere; (d) Main Effect of SM; (e) Effect of SM x Hemisphere; (f) Effect of Location x SM; *p <0.05

4.2.2.6 P2 Power with Temporal Modulation Frequency

The results of the three-factor ANOVA for P2 power and TM (location X hemisphere X TM) revealed a significant main effect of cluster location ($F_{(1,9)}$ = 20.73, p < 0.001) and hemisphere ($F_{(1,9)}$ = 6.72, p = 0.029) on P2 power. Pairwise comparisons show that the P2 was more robust in the frontal region than in the central and parietal (p_{f-p} = 0.001, p_{c-p} = 0.020) regions and more robust in the right hemisphere than in the left. This effect is shown in panels (a) and (b) of Figure 4.14. When location and hemisphere are considered together, panel (c) shows that there was a significant decrease in P2 power from frontal to parietal regions consistent in both left (p_{fl-pl} = 0.048) and right (p_{fr-pr} = 0.007, p_{cr-pr} = 0.013) hemispheres and hence there was no significant interaction of location and hemisphere. Pairwise comparisons of P2 power for each electrode cluster across location and hemisphere showed that there was no significant difference in P2 power between the right and left hemispheres in the frontal, central and parietal regions. There was a significant difference between P2 power at midline versus frontal left but not frontal right regions (p_{fl-m} = 0.001), at midline versus central left and right (p_{cl-m} < 0.001, p_{cr-m} = 0.017) and between midline and parietal left and right (p_{pl-m} = 0.001, p_{pr-m} = 0.001). Figure 4.14 panel (d) shows the effect of TM frequency on P2 power. Although there was a trend for an initial increase in P2 power at 2 Hz and subsequent decrease with increasing TM frequency, this effect was not statistically significant. Panels (e) and (f) show the change in P2 power with hemisphere and TM and with location and TM. In panel (e), we observe an increase in P2 power at 2 Hz, a decrease in P2 power with increasing TM frequency up to 32 Hz, and an increase at 64 Hz in the right hemisphere but decrease in P2 power at 64 Hz in the left hemisphere. As a result, there is a significant interaction of hemisphere and TM ($F_{(4,9)}$ = 4.37, p = 0.031). However, there is no significant interaction of location and TM from Table 4.2.
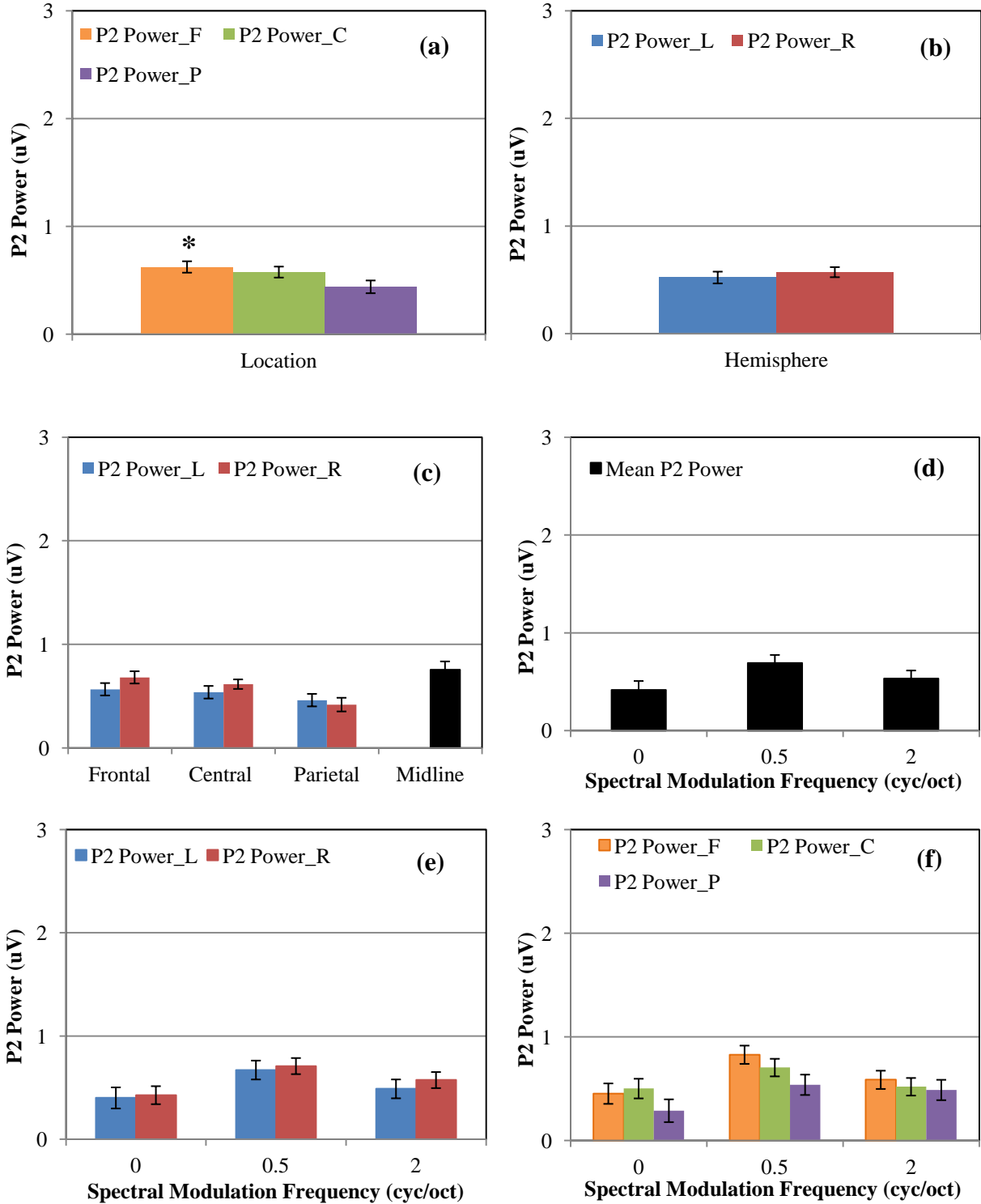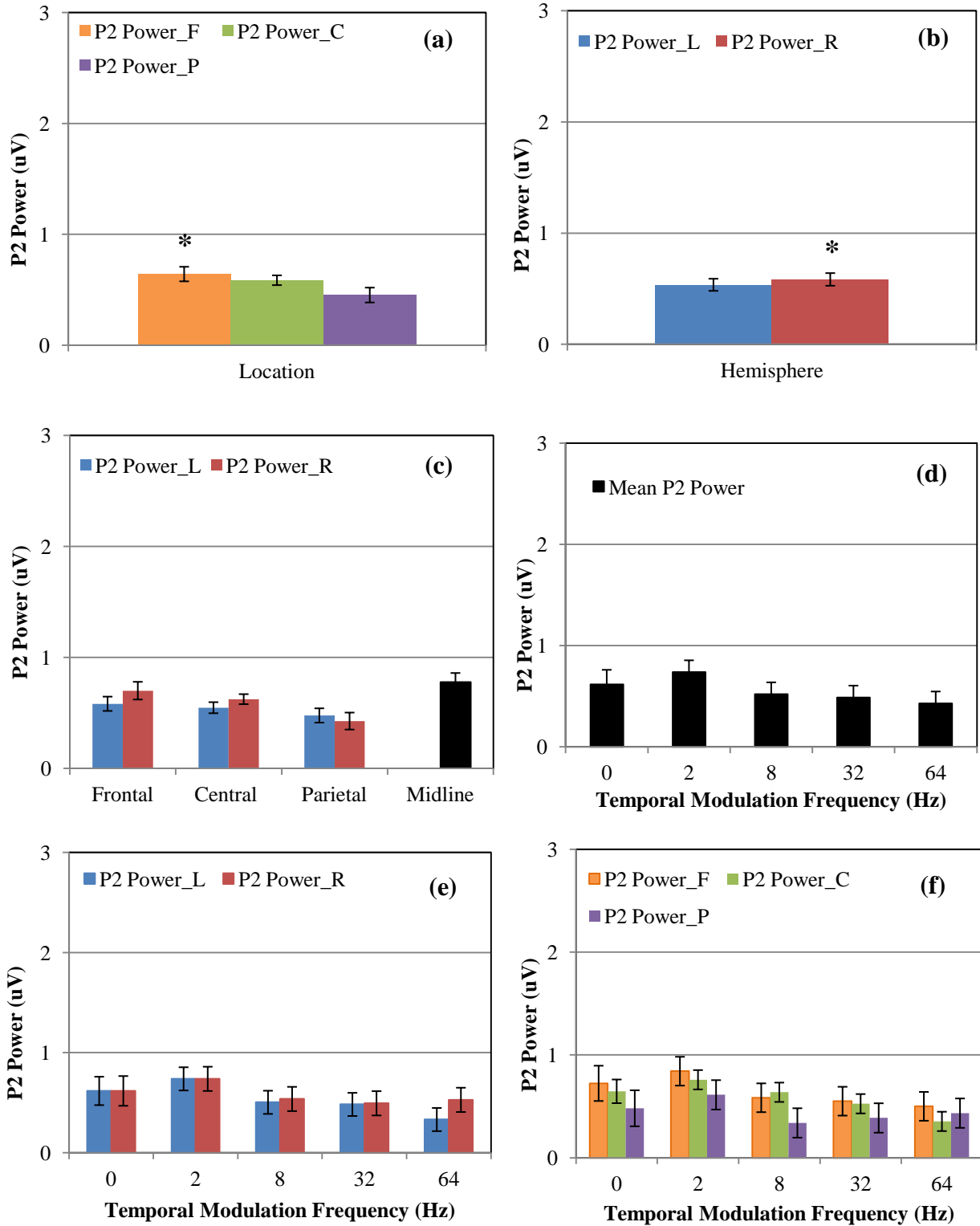
Figure 4.14 Main effects of location, hemisphere and TM and their interactions on P2 power. (a) Main Effect of Location; (b) Main Effect of Hemisphere; (c) Effect of Location x Hemisphere; (d) Main Effect of TM; (e) Effect of TM x Hemisphere; (f) Effect of Location x TM; *$p < 0.05$

4.2.2.7 P2 Latency with Spectral Modulation Frequency

The results of the three-factor ANOVA for P2 latency and SM (location X hemisphere X SM) revealed no significant main effect of cluster location or hemisphere on P2 latency. This result is shown in panels (a) and (b) of Figure 4.15. When location and hemisphere are considered together, panel (c) shows that there was no significant change in P2 latency across location in the right hemisphere, but there was a significant change in the left hemisphere between frontal and central left ($p_{\text{fl-cl}} = 0.030$) and between central and parietal left regions ($p_{\text{cl-pl}} = 0.026$). But this effect was not significant to cause an overall interaction between hemisphere and location. Pairwise comparisons of P2 latency for each electrode cluster across location and hemisphere show that there was a significant difference between P2 latency at the midline versus frontal left and right ($p_{\text{fl-m}} = 0.006$, $p_{\text{fl-m}} = 0.008$) and parietal left and right ($p_{\text{pl-m}} = 0.002$; $p_{\text{pr-m}} = 0.006$) regions but not between the midline versus central left and right regions.

Figure 4.15 panel (d) shows the effect of SM frequency on P2 latency. Although there was a small increase in P2 latency with increasing spectral modulation frequency, this change was not statistically significant. Panels (e) and (f) show the change in P2 latency with hemisphere and SM and with location and SM. As shown in Table 4.1, there is no significant interaction of hemisphere or location on P2 latency with SM. The observed variation in P2 latency with SM frequency is similar in both hemispheres and all three regions.

Figure 4.15 Main effects of location, hemisphere and SM and their interactions on P2 latency. (a) Main Effect of Location; (b) Main Effect of Hemisphere; (c) Effect of Location x Hemisphere; (d) Main Effect of SM; (e) Effect of SM x Hemisphere; (f) Effect of Location x SM; *$p < 0.05$

4.2.2.8 P2 Latency with Temporal Modulation Frequency

The results of the three-factor ANOVA for P2 latency and temporal TM (location X hemisphere X TM) revealed no significant main effect of cluster location or hemisphere on P2 latency. This effect is shown in panels (a) and (b) of Figure 4.16. When location and hemisphere are considered together, panel (c) shows that there was a decrease in P2 latency from frontal to central regions and a significant increase in P2 latency from central to parietal regions consistent in both the right ($p_{cr-pr} = 0.008$) and left ($p_{cl-pl} = 0.021$) hemispheres, hence there is no significant interaction of location and hemisphere. Pairwise comparisons of P2 latency for each electrode cluster across location and hemisphere show that there was no significant difference in P2 latency between the right and left hemispheres in the frontal, central and parietal regions. There was, however, a significant difference between P2 latency at the midline versus frontal left and right ($p_{fl-m} = 0.021$, $p_{fl-m} = 0.006$) and parietal left and right ($p_{pl-m} = 0.003$; $p_{pr-m} = 0.009$) regions but not between the midline and central left and right regions.

Figure 4.16 panel (d) shows the effect of TM frequency on P2 latency. Although there was a slight decrease in P2 latency with increasing temporal modulation frequency up to 8 Hz and an increase in P2 latency from 8 to 64 Hz, this effect was not statistically significant. Panels (e) and (f) show the change in P2 latency with hemisphere and TM and with location and TM. As shown in Table 4.2, there is no significant interaction of hemisphere or location on P2 latency with TM. The observed variation in P2 latency with TM frequency is similar in both hemispheres and all three regions.
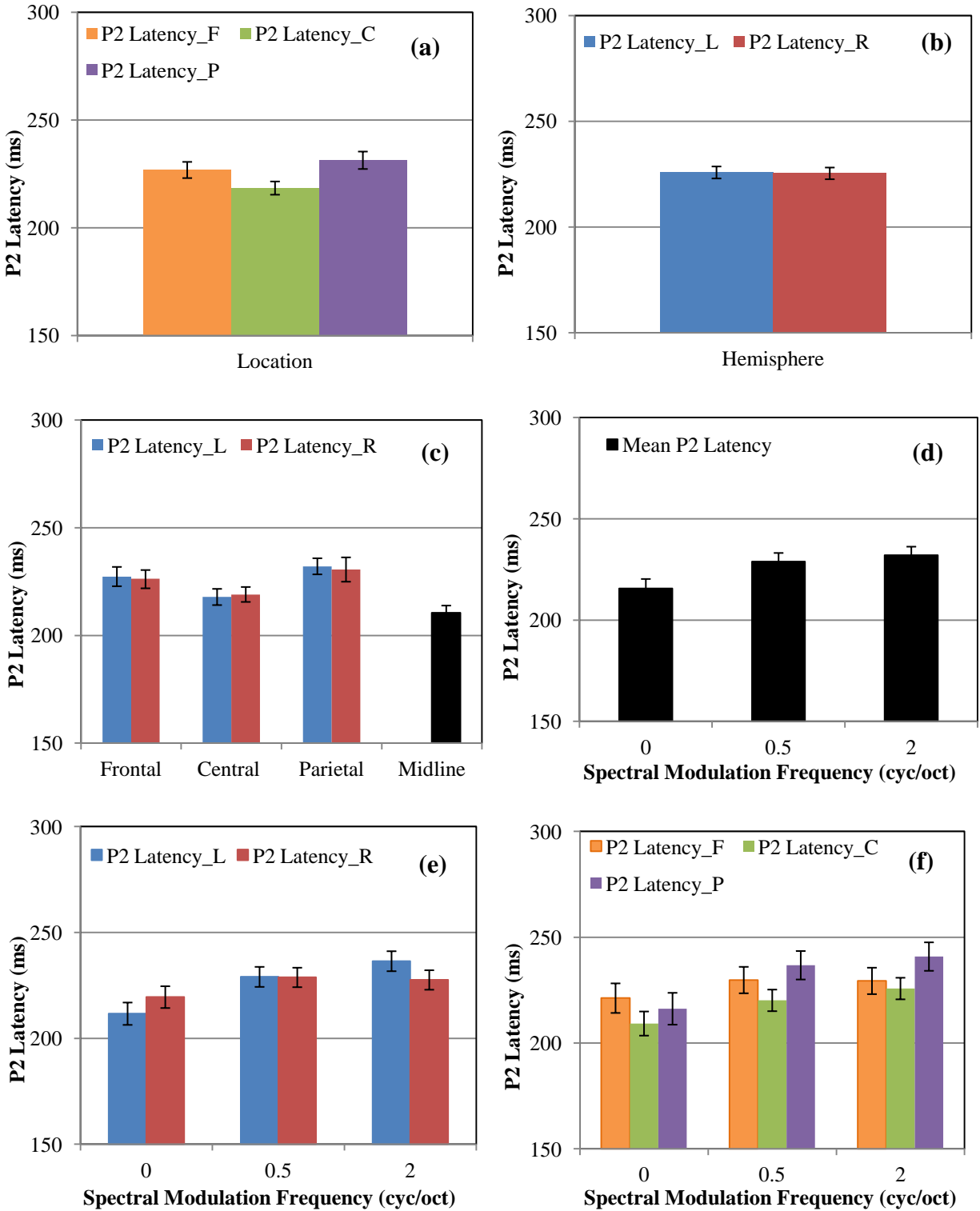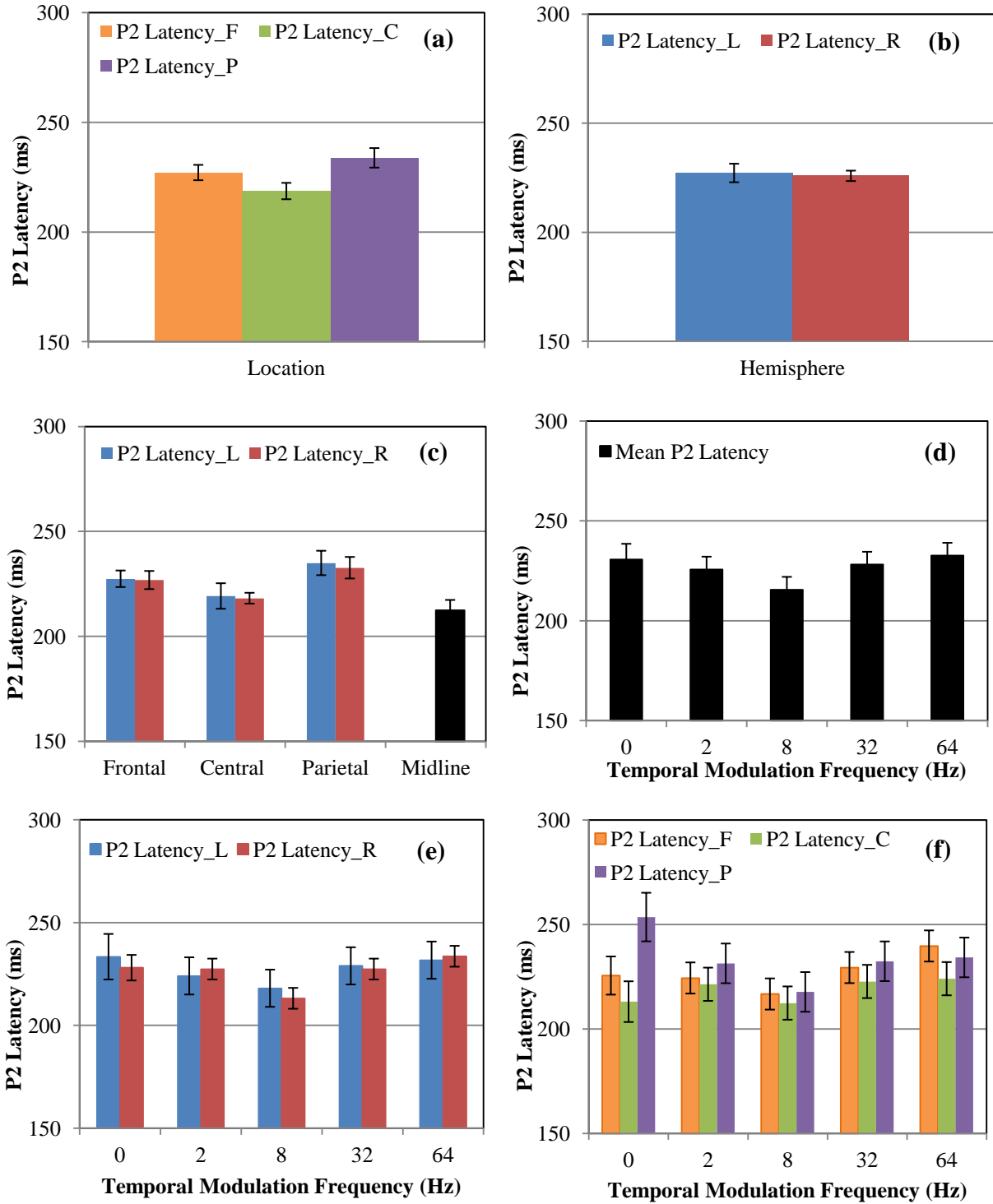
Figure 4.16 Main effects of location, hemisphere and TM and their interactions on P2 latency. (a) Main Effect of Location; (b) Main Effect of Hemisphere; (c) Effect of Location x Hemisphere; (d) Main Effect of TM; (e) Effect of TM x Hemisphere; (f) Effect of Location x TM; *p <0.05

4.2.2.9 N1-P2 Amplitude with Spectral Modulation Frequency

The results of the three-factor ANOVA for N1-P2 amplitude and SM (location X hemisphere X SM) revealed a significant main effect of cluster location ($F_{(1,11)} = 51.37$, $p < 0.001$) and hemisphere ($F_{(1,11)} = 112.26$, $p < 0.001$) on N1-P2 amplitude. Pairwise comparisons showed that the N1-P2 amplitude was more robust in the parietal region than in the frontal and central ($p_{f-p} < 0.001$, $p_{c-p} < 0.001$) regions and more robust in the right hemisphere than in the left. This effect is shown in panels (a) and (b) of Figure 4.17. When location and hemisphere are considered together, panel (c) shows that there was a significant decrease in N1-P2 amplitude from frontal to central region ($p_{fr-cr} = 0.001$, $p_{fr-pr} < 0.001$) but not from central to parietal regions in the right hemisphere, and a significant increase in N1-P2 amplitude from frontal to parietal region in the left hemisphere ($p_{fl-cl} = 0.011$, $p_{fl-pl} < 0.001$, $p_{cl-pl} < 0.001$). Hence, there was a significant interaction of location and hemisphere ($F_{(1,11)} = 2.87$, $p < 0.001$). Pairwise comparisons of N1-P2 amplitude for each electrode cluster across location and hemisphere showed that N1-P2 amplitude was significantly larger in the right than in the left hemisphere in the frontal and central regions ($p_{fl-fr} < 0.001$, $p_{cl-cr} < 0.001$) but not in the parietal region. There also was a significant difference between N1-P2 amplitude at midline versus frontal left and right ($p_{fl-m} = 0.001$, $p_{fr-m} < 0.001$), central left and right ($p_{cl-m} = 0.001$; $p_{cr-m} < 0.001$) and parietal left and right regions ($p_{pl-m} = 0.006$; $p_{pr-m} = 0.019$). Figure 4.17 panel (d) shows the effect of SM frequency on N1-P2 amplitude but this was not significant. Panels (e) and (f) show the change in N1-P2 amplitude with hemisphere and SM and with location and SM. As shown in Table 4.1, there was no significant interaction of hemisphere and location on N1-P2 amplitude with SM. There was, however, a significant three-way interaction (Loc x Hem x SM) of N1-P2 amplitude and SM processing ($F_{(2,11)} = 6.153$, $p = 0.016$).

Figure 4.17 Main effects of location, hemisphere and SM and their interactions on N1-P2 amplitude. (a) Main Effect of Location; (b) Main Effect of Hemisphere; (c) Effect of Location x Hemisphere; (d) Main Effect of SM; (e) Effect of SM x Hemisphere; (f) Effect of Location x SM; *p <0.05

4.2.2.10 N1-P2 Amplitude with Temporal Modulation Frequency

The results of the three-factor ANOVA for N1-P2 amplitude and TM (location X hemisphere X TM) revealed a significant main effect of cluster location ($F_{(1,9)}$ = 59.63, $p <$ 0.001) and hemisphere ($F_{(1,9)}$ = 101.56, $p <$ 0.001) on N1-P2 amplitude. Pairwise comparisons show that the N1-P2 amplitude is more robust in the parietal region than in the frontal and central ($p_{f-p} <$ 0.001, $p_{c-p} <$ 0.001) regions and more robust in the right hemisphere than in the left. This effect is shown in panels (a) and (b) of Figure 4.18. When location and hemisphere are considered together, panel (c) shows that there was a significant decrease in N1-P2 amplitude from frontal to central region (p_{fr-cr} = 0.001, p_{fr-pr} = 0.004) but not from central to parietal regions in the right hemisphere and a significant increase in N1-P2 amplitude from frontal to parietal region in the left hemisphere (p_{fl-cl} = 0.008, $p_{fl-pl} <$ 0.001, $p_{cl-pl} <$ 0.001). Hence there was a significant interaction of location and hemisphere ($F_{(1,9)}$ = 39.77, $p <$ 0.001). Pairwise comparisons of N1-P2 amplitude for each electrode cluster across location and hemisphere, show that N1-P2 amplitude was significantly larger in the right than in the left hemisphere in the frontal and central regions ($p_{fl-fr} <$ 0.001, $p_{cl-cr} <$ 0.001) but not in the parietal region. There also was a significant difference between N1-P2 amplitude at midline versus frontal left and right (p_{fl-m} = 0.001, $p_{fr-m} <$ 0.001), central left and right (p_{cl-m} = 0.002; $p_{cr-m} <$ 0.001) and parietal left and right regions (p_{pl-m} = 0.005; p_{pr-m} = 0.018). Figure 4.18 panel (d) shows the effect of TM frequency on N1-P2 amplitude that was not significant. Panels (e) and (f) show the change in N1-P2 amplitude with hemisphere and TM and with location and TM. As shown in Table 4.2, there was no significant interaction of hemisphere or location on N1-P2 amplitude with TM.
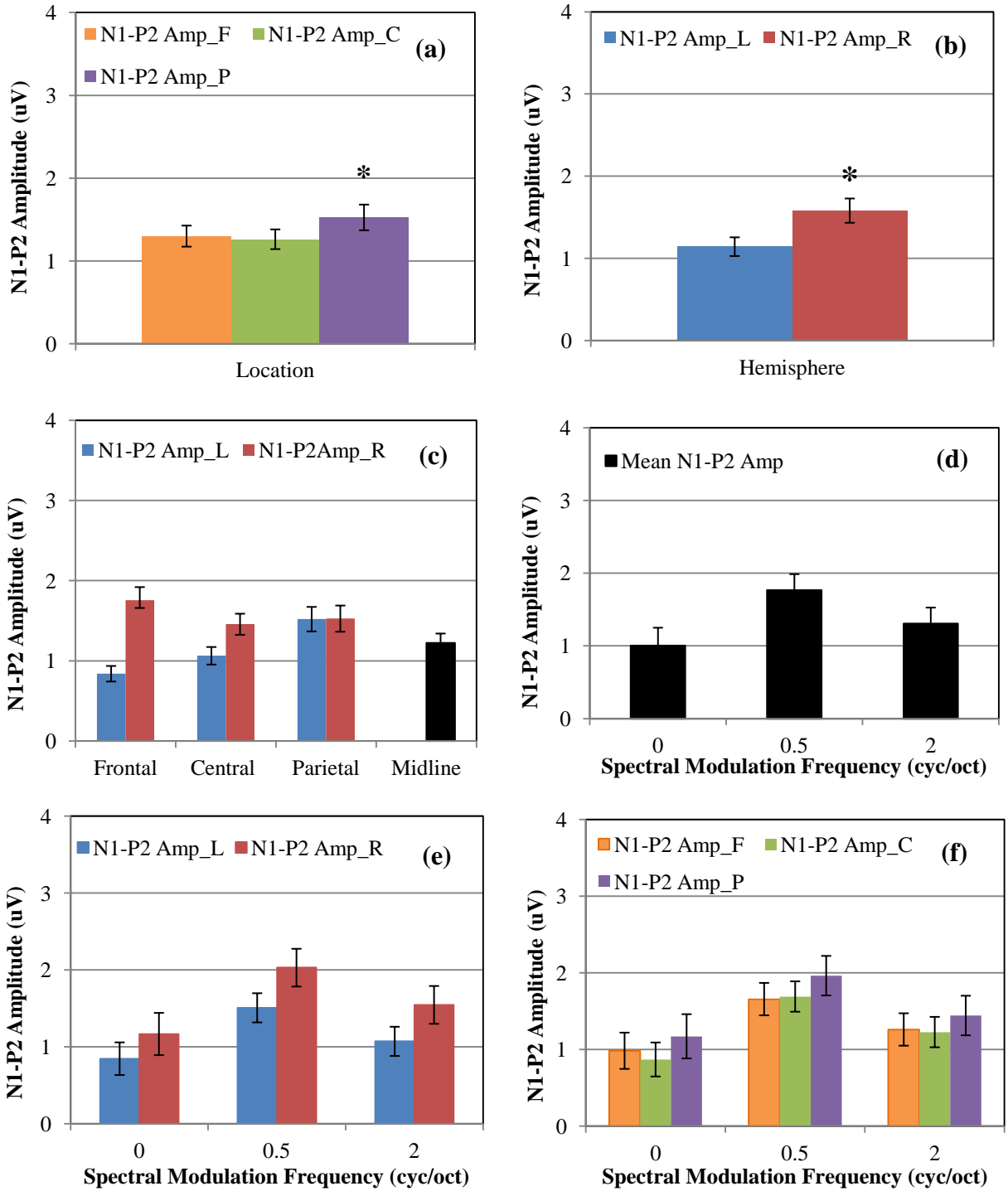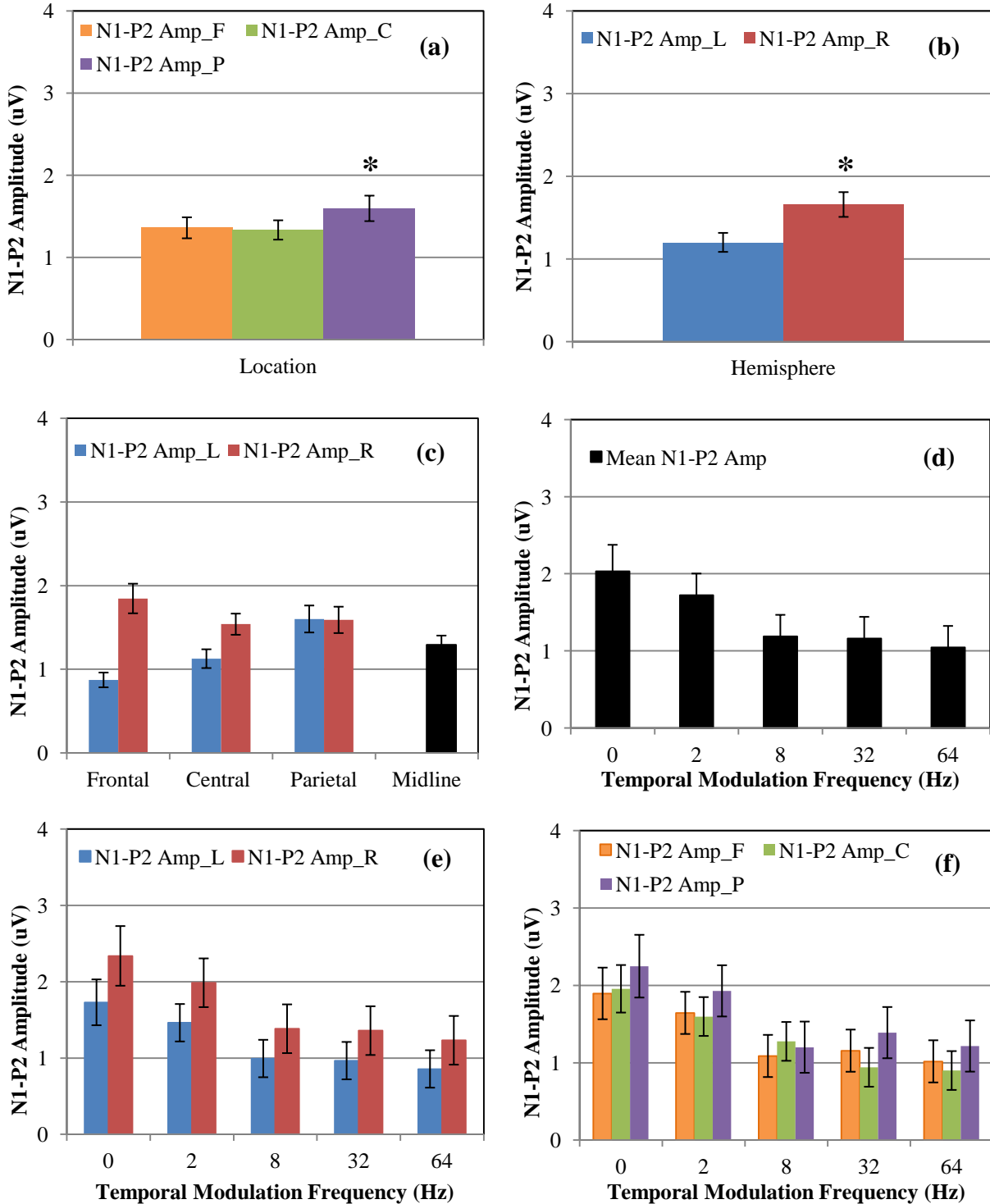
Figure 4.18 Main effects of location, hemisphere and TM and their interactions on N1-P2 amplitude. (a) Main Effect of Location; (b) Main Effect of Hemisphere; (c) Effect of Location x Hemisphere; (d) Main Effect of TM; (e) Effect of TM x Hemisphere; (f) Effect of Location x TM *$p < 0.05$

4.2.3 Individual Data Results

As mentioned earlier in this chapter, the N1-P2 amplitude and the N1 latency were computed from the average cluster waveforms of the individual data. The results of the spectral, temporal and spectro-temporal modulations were analyzed separately. A three factor ANOVA was performed with location and hemisphere as within subject variables and SM, TM or STM frequency as between subject variables on both N1-P2 amplitude and N1 latency. The results are summarized below.

4.2.3.1 Spectral Modulation Results

The results of the three-factor ANOVA for N1-P2 amplitude and SM (location X hemisphere X SM) revealed a significant main effect of cluster location ($F_{(1,16)} = 11.93$, $p = 0.003$) and hemisphere ($F_{(1,16)} = 31.39$, $p < 0.001$) on N1-P2 amplitude. Pairwise comparisons show that the N1-P2 amplitude is more robust in the parietal region than in the frontal ($p_{f\text{-}p} = 0.003$) but not significantly different from central region and more robust in the right hemisphere than in the left. This effect is shown in panels (a) and (b) of Figure 4.19. When location and hemisphere are considered together, panel (c) shows that there was a decrease in N1-P2 amplitude from frontal to central region and a slight increase from central to parietal regions in the right hemisphere and a significant increase in N1-P2 amplitude from frontal to parietal region in the left hemisphere ($p_{fl\text{-}pl} = 0.001$, $p_{cl\text{-}pl} < 0.014$). Hence there was a significant interaction of location and hemisphere ($F_{(1,16)} = 6.70$, $p = 0.020$). Pairwise comparisons of N1-P2 amplitude for each electrode cluster across location and hemisphere, show that N1-P2 amplitude was significantly larger in the right than in the left hemisphere in the frontal and central regions ($p_{fl\text{-}fr} = 0.001$, $p_{cl\text{-}cr} = 0.001$) but not in the parietal region. There was no significant difference between

N1-P2 amplitude at midline versus the different clusters. There was no significant main effect of SM, shown in panel (d) or significant interactions of SM with location or hemisphere.

Figure 4.19 Main effects of location, hemisphere and their interactions on N1-P2 amplitude and the main effect of SM. (a) Main Effect of Location; (b) Main Effect of Hemisphere; (c) Effect of Location x Hemisphere; (d) Main Effect of SM; *p <0.05

The results of the three-factor ANOVA for N1 latency and SM (location X hemisphere X SM) revealed no significant main effect of cluster location or hemisphere on N1 latency. This effect is shown in panels (a) and (b) of Figure 4.20. When location and hemisphere are considered together, panel (c) shows that although there was a slight decrease in N1 latency from frontal to central region and a slight increase from central to parietal regions in the right

hemisphere and an increase in N1 latency from frontal to parietal region in the left hemisphere this was not significant enough to cause an interaction. Pairwise comparisons of N1 latency for each electrode cluster across location and hemisphere show that there was no significant difference in N1 latency between the frontal, central and parietal right and left regions. There was no significant difference between N1 latency at midline versus the different clusters except central right ($p_{cr-m} = 0.011$). There was no significant main effect of SM, shown in panel (d) of Figure 4.20 or significant interactions of SM with location or hemisphere.
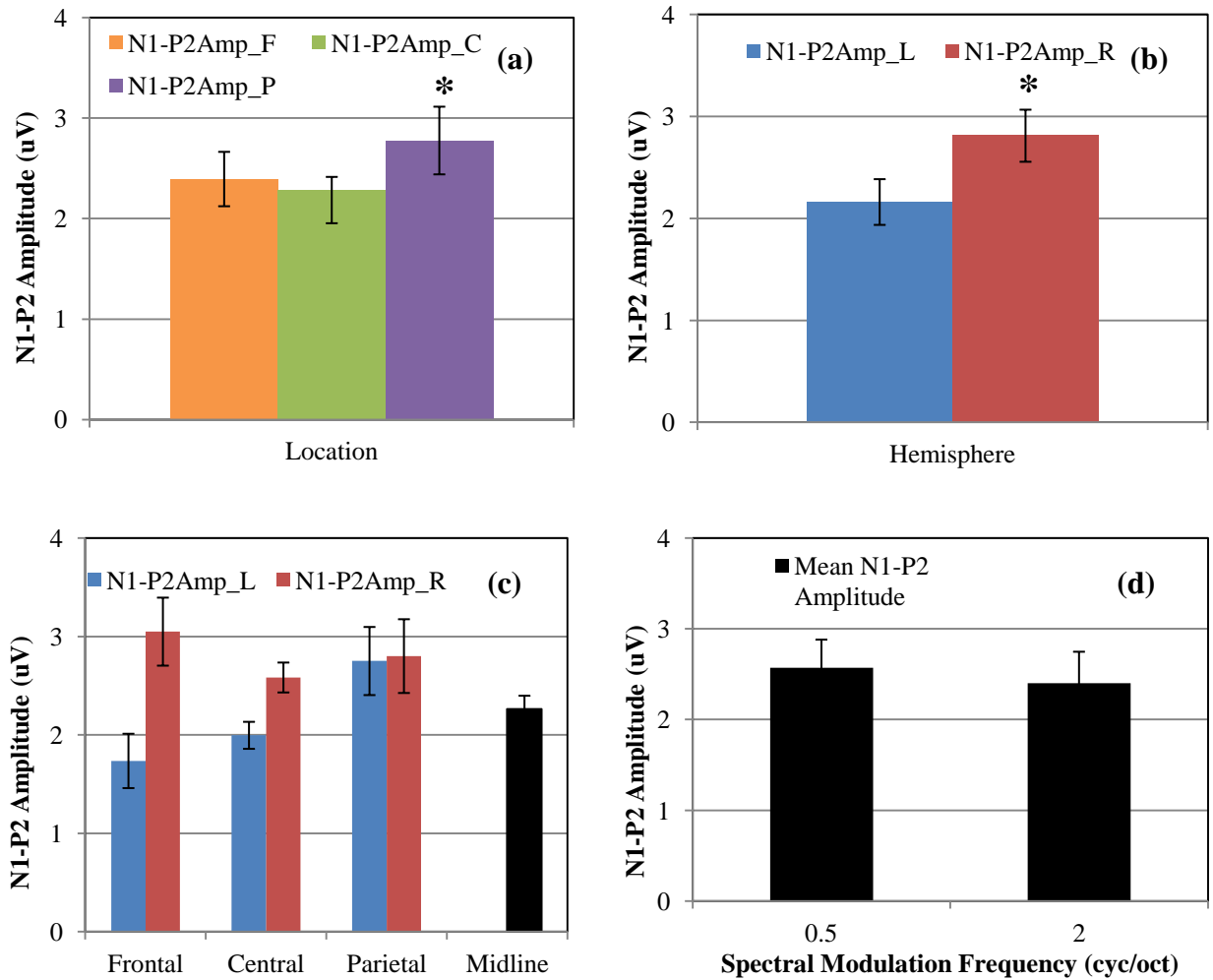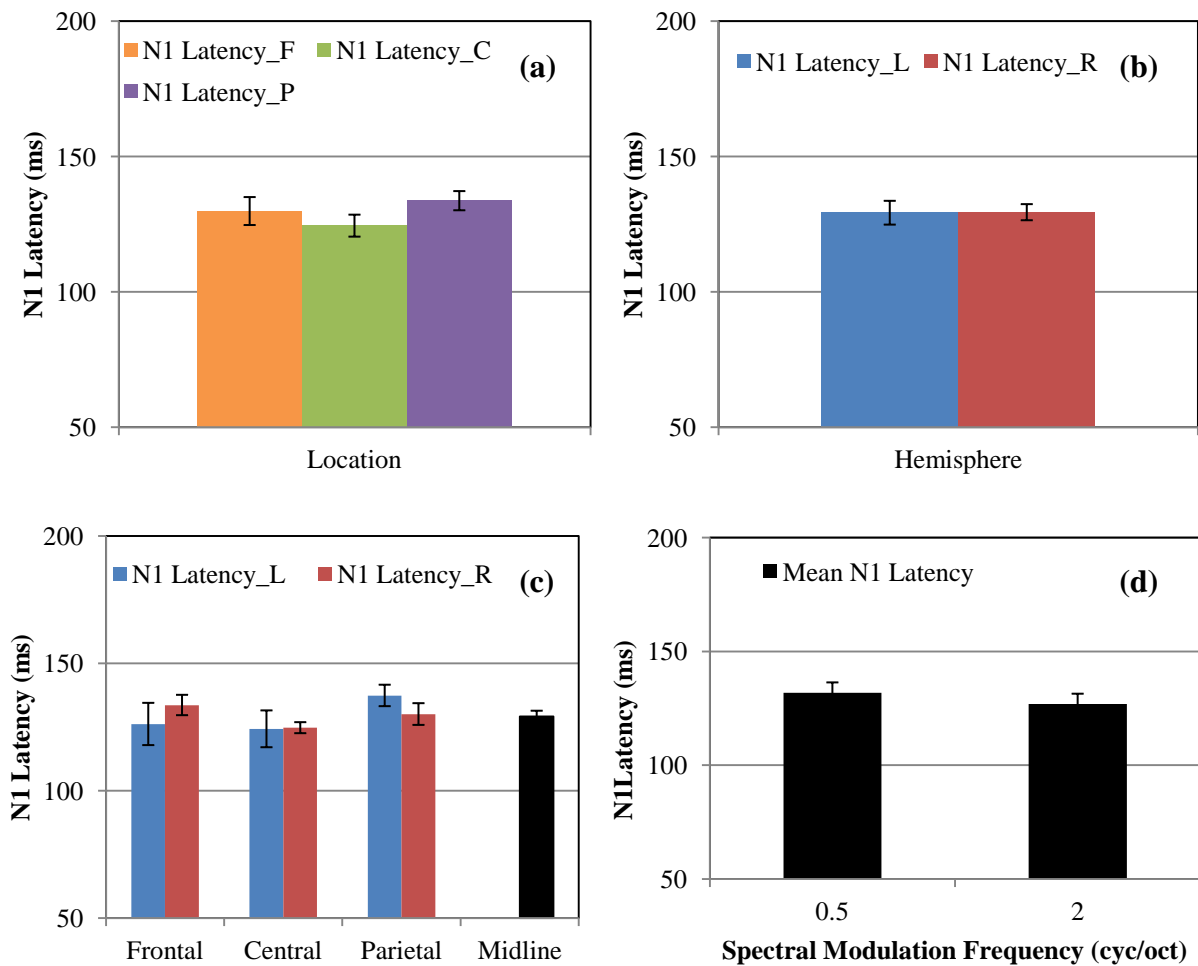

Figure 4.20 Main effects of location, hemisphere and their interactions on N1 latency and the main effect of SM. (a) Main Effect of Location; (b) Main Effect of Hemisphere; (c) Effect of Location x Hemisphere; (d) Main Effect of SM; *$p <0.05$

4.2.3.2 Temporal Modulation Results

The results of the three-factor ANOVA for N1-P2 amplitude and TM (location X hemisphere X TM) revealed a significant main effect of cluster location ($F_{(1,30)}$ = 21.05, $p <$ 0.001) and hemisphere ($F_{(1,30)}$ = 26.91, $p <$ 0.001) on N1-P2 amplitude. Pairwise comparisons show that the N1-P2 amplitude is more robust in the parietal region than in the frontal and central regions ($p_{f-p} <$ 0.001, $p_{c-p} <$ 0.001, p_{f-c} = 0.001) and more robust in the right hemisphere than in the left. This effect is shown in panels (a) and (b) of Figure 4.21. When location and hemisphere are considered together, panel (c) shows that there was a significant decrease in N1-P2 amplitude from frontal to central region and a significant increase from central to parietal regions in the right hemisphere ($p_{fr-cr} <$ 0.001, p_{cr-pr} = 0.004) and a significant increase in N1-P2 amplitude from frontal to parietal region in the left hemisphere ($p_{fl-pl} <$ 0.001, $p_{cl-pl} <$ 0.001). Hence there was a significant interaction of location and hemisphere ($F_{(1,30)}$ = 6.83, p = 0.014). Pairwise comparisons of N1-P2 amplitude for each electrode cluster across location and hemisphere, show that N1-P2 amplitude was significantly larger in the right than in the left hemisphere in the frontal and central regions ($p_{fl-fr} <$ 0.001, p_{cl-cr} = 0.001) but not in the parietal region. There was a significant difference between N1-P2 amplitude at midline versus the frontal right ($p_{fr-m} <$ 0.001), central left ($p_{cl-m} <$ 0.001) and the parietal left and right regions (p_{pl-m} = 0.001, $p_{pr-m} <$ 0.004) but not the rest. There was a significant effect of TM ($F_{(3,30)}$ = 2.96, p = 0.048) shown in panel (d). Pairwise comparisons reveal that there is a significant difference between the N1-P2 amplitudes of 2 Hz and 8 Hz (p = 0.029) and 2 Hz and 64 Hz (p = 0.009) but no significant interactions of TM with location or hemisphere.

Figure 4.21 Main effects of location, hemisphere and their interactions on N1-P2 amplitude and the main effect of TM. (a) Main Effect of Location; (b) Main Effect of Hemisphere; (c) Effect of Location x Hemisphere; (d) Main Effect of TM; *$p < 0.05$

The results of the three-factor ANOVA for N1 latency and TM (location X hemisphere X TM) revealed a significant main effect of cluster location ($F_{(1,32)} = 4.52$, $p = 0.041$) and hemisphere ($F_{(1,33)} = 5.83$, $p = 0.021$) on N1 latency. This effect is shown in panels (a) and (b) of Figure 4.22. When location and hemisphere are considered together, panel (c) shows that there is a significant decrease in N1 latency from frontal to central region ($p_{fr-cr} = 0.041$) but no significant increase from central to parietal regions in the right hemisphere and a significant increase in N1 latency from frontal to parietal region ($p_{fl-pl} = 0.016$, $p_{fl-pl} = 0.041$) in the left

hemisphere. Hence there was a significant interaction of location and hemisphere ($F_{(1,32)} = 9.60$, $p = 0.004$). Pairwise comparisons of N1 latency for each electrode cluster across location and hemisphere show that there was a significant difference in N1 latency between the central left and right ($p_{cl-cr} < 0.001$) and parietal left and right regions ($p_{pl-pr} < 0.001$) but not frontal left and right regions. There was no significant difference between N1 latency at midline versus the different clusters except central left ($p_{cl-m} < 0.001$) and parietal left regions ($p_{pl-m} = 0.001$). Panel (d) shows that there was a significant main effect of TM ($F_{(3,32)} = 3.54$, $p = 0.025$). Pairwise comparisons reveal that there is a significant difference between the N1 latencies of 2 Hz and 64 Hz ($p = 0.004$) but there were no significant interactions of TM with location or hemisphere.
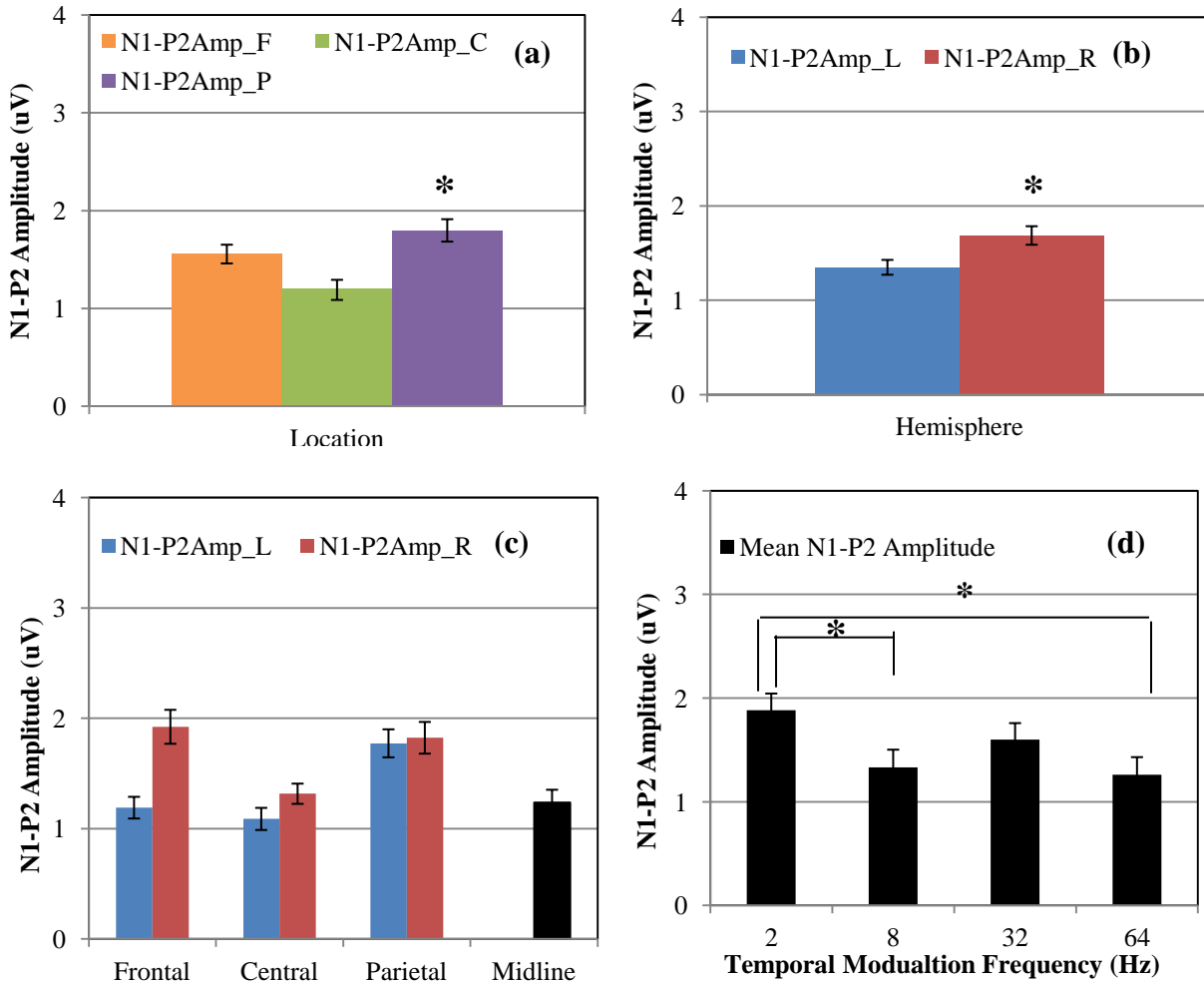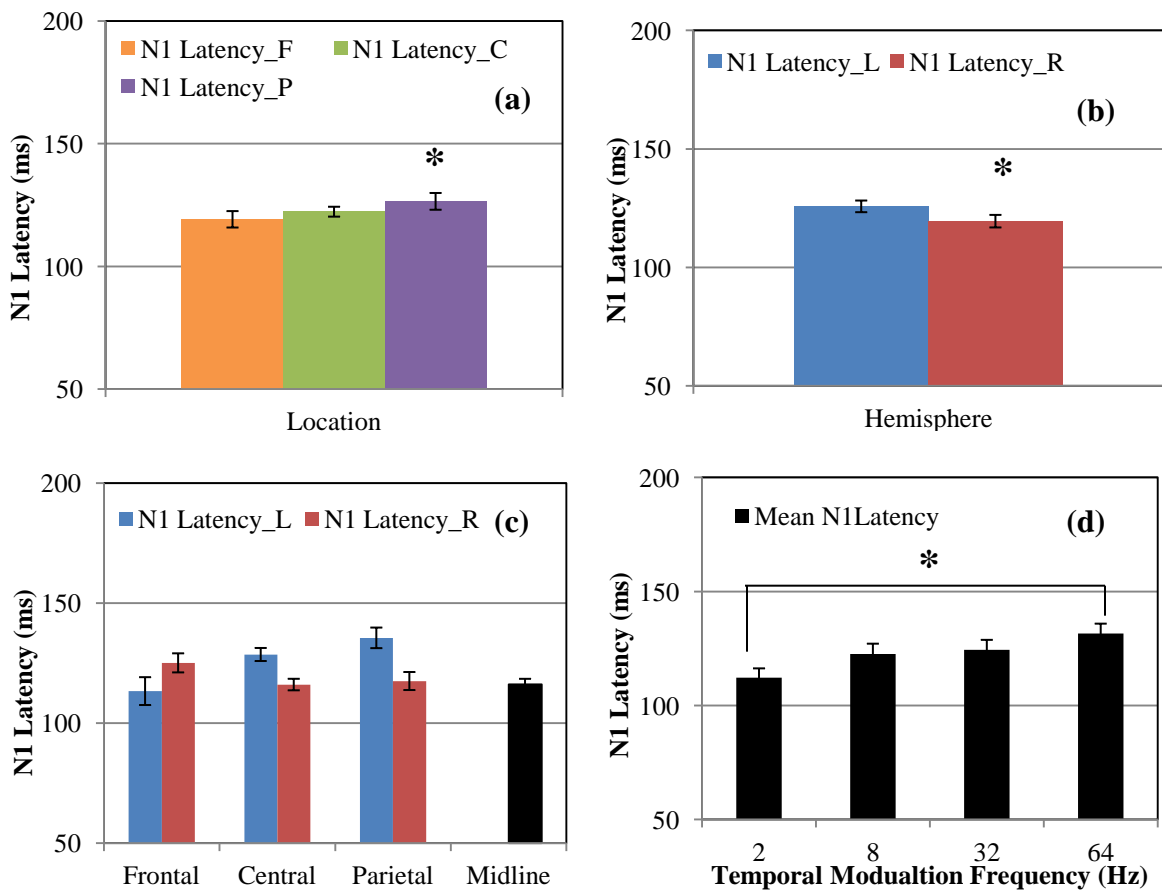

Figure 4.22 Main effects of location, hemisphere and their interactions on N1 latency and the main effect of TM. (a) Main Effect of Location; (b) Main Effect of Hemisphere; (c) Effect of Location x Hemisphere; (d) Main Effect of TM; *$p < 0.05$

4.2.3.3 Spectro-temporal Modulation Results

The results of the three-factor ANOVA for N1-P2 amplitude and STM (location X hemisphere X STM) revealed a significant main effect of cluster location ($F_{(1,65)}$ = 61.53, p < 0.001) and hemisphere ($F_{(1,65)}$ = 31.05, p < 0.001) on N1-P2 amplitude. Pairwise comparisons show that the N1-P2 amplitude is more robust in the parietal region than in the frontal and central regions (p_{f-p} < 0.001, p_{c-p} < 0.001, p_{f-c} = 0.014) and more robust in the right hemisphere than in the left. This effect is shown in panels (a) and (b) of Figure 4.23. When location and hemisphere are considered together, panel (c) shows that there was a significant decrease in N1-P2 amplitude from frontal to central region and a significant increase from central to parietal regions in the right hemisphere (p_{fr-cr} < 0.001, p_{cr-pr} = 0.001) and a significant increase in N1-P2 amplitude from frontal to parietal region in the left hemisphere (p_{fl-pl} < 0.001, p_{cl-pl} < 0.001). Hence there was a significant interaction of location and hemisphere ($F_{(1,65)}$ = 28.84, p < 0.001). Pairwise comparisons of N1-P2 amplitude for each electrode cluster across location and hemisphere, show that N1-P2 amplitude was significantly larger in the right than in the left hemisphere in the frontal and central regions (p_{fl-fr} < 0.001, p_{cl-cr} = 0.001) but not in the parietal region. There was a significant difference between N1-P2 amplitude at midline versus all the cluster regions (p_{fl-m} = 0.010, p_{fr-m} < 0.001, p_{cl-m} = 0.010, p_{cr-m} = 0.010, p_{pl-m} < 0.001, p_{pr-m} < 0.001). Panel (d) shows the significant main effect of STM ($F_{(7,30)}$ = 5.34, p < 0.001). At 0.5 cyc/oct there was no significant difference between the different TM conditions, but at 2 cyc/oct the 2 Hz TM condition was significantly different from the other TM conditions. However, there were no significant interactions of STM with location or hemisphere.

Figure 4.23 Main effects of location, hemisphere and their interactions on N1-P2 amplitude and the main effect of STM. (a) Main Effect of Location; (b) Main Effect of Hemisphere; (c) Effect of Location x Hemisphere; (d) Main Effect of STM; $*p < 0.05$

The results of the three-factor ANOVA for N1 latency and STM (location X hemisphere X STM) revealed no significant main effects of cluster location or hemisphere on N1 latency. This effect is shown in panels (a) and (b) of Figure 4.24. When location and hemisphere are considered together, panel (c) shows that there is a significant decrease in N1 latency from frontal to parietal region ($p_{\text{fr-pr}} = 0.002$) in the right hemisphere and a significant increase in N1 latency from frontal to parietal region ($p_{\text{fl-cl}} = 0.006$, $p_{\text{fl-pl}} = 0.002$) in the left hemisphere. Hence there was a significant interaction of location and hemisphere ($F_{(1,70)} = 16.57$, $p < 0.001$).

Pairwise comparisons of N1 latency for each electrode cluster across location and hemisphere show that there was a significant difference in N1 latency between the frontal left and right ($p_{\text{fl-fr}}$ = 0.027), central left and right ($p_{\text{cl-cr}}$ < 0.001) and parietal left and right regions ($p_{\text{pl-pr}}$ < 0.001). There was no significant difference between N1 latency at midline versus the different clusters except central left ($p_{\text{cl-m}}$ = 0.001) and parietal left regions ($p_{\text{pl-m}}$ = 0.005). Panel (d) shows that there was no significant main effect of STM. There were no significant interactions of STM with location or hemisphere either.
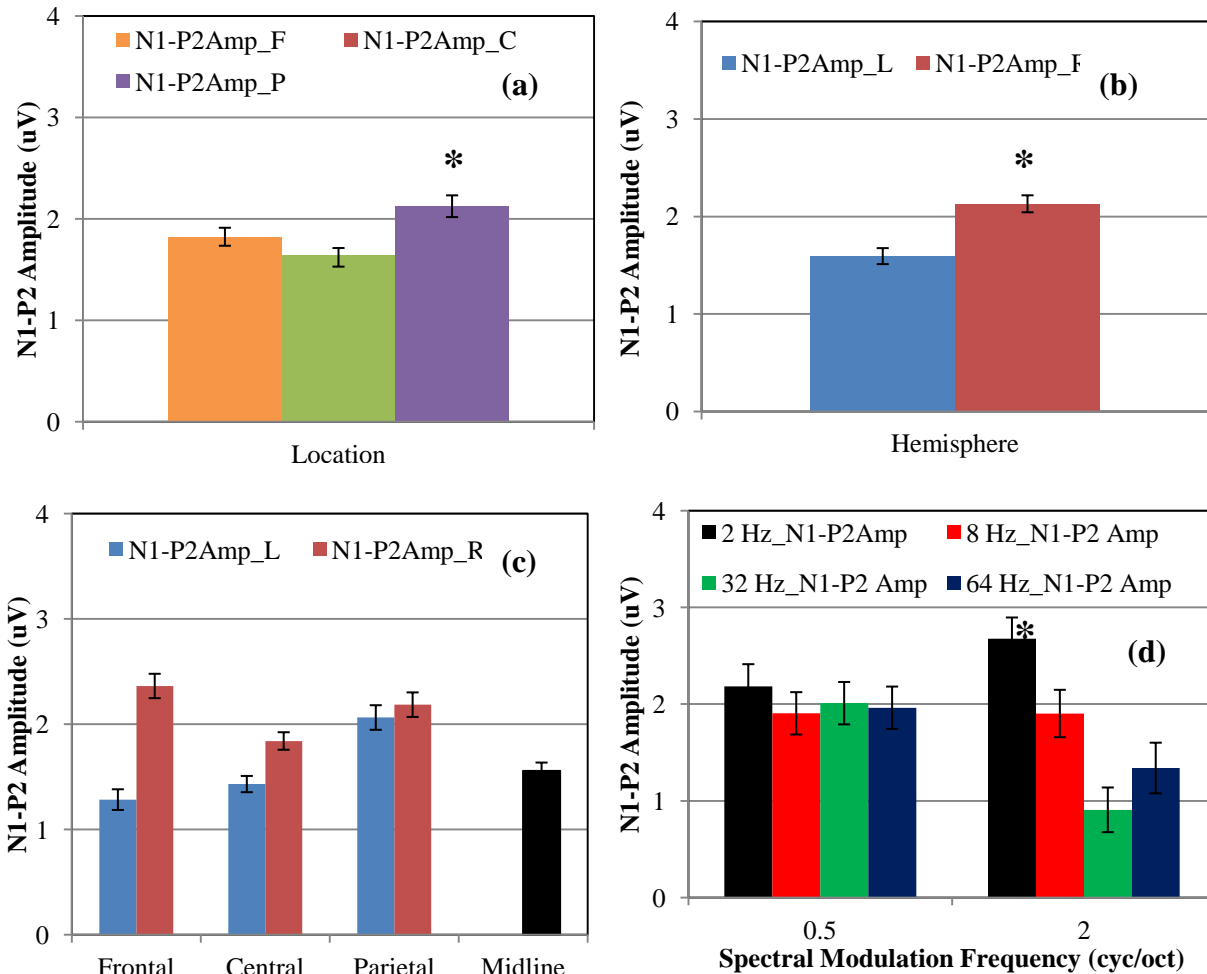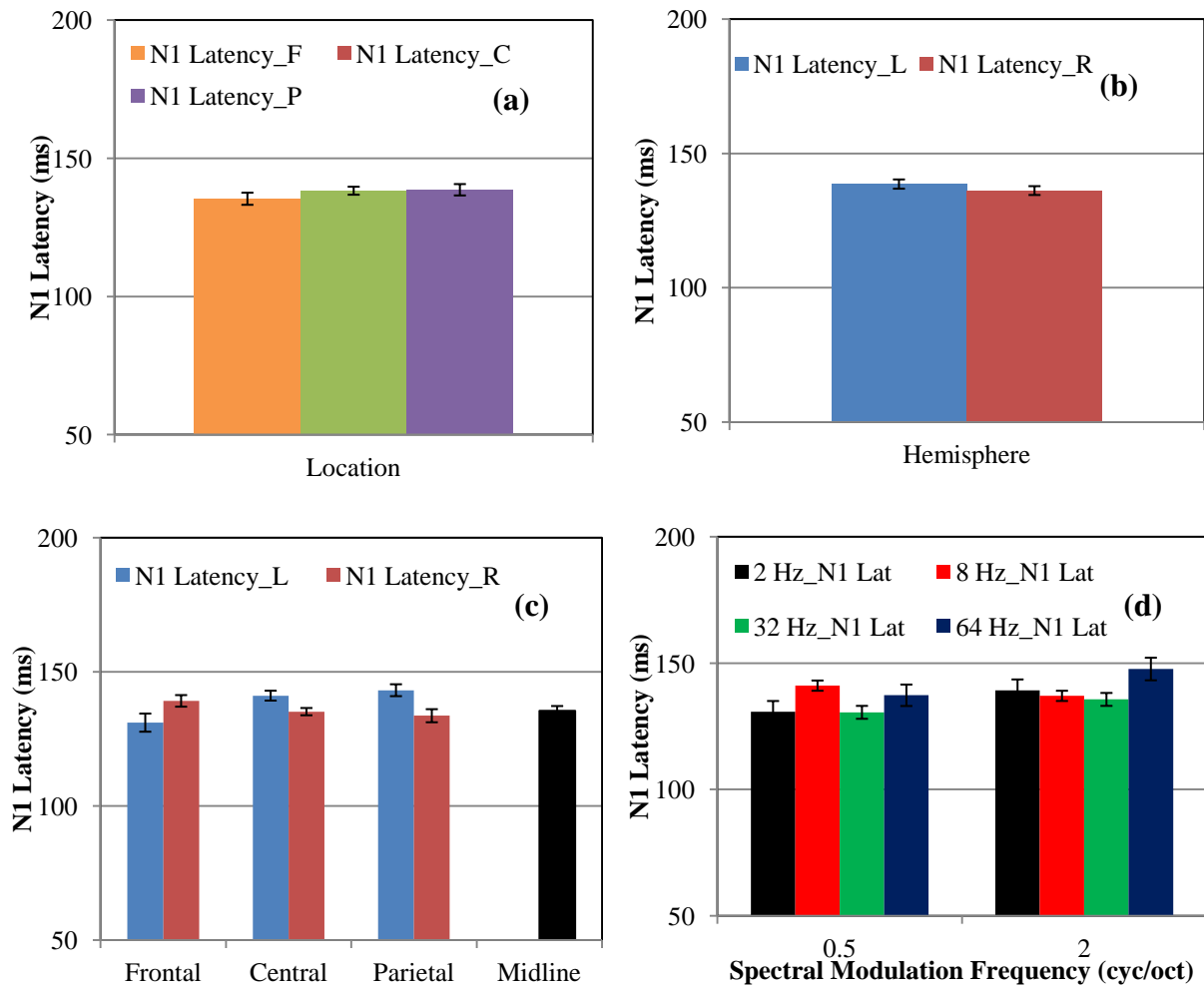

Figure 4.24 Main effects of location, hemisphere and their interactions on N1 latency and the main effect of STM. (a) Main Effect of Location; (b) Main Effect of Hemisphere; (c) Effect of Location x Hemisphere; (d) Main Effect of STM; *p <0.05

4.2.3.4 Correlation of Behavior and Electrophysiology Results

Until now we have been looking at the characteristics of the different behavior and physiological correlates of spectral, temporal and spectro-temporal modulation. In order to understand which of these physiological measures would be closely related to the behavioral measures of spectral, temporal and spectro-temporal sensitivity, a correlation between the behavioral thresholds and the N1-P2 amplitudes and N1 latencies obtained from each of the cluster groups was studied. In addition, an average measure of N1-P2 amplitude and N1 latency was calculated across the different cluster groups and their correlation with the behavioral thresholds were studied. A Pearson's product-moment correlation coefficient was used as a measure to evaluate the degree of correlation between the different pairs. The ρ values and associated p-values for the correlation of N1-P2 amplitudes and N1 latencies with behavioral thresholds for spectral, temporal and spectro-temporal modulation are shown in Tables 4.3 – 4.8.

From Table 4.3 and 4.4 we observe that the behavioral thresholds are significantly correlated with the N1-P2 amplitudes obtained from CR (central right) cluster but not significantly correlated with the N1 latencies obtained from any of the clusters. However, when the thresholds were grouped by SM frequency, we observe a significant correlation at 0.5 cyc/oct in the PR (parietal right) cluster.

From Tables 4.5 and 4.6 we observe the behavioral thresholds are not significantly correlated with the N1-P2 amplitude obtained from any of the clusters or the average. However, when the thresholds are grouped by temporal modulation frequency, a significant correlation is observed between the behavioral thresholds and the N1-P2 amplitude obtained from the CR

(central right) cluster at 32 Hz. The behavioral thresholds are also significantly correlated with the N1 latency measures obtained from the CR (central right) electrode cluster.

From Table 4.7, we observe a strong correlation between the behavioral thresholds and the N1-P2 amplitudes obtained from all the electrode clusters. This is depicted in panel (a) of Figure 4.25. From panel (b) of Figure 4.25, we observe that when the data is grouped by spectral modulation frequency, there is a significant correlation between behavioral thresholds and the N1-P2 amplitudes obtained from all the clusters, at 2 cyc/oct. When the data is grouped by temporal modulation frequency, a strong correlation is observed between the behavioral thresholds and the N1-P2 amplitudes obtained from FR (frontal right) and PR clusters.

From Table 4.8, a strong correlation is observed between the behavioral thresholds and the N1 latency obtained from the CL (central left), CR and Midline clusters and is shown in panel (a) of Figure 4.26. From panel (b) of Figure 4.26, we observe that when the data is grouped by spectral modulation frequency, there is a significant correlation between behavioral thresholds and the N1 latency obtained from the CR and Midline clusters at 2 cyc/oct. When the data is grouped by temporal modulation frequency a strong correlation is observed between the behavioral thresholds and the N1 latencies obtained from the CR, Midline clusters and the average N1 latency at 64 Hz.

Table 4.3 Correlation coefficients of behavior thresholds with N1-P2 amplitude from different clusters for pure spectral modulation

Behavior threshold	FL	FR	CL	CR	PL	PR	Midline	N1P2 Average
Ungrouped	ρ= -0.003, p = 0.991	ρ= 0.206, p = 0.383	ρ= 0.287, p = 0.221	**ρ= 0.454, p = 0.044**	ρ= 0.089, p = 0.725	ρ= 0.038, p = 0.729	ρ= 0.263, p = 0.263	ρ= 0.218, p = 0.356
Grouped by 0.5cyc/oct	ρ= -0.191, p = 0.597	ρ= -0.025, p = 0.945	ρ= -0.222, p = 0.537	ρ= 0.302, p = 0.396	ρ= 0.013, p = 0.973	ρ= -0.051, p = 0.888	ρ= -0.419, p = 0.228	ρ= -0.085, p = 0.815
Grouped by 2 cyc/oct	ρ= 0.303, p = 0.395	ρ= 0.121, p = 0.739	ρ= 0.307, p = 0.389	ρ= 0.594, p = 0.070	ρ= 0.284, p = 0.496	ρ= 0.190, p = 0.599	ρ= 0.493, p = 0.148	ρ= 0.343, p = 0.332

Table 4.4 Correlation coefficients of behavior thresholds and N1 latency from different clusters for pure spectral modulation

Behavior threshold	FL	FR	CL	CR	PL	PR	Midline	N1 Latency Average
Ungrouped	ρ= 0.401, p = 0.080	ρ= 0.274, p = 0.243	ρ= 0.256, p = 0.276	**ρ= 0.059, p = 0.806**	ρ= 0.309, p = 0.185	ρ= 0.195, p = 0.409	ρ= -0.015, p = 0.949	ρ= 0.414, p = 0.070
Grouped by 0.5cyc/oct	ρ= 0.556, p = 0.095	ρ= 0.489, p = 0.152	ρ= 0.409, p = 0.240	ρ= 0.396, p = 0.257	ρ= 0.372, p = 0.289	**ρ= 0.703, p = 0.023**	ρ= 0.131, p = 0.718	ρ= 0.609, p = 0.061
Grouped by 2 cyc/oct	ρ= 0.317, p = 0.373	ρ= -0.085, p = 0.815	ρ= 0.299, p = 0.402	ρ= 0.046, p = 0.899	ρ= 0.404, p = 0.246	ρ= 0.124, p = 0.733	ρ= 0.377, p = 0.283	ρ= 0.428, p = 0.218

Table 4.5 Correlation coefficients of behavior thresholds and N1-P2 amplitude from different clusters for pure temporal modulation

Behavior threshold	FL	FR	CL	CR	PL	PR	Midline	N1P2 Average
Ungrouped	ρ= -0.063, p = 0.699	ρ= -0.040, p = 0.805	ρ= -0.173 p = 0.287	ρ= -0.304, p = 0.056	ρ= -0.032, p = 0.853	ρ= 0.215, p = 0.195	ρ= -0.273, p = 0.089	ρ= -0.123, p = 0.448
Grouped by 2 Hz	ρ= -0.305, p = 0.391	ρ= -0.370, p = 0.293	ρ= 0.2 p = 0.579	ρ= 0.310, p = 0.383	ρ= 0.109, p = 0.779	ρ= 0.559, p = 0.067	ρ= 0.270, p = 0.450	ρ= 0.443, p = 0.200
Grouped by 8 Hz	ρ= 0.375, p = 0.286	ρ= -0.045, p = 0.902	ρ= -0.408 p = 0.241	ρ= -0.339, p = 0.337	ρ= 0.272, p = 0.478	ρ= 0.376, p = 0.318	ρ= -0.542, p = 0.105	ρ= -0.082, p = 0.821
Grouped by 32 Hz	ρ= -0.227, p = 0.528	ρ= -0.084, p = 0.818	ρ= -0.202 p = 0.575	**ρ= -0.848, p = 0.002**	ρ= -0.097, p = 0.804	ρ= 0.137, p = 0.705	ρ= -0.319, p = 0.369	ρ= -0.238, p = 0.507
Grouped by 64 Hz	ρ= -0.446, p = 0.196	ρ= 0.003, p = 0.993	ρ= -0.540 p = 0.107	ρ= -0.318, p = 0.371	ρ= 0.311, p = 0.415	ρ= -0.288, p = 0.452	ρ= -0.614, p = 0.059	ρ= -0.275, p = 0.441

Table 4.6 Correlation coefficients of behavior thresholds and N1 latency from different clusters for pure temporal modulation

Behavior threshold	FL	FR	CL	CR	PL	PR	Midline	N1 Latency Average
Ungrouped	ρ= 0.011, p = 0.945	ρ= -0.018, p = 0.911	ρ= 0.308 p = 0.053	ρ= 0.354, p = 0.025	ρ= -0.139, p = 0.413	ρ= 0.085, p = 0.603	ρ= 0.266, p = 0.097	ρ= 0.191, p = 0.237
Grouped by 2 Hz	ρ= -0.140, p = 0.700	ρ= -0.339, p = 0.337	ρ= -0.051 p = 0.888	ρ= -0.128, p = 0.725	ρ= -0.450, p = 0.192	ρ= -0.344, p = 0.331	ρ= 0.134, p = 0.711	ρ= -0.391, p = 0.263
Grouped by 8 Hz	ρ= 0.380, p = 0.279	ρ= 0.203, p = 0.575	ρ= 0.486 p = 0.154	ρ= -0.131, p = 0.718	ρ= 0.041, p = 0.916	ρ= 0.576, p = 0.104	ρ= -0.338, p = 0.339	ρ= 0.215, p = 0.550
Grouped by 32 Hz	ρ= 0.220, p = 0.541	ρ= 0.374, p = 0.286	ρ= 0.298 p = 0.402	ρ= -0.263, p = 0.463	ρ= -0.141, p = 0.717	ρ= -0.199, p = 0.582	ρ= -0.143, p = 0.693	ρ= -0.119, p = 0.743
Grouped by 64 Hz	ρ= -0.438, p = 0.206	ρ= 0.103, p = 0.776	ρ= -0.022 p = 0.953	ρ= -0.307, p = 0.387	ρ= -0.443, p = 0.233	ρ= -0.261, p = 0.466	ρ= -0.480, p = 0.161	ρ= -0.118, p = 0.746
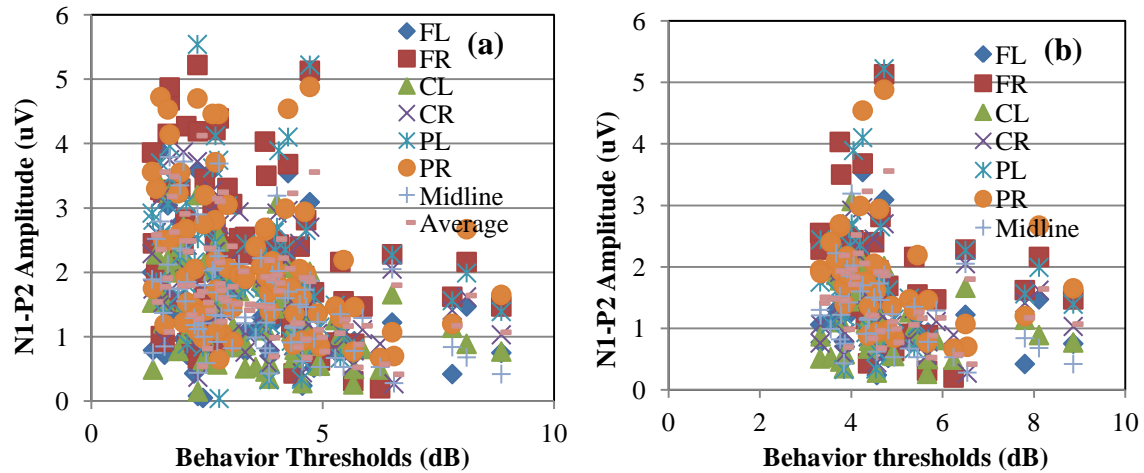
Figure 4.25 Correlation of behavior thresholds with N1-P2 amplitudes for spectro-temporal modulation conditions. (a) For all STM conditions (b) Grouped by SM − 2 cyc/oct
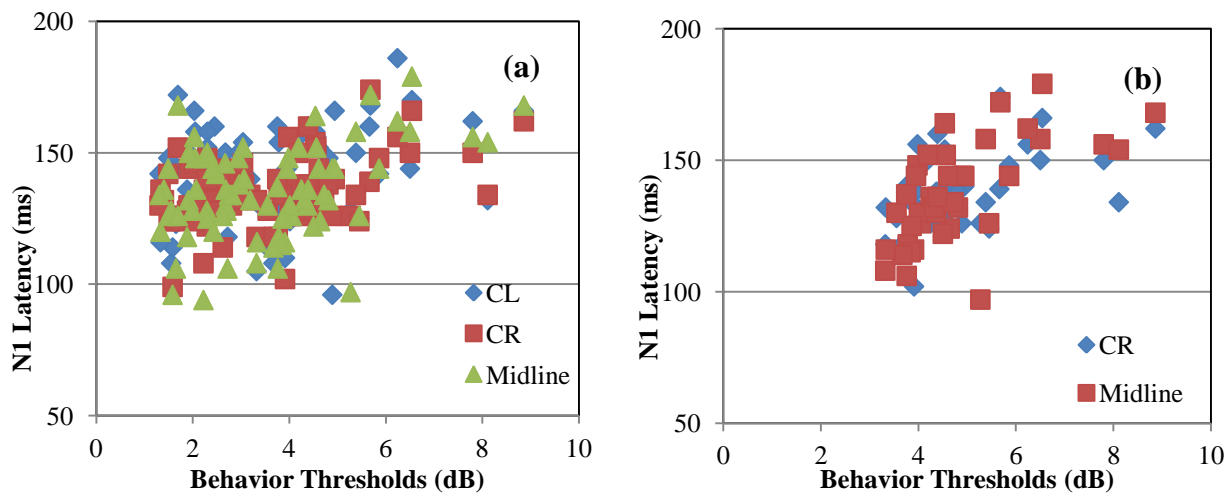
Figure 4.26 Correlation of behavior thresholds with N1 latencies for spectro-temporal modulation conditions. (a) For all STM conditions (b) Grouped by SM − 2 cyc/oct

When the behavioral thresholds and the average N1-P2 amplitude from all clusters are plotted together, we observe a very close relationship between the two (Figure 4.27). Here we observe that as the sensitivity to modulation decreases behaviorally there is a decrease in N1-P2 amplitude and this effect is monotonic. The change is more prominent at 2 cyc/oct than at 0.5 cyc/oct.

Table 4.7 Correlation coefficients of behavior thresholds and N1-P2 amplitude from different clusters for spectro-temporal modulation

Behavior threshold	FL	FR	CL	CR	PL	PR	Midline	N1P2 Average
Ungrouped	**ρ= -0.279, *p* = 0.012**	**ρ= -0.398, *p* < 0.001**	**ρ= -0.417, *p* < 0.001**	**ρ= -0.408, *p* < 0.001**	**ρ= -0.304, *p* < 0.001**	**ρ= -0.348, *p* < 0.001**	**ρ= -0.456, *p* < 0.001**	**ρ= -0.443, p < 0.001**
Grouped by 0.5cyc/oct	ρ= -0.171, *p* = 0.292	ρ= 0.125, *p* = 0.442	ρ= -0.096, *p* = 0.554	ρ= -0.001, *p* = 0.993	ρ= 0.119, *p* = 0.466	ρ= 0.154, *p* = 0.349	ρ= -0.189, *p* = 0.243	ρ= 0.085, p = 0.603
Grouped by 2 cyc/oct	**ρ= -0.444, p = 0.004**	**ρ= -0.602, *p* < 0.001**	**ρ= -0.520, *p* = 0.001**	**ρ= -0.534, *p* < 0.001**	**ρ= -0.573, *p* < 0.001**	**ρ= -0.546, *p* < 0.001**	**ρ= -0.562, *p* < 0.001**	**ρ= -0.616, p < 0.001**
Grouped by 2 Hz	ρ= -0.097, *p* = 0.683	ρ= 0.903, *p* = 0.696	ρ= 0.122, *p* = 0.609	ρ= 0.118, *p* = 0.620	ρ= -0.063, *p* = 0.791	ρ= -0.156, *p* = 0.523	ρ= 0.143, *p* = 0.548	ρ= 0.046, p = 0.914
Grouped by 8 Hz	ρ= 0.133, *p* = 0.575	ρ= 0.237, *p* = 0.314	ρ= 0.356, *p* = 0.123	ρ= 0.416, *p* = 0.068	ρ= -0.047, *p* = 0.854	ρ= 0.072, *p* = 0.763	ρ= 0.345, *p* = 0.137	ρ= 0.314, p = 0.178
Grouped by 32 Hz	ρ= -0.265, *p* = 0.258	**ρ= -0.534, *p* = 0.015**	ρ= -0.179, *p* = 0.451	ρ= -0.358, *p* = 0.121	ρ= -0.163, *p* = 0.506	**ρ= -0.493, *p* = 0.027**	ρ= -0.294, *p* = 0.221	**ρ= -0.445, p = 0.049**
Grouped by 64 Hz	ρ= -0.296, *p* = 0.206	ρ= -0.319, *p* = 0.170	ρ= -0.420, *p* = 0.079	ρ= -0.358, *p* = 0.122	ρ= -0.177, *p* = 0.498	ρ= -0.289, *p* = 0.230	**ρ= -0.549, *p* = 0.012**	ρ= -0.346, p = 0.102

Table 4.8 Correlation coefficients of behavior thresholds and N1 latency from different clusters for spectro-temporal modulation

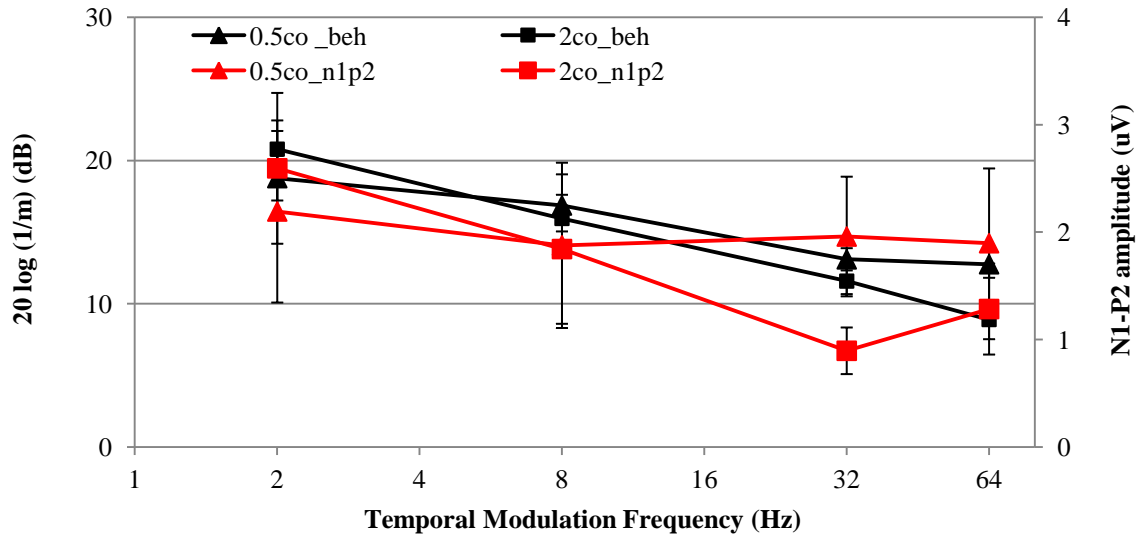| Behavior threshold	FL	FR	CL	CR	PL	PR	Midline	N1 Latency Average
Ungrouped	ρ= -0.001, p = 0.991	ρ= 0.198, p = 0.078	**ρ= 0.233, p = 0.038**	**ρ= 0.432, p < 0.001**	**ρ= -0.121, p = 0.286**	**ρ= 0.054, p = 0.641**	**ρ= 0.391, p < 0.001**	**ρ= -0.211, p = 0.060**
Grouped by 0.5cyc/oct	ρ= -0.041, p = 0.802	ρ= 0.165, p = 0.308	ρ= -0.054, p = 0.739	ρ= 0.304, p = 0.056	ρ= -0.115, p = 0.479	ρ= 0.053, p = 0.751	ρ= 0.055, p = 0.737	ρ= 0.050, p = 0.759
Grouped by 2 cyc/oct	ρ= 0.022, p = 0.892	ρ= 0.197, p = 0.223	ρ= 0.288, p = 0.072	**ρ= 0.457, p = 0.003**	ρ= -0.142, p = 0.387	ρ= 0.009, p = 0.956	**ρ= -0.460, p = 0.003**	ρ= 0.217, p = 0.178
Grouped by 2 Hz	ρ= -0.130, p = 0.584	ρ= -0.018, p = 0.941	ρ= 0.277, p = 0.237	ρ= 0.055, p = 0.817	ρ= 0.056, p = 0.814	ρ= 0.193, p = 0.428	ρ= 0.199, p = 0.401	ρ= 0.104, p = 0.662
Grouped by 8 Hz	ρ= -0.410, p = 0.073	ρ= 0.166, p = 0.484	ρ= -0.227, p = 0.336	ρ= 0.252, p = 0.283	ρ= -0.018, p = 0.939	ρ= 0.238, p = 0.311	ρ= 0.253, p = 0.282	ρ= 0.153, p = 0.519
Grouped by 32 Hz	ρ= 0.340, p = 0.143	ρ= 0.037, p = 0.878	**ρ= -0.448, p = 0.048**	ρ= 0.325, p = 0.161	ρ= 0.139, p = 0.560	ρ= 0.330, p = 0.156	ρ= 0.286, p = 0.235	ρ= 0.417, p = 0.069
Grouped by 64 Hz	ρ= 0.092, p = 0.700	ρ= 0.375, p = 0.103	ρ= 0.393, p = 0.086	**ρ= 0.449, p = 0.047**	ρ= -0.128, p = 0.602	ρ= 0.174, p = 0.477	**ρ= 0.698, p = 0.001**	**ρ= 0.448, p = 0.048**

Figure 4.27 Relationship between behavioral spectro-temporal modulation transfer function and average N1-P2 amplitudes for the corresponding spectro-temporal conditions.

4.2.4 Discussion

Several previous studies have demonstrated that spectral and temporal changes in the acoustic stimuli were encoded differentially in the two hemispheres (spectral change − right dominate; temporal change − left dominant; e.g., Zattore and Belin, 2001; Jamison *et al*., 2005; Zaehle *et al*., 2009). The current results indicate greater global field power of N1 and P2 components and N1-P2 amplitudes in the right hemisphere for both spectral and temporal changes. To explain these disparate results, one may consider differences in methodology across studies. A primary difference is the nature of the stimuli and the stimulus change. Secondary differences include method of stimulus delivery and subject state.

Comparing the results of the current study with the findings of Zatorre and Belin (2001), Jamison *et al*. (2005) and Zaehle *et al*. (2009), we observe a major difference between the nature of the stimuli used in those studies and the stimuli used in the current study. The spectral changes in the previous studies can be characterized by a change in the center frequency of relatively

narrowband stimuli (Zaehle *et al*., 2009) or change in frequency separation of tonal components (Zatorre and Belin, 2001; Jamison *et al*., 2005). In the current study, the spectral change was produced by introducing spectral modulation to the relatively broadband (3 octaves) spectral envelope. So the carrier remained the same throughout the study, while spectral modulation superimposed a distinct spectral shape. Thus, the current stimuli involved a change in spectral pattern rather than absolute audio frequency. Similarly, the temporal change in the previous studies can be characterized by a change in duration of the temporal gap (Zaehle *et al*., 2009) or change in duration of the tonal components (Zatorre and Belin, 2001; Jamison *et al*., 2005). In the current study, again the carrier remained constant and the temporal change was represented by the introduction of temporal modulation. We observe that detection of change in center frequency, detection of frequency separation, and spectral envelope detection (current study) produce similar lateralization of the measured neural correlates (right lateralization), but the neural correlates of changes in gap duration or overall stimulus duration tended to be left lateralized while the neural correlates of temporal modulation detection in the current study is right lateralized. Apart from differences in stimuli, the differences in presentation paradigms could also contribute to the differences in results. Zatorre and Belin (2001) presented their stimuli continuously. Jamison *et al*. (2005) presented their stimuli in a change detection paradigm with the 6 s stimulus occurring every 23 seconds with silence when no stimulus is being presented. Zaehle *et al*. (2009) presented their stimuli in an oddball paradigm with a stimulus-onset-asynchrony (SOA) of 750 ms. The current study uses a change detection paradigm in which sound is continuously present and the infrequent stimulus occurred once every 1600 ms. A third difference among the previous studies and the current study was ear of

88

presentation. The previous studies presented all stimuli diotically, whereas the current study presented stimuli monaurally (to the left ear only).

Okamoto *et al*. (2012) demonstrated that the N1m latency of the response to their temporal change stimuli was longer than the latency to their spectral-temporal change stimuli. Recall that their temporal change involved the superposition of 40 Hz sinusoidal amplitude modulation to tonal carriers in either the first or second 800-ms interval of a 1600-ms stimulus. The major differences between this study and the current study is the use of 40 Hz versus 2, 8, 32, 64 Hz modulation frequency, the use of tonal versus 3-octave wide band-pass noise carriers, and the use of "burst" versus "continuous" stimulus presentation, and diotic versus monotic stimulus presentation. Contrary to the results of Okamoto *et al*. (2012), the current results indicated a significantly shorter latency for the temporal modulation compared to the spectro-temporal modulation conditions (Figure 4.11 panel (d)). Interestingly, the temporal change in the two studies are comparable (change from no temporal modulation to temporal modulation) while the spectral change is quite different across studies (change in carrier frequency versus presence/absence of spectral modulation). Thus, one possible explanation for the disparate latencies is that the more complex spectral change paradigm used here results in longer-latency cortical evoked responses.

Rao *et al*. (2010) simultaneously recorded behavioral and evoked potential responses to their different pitch perception conditions. They reported frontal and central activity of the N1 and P2 responses whereas we observe that the N1-P2 amplitude is maximal at the parietal sites (panel (a) of Figures 4.19, 4.21 and 4.23). In panel (c) of the same figures, we observe that the N1-P2 complex is strongly lateralized to the right in the front and there is a loss of laterality as we go to the parietal region. Thus when the responses are collapsed across regions the effect of

laterality is washed out, resulting in a net increase in N1-P2 amplitude in the parietal region. Since the N1-P2 is a sensory response, the results from Rao *et al.*, study give us a sense of direction of what to expect from the N1-P2 when analyzing multi-channel recordings. The main difference between the current study and Rao *et al.* (2010) is that the current study involved passive listening. The stimuli used and the presentation paradigms were also very different. During recording, listeners in the Rao *et al.* study identified the frequency of target stimuli (tones or noises in different conditions). This classification of high/low frequency is quite different from passive exposure to the presence or absence of spectral modulation. Thus, it is likely that the two tasks involve different neural substrates.

From panel (a) of Figures 4.9, 4.10, 4.13 and 4.14, we observe a parietal dominance of N1 power and P2 power when averaged across hemispheres and modulation conditions. Figure 4.28 represents the voltage maps showing the distribution of the N1 and P2 responses of the averaged spectral, temporal and spectro-temporal modulation conditions. From Figure 4.28 we observe that the N1 and P2 components show a very robust fronto-central activity while processing spectral, temporal and spectro-temporal modulations. We also observe the change in laterality in the N1 component going from frontal to parietal regions. Thus without completing additional source localization analyses, it is difficult to determine whether this change in laterality from frontal to parietal locations reflects asymmetric processing gradients for SM, TM, and STM from anterior to posterior primary and non-primary auditory cortices in each hemisphere. Such tuning to STM has been observed at the single voxel level in primary and secondary auditory cortices in humans using fMRI (Schonwiesner and Zatorre, 2009).
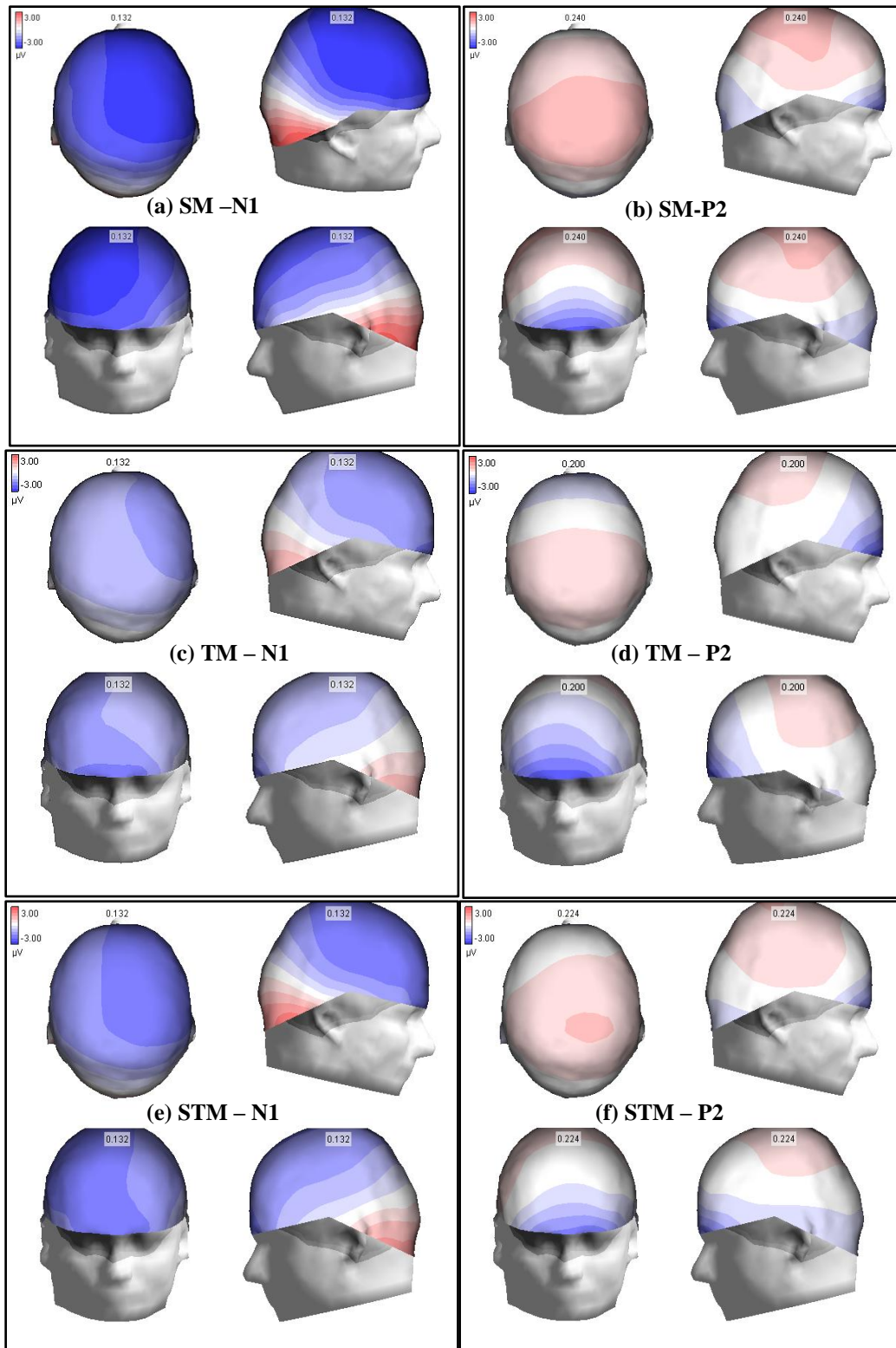
90

Figure 4.28 Average responses at N1 and P2 latencies for pure SM, TM and STM modulation frequencies over 10 subjects.

The correlation of the behavior and the evoked potential components show a weak negative relationship between the N1-P2 amplitude and weak positive relationship with N1 latency. However there is a high degree of variability observed in the correlation. In Figure 4.25 we observe that for low behavioral thresholds, the N1-P2 amplitude obtained from the different sites vary across a 4 uV range and for high behavioral thresholds the N1-P2 amplitudes obtained vary over a 2.5 uV range. When the average N1-P2 amplitude of all the sites is compared with the behavioral sensitivity (Figure 4.27), we observe a close relationship in the shapes of the psychophysical and physiological transfer functions and the effect of modulation frequency on each of them.

4.2.5 Conclusion

The current results indicated robust electrophysiological responses to supra-threshold spectral, temporal, and spectro-temporal modulation. The pattern of physiological results mimicked behavioral results for the same subjects. There was a highly significant but weak to moderate negative relationship between the behavioral thresholds and N1-P2 amplitude. The N1-P2 complex is right lateralized fronto-centrally and loses its laterality at more posterior sites. The nature of the N1-P2 complex is consistent for spectral, temporal and spectro-temporal modulations. The EEG recordings reported here lend themselves to many different possible analyses and this thesis, in many ways, presents a small subset of those analyses. Future work may focus on more comprehensive analysis of results from individual listeners, results from individual electrodes, and time varying responses across spatial location. To better elucidate neural correlates of spectro-temporal processing, future studies may include different modes of stimulation (left, right, diotic), the use of simple spectral changes (e.g., low/high frequency), and

simple changes in stimulus duration. Such measures may help to explain disparate results, in terms of response latency and hemispheric specialization, observed across many studies.

REFERENCES

1. Amagai, S., Dooling, R. J., Shamma, S., Kidd, T. L., and Lohr, B. **(1999).** "Detection of modulation in spectral envelopes and linear-rippled noises by budgerigars (Melopsittacus undulates)," J. Acoust. Soc. Am. **105**, 2029–2035.

2. Berlingeri, M., Danelli, L., Bottini, G., Sberna, M., and Paulesu, E. **(2013).** "Reassessing the HAROLD model: Is the hemispheric asymmetry reduction in older adults a special case of compensatory-related utilisation of neural circuits?," Exp Brain Res. **224**, 393–410.

3. Bernstein, J. G. W., Mehraei, G., Shamma, S., Gallun, F. J., Theodoroff, S. M., and Leek, M. R. **(2013)**. "Spectrotemporal Modulation Sensitivity as a Predictor of Speech Intelligibility for Hearing-Impaired Listeners," J. Am. Acad. Audiol. **24**, 293–306.

4. Chi, T., Gao, Y., Guyton, M. C., Ru, P., and Shamma, S. **(1999).** "Spectro-temporal modulation transfer functions and speech intelligibility," J. Acoust. Soc. Am. **106** (5), 2719-2732.

5. Dau, T., Kollmeier, B., and Kohlraush, A. **(1997).** "Modeling auditory processing of amplitude modulation. I. Detection and masking with narrow-band carriers," J. Acoust. Soc. Am. **102** (5), 2892-2905.

6. Draganova, R., Wollbrink, A., Schulz, M., Okamoto, H., and Pantev, C. **(2009).** "Modulation of auditory evoked responses to spectral and temporal changes by behavioral discrimination training," BMC Neuroscience. **10** (143), 1-18.

7. Eddins, D. A. **(1993)**. "Amplitude modulation detection of narrow-band noise: Effects of absolute bandwidth and frequency region," J. Acoust. Soc. Am. **93** (1), 470-479.

8. Eddins, D.A., and Bero, E. M. **(2007)**. "Spectral modulation detection as a function of modulation frequency, carrier bandwidth, and carrier frequency region," J. Acoust. Soc. Am. **121** (1), 363-372.

9. Frisina, R. D., Smith, R. L., Chamberlain, S. C. **(1985).** "Differential encoding of rapid changes in sound amplitude by second order auditory neurons," Exp. Brain Res. **60**, 417-422.

10. http://commons.wikimedia.org/wiki/File:Spectrogram_of_I_owe_you.png

11. http://www.ant-neuro.com/products/waveguard/electrode-layouts

12. Jamison, H. L., Watkins, K. E., Bishop, D. V. M., and Matthews, P. M. **(2006).** "Hemispheric Specialization for Processing Auditory Nonspeech Stimuli," Cerebral Cortex. **16**, 1266-1275.

13. Korczak, P., Smart, J., Delgado, R., Strobel, T. M., Bradford, C. **(2012).** "Auditory Steady-State Responses," J. Am. Acad. Audiol. **23** (3), 146-170.

14. Langner, G. **(1991).** "Periodicity coding in the auditory system," Hearing Research. **60**, 115-142.

15. Langner, G., and Shreiner, C. E., (**1988).** "Periodicity coding in the inferior colliculus of the cat. I. Neural Mechanisms," J. Neurophysiol. **60**, 1799-1822.

16. Levitt, H. **(1971)**. "Transformed up-down methods in psychoacoustics," J. Acoust. Soc. Am. **49**, 467-477.

17. Luo, H., and Poeppel, D. **(2012).** "Cortical oscillations in auditory perception and speech: evidence for two temporal windows in human auditory cortex," frontiers in psychology. **3** (170), 1-10.

18. Maurits, N. M., Scheeringa, R., van der Hoeven, J. H., and de Jong, R. **(2006).** "EEG Coherence Obtained From an Auditory Oddball Task Increases With Age," J. Clin. Neurophysiol. **23,** 395–403.

19. Okamoto, H., Teismann, H., Kakigi, R., and Pantev, C. **(2012). "**Auditory evoked fields elicited by spectral, temporal, and spectral–temporal changes in human cerebral cortex," frontiers in psychology. **3** (149), 1-11.

20. Rao, A., Zhang, Y., and Miller. S. **(2010)**. "Selective listening of concurrent auditory stimuli: An event-related potential study," Hearing Research. **268**, 123-132.

21. Rodenburg,M . **(1977)**. "Investigation of temporal effects with amplitude modulated signals," Psychophysics and Physiology of Hearing, edited by E. F. Evans and J.P. Wilson (Academic, London), 429-437.

22. Sabin, A. T., Eddins, D. A., and Wright, B. A. **(2012).** "Perceptual Learning Evidence for Tuning to Spectrotemporal Modulation in the Human Auditory System," J. Neuroscience. **32** (19), 6542-6549.

23. Saoji, A. A., and Eddins, D.A. **(2007).** "Spectral modulation masking patterns reveal tuning to spectral envelope frequency," J. Acoust. Soc. Am. **122** (2), 1004-1013.

24. Schönwiesner, M., and Zatorre, R. J. **(2009).**" Spectro-Temporal Modulation Transfer Function of Single Voxels in the Human Auditory Cortex Measured with High-Resolution fMRI," Proceedings of the National Academy of Sciences. **104** (34), 14611-14616.

25. Shamma, S. A., Fleshman, J. W., Wieser, P. R., and Versnel, H. **(1993).** "Organization of response areas in ferret auditory cortex," J. Neurophysiol. **69**, 367–383.

26. Summers, V., and Leek, M. R. **(1994)**. "The internal representation of spectral contrast in hearing-impaired listeners," J. Acoust. Soc. Am. **95**, 3518–3528.

27. Versnel, H., Zwiers, M. P., and van Opstal, J. **(2009). "**Spectrotemporal Response Properties of Inferior Colliculus Neurons in Alert Monkey," J.Neuroscince. **29** (31), 9725-9739.

28. Viemeister,N . F. **(1979).** "Temporal modulation transfer functions based upon modulation thresholds," J. Acoust. Soc. Am. **66,** 1364-1380.

29. Zaehle, T., Jancke, L., Hermann, C. S., and Meyer, M. **(2009)**. "Pre-attentive Spectro-temporal Feature Processing in the Human Auditory System," Brain Topogr. **22**, 97-108.

30. Zatorre, R. J., and Belin, P. **(2001)**. "Spectral and Temporal Processing in Human Auditory Cortex," Cerebral Cortex. **11**, 946-953.

APPENDICES

Appendix A IRB Approval

RESEARCH INTEGRITY AND COMPLIANCE
Institutional Review Boards, FWA No. 00001669
12901 Bruce B. Downs Blvd., MDC035 • Tampa, FL 33612-4799
(813) 974-5638 • FAX (813) 974-7091

1/16/2014

Ann Eddins, Ph.D.
Communication Sciences and Disorders
4202 E. Fowler
Ave. PCD1017
Tampa, FL 33620

RE: **Expedited Approval for Continuing Review**
IRB#: CR1_Pro00011325
Title: Neural correlates of age-related changes in auditory perception

Study Approval Period: 1/31/2014 to 1/31/2015

Dear Dr. Eddins:

On 1/14/2014, the Institutional Review Board (IRB) reviewed and **APPROVED** the above application and all documents outlined below.

Approved Item(s): Protocol Document(s):
AEddins_Neural_Correlates_IRB_Protocol_v4_07-19-2013.docx MoCA-Test-English_7_1.pdf
Neural_Correlates_IRB_Datasheet.xlsx
USF_ASSL_IntakeForms_HazardExposure_071913.docx
USF_ASSL_IntakeForms_Hearing&Medical_071913.docx
USF_ASSL_IntakeForms_NoiseExposure_071913.docx
USF_Neural Correlates_Allergen Questionnaire.docx

Consent/Assent Document(s)*:
Adult IC v2 PRO11325_07_19_13.docx.pdf

*Please use only the official IRB stamped informed consent/assent document(s) found under the "Attachments" tab on the main study's workspace. Please note, these consent/assent document(s) are only valid during the approval period indicated at the top of the form(s) and replace the previously approved versions.

The IRB determined that your study qualified for expedited review based on federal expedited category number(s):

(4) Collection of data through noninvasive procedures (not involving general anesthesia or sedation) routinely employed in clinical practice, excluding procedures involving x-rays or microwaves. Where medical devices are employed, they must be cleared/approved for marketing.

As the principal investigator of this study, it is your responsibility to conduct this study in accordance with IRB policies and procedures and as approved by the IRB. Any changes to the approved research must be submitted to the IRB for review and approval by an amendment.

We appreciate your dedication to the ethical conduct of human subject research at the University of South Florida and your continued commitment to human research protections. If you have
any questions regarding this matter, please call 813-974-5638.

Sincerely,

E. Verena Jorgensen, M.D., Chairperson
USF Institutional Review Board

January 31, 2013

Ann Eddins, PhD
Communication Sciences and Disorders
4202 E. Fowler Ave., PCD1017
Tampa, FL 33620

RE: **Expedited Approval** for Initial Review
IRB#: Pro00011325
Title: Neural correlates of age-related changes in auditory perception

Dear Dr. Eddins:

On 1/31/2013 the Institutional Review Board (IRB) reviewed and **APPROVED** the above referenced protocol**.** Please note that your approval for this study will expire on 01/31/2014.

Approved Items:
Protocol
Document(s):
AEddins_Neural Correlates IRB Protocol_v1_1-30-2013.docx
Neural_Correlates_IRB_Datasheet.xlsx
USF_Neural Correlates_Allergen Questionnaire.docx

Consent/Assent Documents:
Adult IC v1 PRO11325_1_11_13.docx.pdf

It was the determination of the IRB that your study qualified for expedited review which includes activities that (1) present no more than minimal risk to human subjects, and (2) involve only procedures listed in one or more of the categories outlined below. The IRB may review research through the expedited review procedure authorized by 45CFR46.110 and 21 CFR
56.110. The research proposed in this study is categorized under the following expedited review category:

(4) Collection of data through noninvasive procedures (not involving general anesthesia or sedation) routinely employed in clinical practice, excluding procedures involving x-rays or microwaves. Where medical devices are employed, they must be cleared/approved for marketing.

Please note, the informed consent/assent documents are valid during the period indicated by the official, IRB-Approval stamp located on the form. Valid consent must be documented on a copy of the most recently IRB-approved consent form.

As the principal investigator of this study, it is your responsibility to conduct this study in accordance with IRB policies and procedures and as approved by the IRB. Any changes to the approved research must be submitted to the IRB for review and approval by an amendment.

We appreciate your dedication to the ethical conduct of human subject research at the University of South Florida and your continued commitment to human research protections. If you have

any questions regarding this matter, please call 813-974-

5638. Sincerely,

E. Verena Jorgensen, MD, Chairperson
USF Institutional Review Board